

Mathematical and Computer Modelling

Introduction of Intelligent Thermal Module with the Use of Renewable and Alternative Energy Sources to Increase the Efficiency of Power Supply Systems of Military Facilities of the Republic of Kazakhstan

Altai Sh. Alimgazin¹, Mukhtar O. Serkpaev², Khuralay Moldamurat¹, Saule G. Alimgazina³, and Sabina E. Bakhtiyarova³

¹ *L.N. Gumilyov Eurasian National University, Astana, Kazakhstan*

² *Academy of Military Sciences of the Republic of Kazakhstan, Astana, Kazakhstan*

³ *Startup company "BMTU" LLP, Astana, Kazakhstan*

Abstract

The transition to low-carbon development and decarbonization of the national economy of Kazakhstan, including industries related to law enforcement agencies, involves the adoption of drastic measures to improve energy efficiency and introduce energy-saving technologies using non-traditional and renewable energy sources (hereinafter - NRES). The issues of introducing an energy-efficient low-carbon intelligent thermal module (NITM) based on a heat pump unit (HPU) using renewable and alternative energy sources to improve the energy efficiency of both industrial facilities in various sectors of the economy and social facilities, housing and communal services, agro-industrial complex, etc. Republic of Kazakhstan.

Over the past few years, the scientists of NJSC "ENU named after L.N. heat of ventilation emissions, heat of sewage, excess waste heat of industrial enterprises, etc.), for the modernization of their heat and cold supply systems.

Keywords

Decarbonization, intelligent thermal module, low-carbon technologies, energy saving, renewable and alternative energy sources heat pump unit, intelligent control system.

1. Introduction

The practical transition of the leading countries of the world to a new technological order based on the principles of decarbonization of production and carbon neutrality in the framework of the Paris Climate Agreement requires a complete rejection of the use of hydrocarbon raw materials and technologies that cause global climate change and the destruction of the planet's ecosystems already in the second half of this century [1,2].

According to the latest data, Kazakhstan is among the top thirty polluting countries in the global ranking [3]. According to The Global Carbon Atlas, Kazakhstan's contribution to global carbon dioxide emissions in 2019 amounted to 314 megatons of CO₂. In terms of carbon dioxide emissions, Kazakhstan ranked 21st among more than 221 countries.

The transition to low-carbon development and decarbonization of the national economies of the leading countries of the world involves the adoption of drastic measures to improve energy efficiency and introduce new low-carbon technologies [4], while one of the most effective technologies, as shown by world practice in recent years, is PATT [5].

Currently, Kazakhstan is in the process of making decisions in the field of substantiating the national position in the climate negotiation process, implementing the Concept of low-carbon development and achieving low-carbon neutrality until 2060.

2. Objects and methods of research

In recent years, in the Republic of Kazakhstan, at the state level, much attention has been paid to the development and implementation of new energy-saving and energy-efficient technologies using renewable energy sources.

In the period from 2012 to 2021, scientists from the Research Institute "Energy Saving and Energy Efficient Technologies" of the Eurasian National University. L. N. Gumilyov (hereinafter L. N. Gumilyov ENU) developed and patented the foundations of a unique energy-saving "green" technology based on the use of vapor compression heat pump technology in a stationary and block-modular layout using various NRES [6,7,8].

A significant impetus to this direction was given by the holding in 2017 in the Republic of Kazakhstan of the International specialized exhibition "EXPO-2017", which widely presented the latest developments of the world's leading countries in the field of application of renewable energy sources, including scientists of the Republic of Kazakhstan [9,10].

This "green" technology in 2017 was demonstrated among the 25 best scientific projects of the country in the Nur-Alem National Pavilion of the EXPO-2017 International Exhibition, aroused considerable interest among representatives of a number of industrial enterprises of our country, countries of near and far abroad.

In order to study the best practices in the use of alternative energy sources, in accordance with the decision of the Minister of Defense of the Republic of Kazakhstan No. KM-7072 of 07/05/2017, a research group of the International Specialized Exhibition EXPO-2017 was created, which carried out its work during the period of the exhibition from 8 to 11 August 2017.

The report on the results of a military scientific study [11] noted the installation of "green heating" for the energy supply of various objects (RSE "Eurasian National University named after L.N. Gumilyov").

The prospects for its application in the interests of the Armed Forces of the Republic of Kazakhstan are determined - in the design of heating and ventilation systems for new buildings of the Main Directorate for the quartering of troops (GURV).

For many remote facilities of the Ministry of Defense, the Border Service of the KNB, the Ministry of Emergency Situations of the Republic of Kazakhstan (border outposts, technical supervision posts of military units, etc.), the issues of their energy supply are relevant, because. often these facilities are located at a significant distance from settlements where there are systems of central heat and power supply.

Domestic military scientists [12,13] considered the use of low-power autonomous hybrid energy complexes (up to 30 kW) in conjunction with backup autonomous sources of electricity, in particular, diesel generators.

However, the issues of using energy-efficient technologies based on renewable energy sources for solving the issues of heat and cold supply of remote military facilities have not been practically studied.

Ensuring reliable heat and cold supply to such remote military infrastructure facilities, the issues of uninterrupted delivery of the main types of fuel (fuel oil, heating oil, diesel fuel, coal) before the heating period are given great attention in law enforcement agencies.

One of the promising ways to solve this problem of energy supply to remote facilities is the use of new energy-saving environmentally friendly technologies of alternative energy, using the above low-temperature renewable energy sources as a heat source [14,15,16].

When developing the proposed technology, both theoretical methods were used (study of various energy supply schemes, the use of alternative energy sources using dual-purpose NTMs, calculations using T-S diagrams of their thermodynamic characteristics, heat balance diagrams), and computational and analytical methods for studying prospects and ways to introduce energy-efficient low-carbon technologies based on dual-use NITM in the modernization of heat and power supply systems for remote military facilities of the Republic of Kazakhstan.

When evaluating the effectiveness of NITM based on TTT with the use of various types of low-grade

heata special energy conversion coefficient COP (ϕ) is used, indicating how many times more (thermal) energy is produced in comparison with the consumed (electrical energy). This coefficient for the proposed TTT ranges from 3.6 to 8.0. The value of the coefficient depends on the temperature of the cooled water (or other low-potential coolant).

COP NITM is determined by the formula [17]:

$$\phi = \frac{Q_{cond}}{N_{comp}} = \alpha \times \frac{T_{cond}}{(T_{cond} - T_{sp})}, \quad (1)$$

where - Q_{cond} - heat removed from the condenser;

N_{comp} - power consumed by the compressor;

T_{cond} - temperature of the working fluid at the outlet of the condenser;

T_{sp} - temperature of the working fluid at the outlet of the evaporator;

α is the total loss factor of the device (cycle losses, compressor losses, losses from irreversibility during heat transfer, etc.).

Table 1 below shows the average annual values of the coefficient ϕ for different temperatures of the cooled water:

Table 1

Values ϕ for different temperatures of the cooled medium [18]

(t_c)	5	10	15	20	25	30	35	40
(ϕ)	3.6	4.06	4.6	5.35	5.98	6.64	7.19	7.93

Studies have been carried out on promising schemes for the use of dual-use NITM with the above various types of renewable energy sources for a typical remote military infrastructure facility. A pilot model of a dual-purpose ITM with an intelligent monitoring system based on TTT has been manufactured for the power supply system of a remote pilot facility of the Border Guard Department of a specific region of the country, it is planned to test its operation.

NITM are metal insulated containers of various sizes with installed equipment (TTT of low and medium thermal power, power and communication cabinets, automation equipment, an intelligent control system unit (ICS), solar panels, batteries, etc.) (Fig. 1).

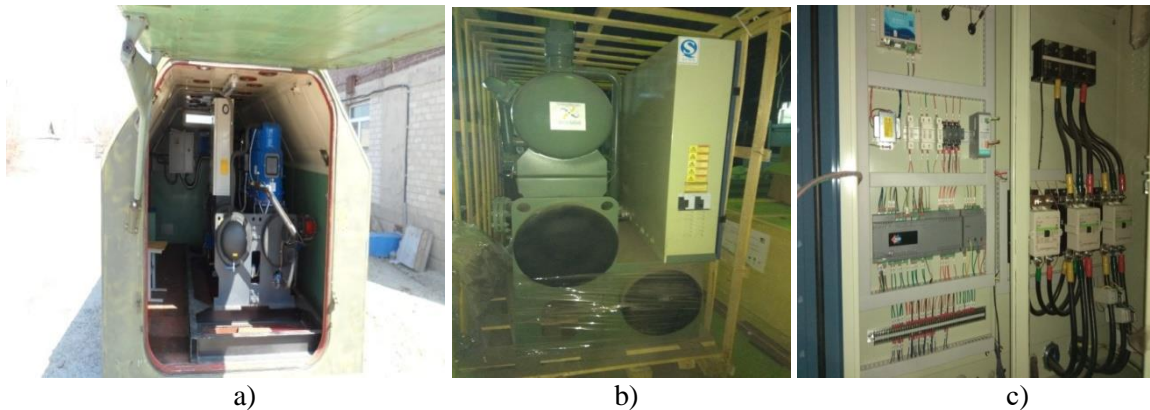


Figure 1: General view of NITM of various thermal power
 a) low power (up to 50 kW) b, c) medium power (up to 500 kW)

A dual-purpose NITM is designed to operate as an energy source for power supply systems of various facilities, in which the sources of heat and electricity and the consumers it serves are located within one building, its part, or several closely spaced buildings.

NITM dual purpose [19,20], locally connected by two pipelines with various sources of low-grade heat (supply of coolant with a temperature of +5 to 350C and its removal after cooling), and also connected to two pipelines (supply and return lines) of the heat supply system remote object.

Other practical advantages of dual-purpose NITM are the possibility of using the utilized heat of ventilation emissions, waste heat from wastewater, using modern heat recovery systems [21,22].

This solution will provide maximum (up to 90%) recovery of waste heat of the utilized air and waste water heat from the premises, will be fully integrated into the overall building management system, has a closed loop, automation

Conducting research on the use of dual-use NITM using various types of renewable energy sources as a source will make it possible [23]:

- the use of alternative types of energy for the needs of heat and power supply of isolated objects of specifically selected regions of the Republic of Kazakhstan;
- assessment of fossil fuel savings at existing remote facilities using dual-use NITM (according to the heat load substitution scheme), which, ultimately, occurs due to the beneficial use of various alternative energy sources in specifically studied regions.

The creation and practical application of intelligent control systems (ICS) in modern energy-saving technologies and equipment, which include dual-use NITM, is one of the most important features of the proposed technology [24,25].

Research and evaluation of the effectiveness of various schemes for the use of NITM using various NRES [26].

2.1. Results and discussion

According to the developed calculation method [27] analytical studies of one of the schemes of work were carried out NIT Musing the heat of the soil (variant of scheme 6 - using vertical ground heat exchanger operating in conjunction with a heat pump - the basic element of the proposed NITM).

The length of the vertical ground heat exchanger (VGHE) depends on the properties of the ground and on the characteristics of the heat pump system. Consider a schematic diagram of the use of VGHE in a heat supply system with a heat pump (Fig. 2).

The VGHE contains a U-shaped polyethylene pipeline, through which an aqueous solution of glycol circulates, pumped by the circulation pump 6 through the evaporator 3 of the heat pump. The refrigerant boiling in the evaporator is compressed by the compressor 2. The heat of condensation is removed in the condenser 4 by the coolant of the heating system 5 supplied by the pump 7.

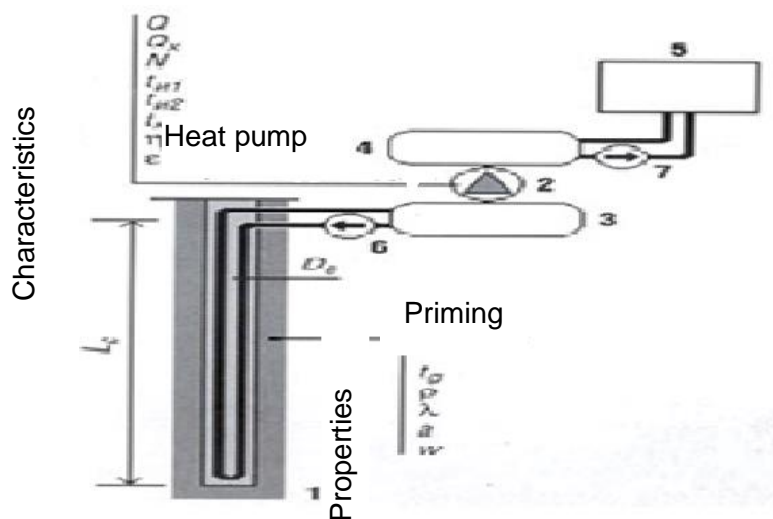


Figure 2: Scheme of a soil heat exchanger - an NITM element:
 1- VGHE, 2 - compressor, 3 - evaporator, 4 - condenser, 5 - heating system,
 6 - circulation pump VGHE, 7 - pump of the heating system

The influence on the intensity of heat transfer in the soil is exerted by its properties such as temperature t_g in the natural state, density ρ , thermal conductivity λ , thermal diffusivity α and moisture content w .

An equally important role in determining the length of the heat exchanger LC is played by the value of its equivalent diameter De , as well as the heat output Q of the heat pump. In the case of using the VGHE for heat removal in the air conditioning mode, it is necessary to take into account the cooling power QX and the electric power N . The intensity of heat transfer in the soil is largely determined by the liquid temperatures t_{u1} and t_{u2} at the inlet to the VGHE and at the outlet from it, and the temperature at the outlet of the condenser t_k is decisive in determining the conversion coefficients of the heat pump η and the cooling coefficient ε , which characterize the energy efficiency of the system.

Because it is planned to carry out work on the implementation of NIRM at remote facilities of law enforcement agencies in various climatic regions of the Republic of Kazakhstan, including facilities in mountainous areas, it is necessary for preliminary studies to have a reliable technique for engineering calculations of VGHE in various soils under a wide variety of external conditions.

The calculation is based on a simple physical dependence [28]

$$q = LC - (t_g - t_w)/R, \quad (2)$$

which includes the value of the heat flow q , the length of the wells LC , the temperature of the soil in its natural state t_g and the temperature of the fluid circulating in the VGHE t_w , as well as the linear (related to one meter of the length of the well) resistance to heat transfer R from the soil to the liquid.

The total length of wells LC , m, used for heat exchange with the ground in heat supply systems with heat pumps, is determined by formula (3), where the following symbols are used:

$$LC = \frac{q_a \cdot R_{ga} + (q_H - N_{HP}) \cdot (R_b + k_m \cdot R_{gm} + R_{gd} \cdot k_{HL})}{t_g - 0,5 \cdot (t_{1H} + t_{2H}) - \Delta t}, \quad (3)$$

$$q_a = \frac{-Q_c \cdot \frac{\varepsilon + 1}{\varepsilon} + Q_H \cdot \frac{\eta - 1}{\eta}}{31536000} = 31,37 \left(-Q_c \cdot \frac{\varepsilon + 1}{\varepsilon} + Q_H \cdot \frac{\eta - 1}{\eta} \right), \quad (4)$$

where q_a is the yearly averaged value of the heat flux, W, from the soil;

R_{ga} – linear thermal resistance of soil, $m \cdot K/W$;

q_H - design thermal power, W, heating systems;

NHP - electric power, W, heat pump;

R_b , – linear thermal resistance, $m \cdot K/W$, wells;

k_m is the coefficient averaging the peak heat load;

R_{gm} – linear thermal resistance, $m \cdot K/W$, of soil during the calculation month;

R_{gd} – linear thermal resistance, $m \cdot K/W$, of soil during the calculation day;

k_{HL} - coefficient taking into account heat losses, which is taken equal to 1.04;

t_{2H} , t_{1H} – temperatures, °C, of fluid at the well inlet and outlet;

t_g is the natural temperature, °C, of the soil;

Δt – correction, °C, taking into account the effect on heat transfer of neighboring wells, if the distance between them is less than 6 meters.

The yearly averaged value of the heat flux q_a , W, into the soil is determined by formula (4), where Q_C is the annual need for cold, GJ; Q_H – annual heat demand, GJ; 31536000 is the number of seconds in a year. ε and η are the coefficient of performance and conversion coefficient of the heat pump, determined from the equipment catalogs at the calculated boiling and condensing temperatures of the refrigerant.

When discussing the advantages of using a VGHE together with a heat pump, attention is always paid to the possibility of using a soil massif in summer when the heat of condensation is removed from the refrigeration machines of the air conditioning system. It is obvious that in this case the heat flux from the soil increases in winter, but dependence (4) makes it possible to quantify this increase [29].

Linear thermal resistance of soil R_{ga} , $m \cdot K/W$, is determined by the formula:

$$R_{ga} = G/\lambda, \quad (5)$$

where λ is the thermal conductivity of the soil, $W/(K \cdot m)$, G is a factor that takes into account the non-stationarity of heat transfer in the soil during alternating cycles of the direction of the heat flow from the cylindrical heat exchanger to the soil and from the soil to the heat exchanger. The value of this factor is related to the Fourier criterion F_o :

$$G = f(F_o), \quad (6)$$

As is known, the Fourier number is one of the criteria for the similarity of non-stationary thermal processes, which characterizes the relationship between the rate of change in thermal conditions in the environment and the rate of restructuring of the temperature field inside the system under consideration. The Fourier number depends on the dimensions of the body and its thermal diffusivity. With regard to the problem under consideration:

$$F_o = \frac{\alpha \tau}{d^2}, \quad (7)$$

where α is the soil thermal diffusivity, m^2/day ;

τ is the cycle in days during which the direction of the heat flow changes;

d is the equivalent diameter, m, of one VGHE U-shaped pipeline, determined from Table 1 [30].

It is necessary to calculate the Fourier number three times, since it affects the values of R_{ga} , R_{gm} and R_{gd} . The authors of the methodology recommend that the values $\tau = 3650$, 30 and 0.25 days, respectively,

be set, which corresponds to time intervals of ten years, one month and six hours.

Data on thermal conductivity and thermal diffusivity of sandy and clay soils are presented in Table 2 [18]. All other types of soils can be considered on the basis of thermal properties as a combination of sand and clay in various proportions, and the corresponding values are determined using the data in Table 2 [30] by interpolation.

In Table 3 shows data on soils obtained during surveys at the construction sites in Astana, Almaty.

Density ρ , moisture content w , coefficients of thermal conductivity λ , and thermal diffusivity α of soils typical for Astana.

After the criterion F_o is calculated, it is necessary to determine the auxiliary value G , the dependence of which on F_o is presented graphically in the form of a diagram in logarithmic coordinate axes [30]. Using Excel, it is not difficult to represent this empirical dependence analytically:

$$G = 0.0756 - \ln(F_o) + 0.0927, \quad (8)$$

Linear thermal resistance R_b , $m \cdot K / W$, of the material filling the well, is taken according to Table if the well is filled with soil removed from the well during drilling. To the value of R_b , determined according to the table, a correction is introduced if the well is filled with a solution whose thermal conductivity differs from that of the soil surrounding the well.

The value of the coefficient k_t , averaging the peak heat load, is determined by the formula:

$$k_m = 10^9 \cdot \frac{Q_H}{q_H \cdot z}, \quad (9)$$

where z is the number of seconds of the heating period.

The values of effective linear thermal resistance, R_{gm} , and R_{gd} , $m \cdot K/W$, of the soil during the calculation month and calculation day are determined by formulas (5)-(7) with the corresponding values $\tau = 30$ and $\tau = 0.25$.

The values of thermal loads q_H and q_c , as well as soil temperatures t_g are taken according to the design data. The temperature t_{II} and the glycol cooled in the evaporator of the heat pump is recommended to be calculated according to formula (3), based on the given values of the conversion coefficient and the temperature of the coolant in the heating system, and the temperature t_{II} of the glycol at the outlet of the VGHE is assumed to be 5°C higher [31].

Thus, all the symbols of the main calculation formula (3) are explained.

You can verify the reliability of these explanations and the correctness of the dependence itself by the example of calculating the application of NIRM for one remote frontier outpost facility in the Southern Border District of the Republic of Kazakhstan.

It is necessary to calculate the field of vertical ground heat exchangers (VGHE) for heating and air conditioning of the building of a remote military facility, built on a terrain in which the natural temperature of the soil at a depth of more than 6 meters $t_g = 10^\circ C$, and the duration of the heating period is 170 days ($z = 14688000$ s).

VGHE is designed from polyethylene pipes with a conditional bore of 25 mm, installed in wells with a diameter of 150 mm. The density of the soil in which the VGHE is installed is $\rho = 1318$ kg/m³, the humidity is 15%, the coefficients of thermal conductivity and thermal diffusivity are, respectively, 2.076 W/(K · m) and 0.087 m²/day.

The project has established that the peak thermal power of the heating system is $q_H = 500$ kW, and the refrigeration power of the air conditioning system is $q_C = 800$ kW. Annual heat consumption by the heating system is estimated at $Q_H = 3230$ GJ, and cold is generated at $Q_C = 1556$ GJ during the summer period.

It is assumed that the conversion factor η should not be lower than 4, and the average cooling factor for

the summer period $\varepsilon = 4.2$.

The heating system of the building is designed taking into account the water temperature at the outlet of the condenser $t_{2k} = 35^\circ\text{C}$.

The yearly averaged value of the heat flux q_a from the heat pump into the ground is determined by formula (7):

$$q_a = 31.71 \cdot (-1556 \cdot (4.2 + 1) / 4.2 + 3230 \cdot (4.0 - 1) / 4.0) = 15796 \text{ W}$$

The Fourier criterion F_o of a ten-year (3650 days) cycle is determined by formula (7):

$$F_o = (0.087 \cdot 3650) / 0.0542 = 106030$$

Factor G , which takes into account the non-stationarity of heat transfer in the soil, is determined by formula (8):

$$G = 0.0756 \times 2.3 \times \lg(106030) + 0.0927 = 0.967$$

The value of the effective linear thermal resistance of the soil R_{ga} is determined by the formula (8):

$$R_{ga} = 0.967 / 2.076 = 0.466 \text{ m} \cdot \text{K} / \text{W}$$

Let us determine the electrical power of the NHP heat pump engine based on the specified minimum value of the conversion factor $\eta = 4.0$:

$$N_{HP} = 103 \cdot \left(\frac{q_H}{\eta} \right) = 125000 \text{ W}, \quad (10)$$

The value R_b of the linear thermal resistance of the well depends on the velocity of the fluid through the pipeline submerged in this well. In order to preliminarily determine this speed, it is necessary to specify the number of wells connected in parallel, without going into the subtleties of the hydraulic calculation.

With a heat pump heat output of 500 kW and a water temperature difference, (the properties of ethylene glycol can be ignored in this calculation), at the inlet to the evaporator and at the outlet of 5°C , the following should circulate through the wells:

$$(500 - 125) \cdot 0.86 / 5 = 64.5 \text{ t} / h_{\text{liquid}}$$

If you set the number of VGHEs, for example 80, then $64.5 / 80 = 0.81 \text{ t} / \text{h}$ will circulate through each of them.

The inner diameter of the Dy25 polyethylene pipe is 27.4 mm. The speed of the fluid in it is: $(0.81 / 3600) / (\pi \cdot 0.02742 / 4) = 0.382 \text{ m/s}$.

According to the table, we determine the linear thermal resistance R_b of the well, taking into account its filling with heat-conducting bentonite:

$$R_b = 0.081 - 0.012 = 0.069 \text{ m} \cdot \text{K} / \text{W}, \quad (11)$$

The value of the coefficient kt , averaging the peak heat load, is determined by formula (12):

$$109 \cdot 3230 / (500000 - 14688000) = 0.44$$

The values of the effective linear thermal resistance, R_{gm} , and $R_{gd} \text{ m} \cdot \text{K/W}$, of the soil are determined

by formulas (5)...(9).

The Fourier criterion for the monthly cycle (30 days) is determined by the formula (7):

$$F_o = (0.087 * 30) / 0.0542 = 871$$

Factor G is determined by formula (11):

$$G = 0.0756 \times 2.3 \times \lg(871) + 0.0927 = 0.604$$

The value of the effective linear thermal resistance of the soil is determined by the formula (5):

$$R_{gm} = 0.604 / 2.076 = 0.291 \text{ m} \cdot \text{K} / \text{W}$$

For a six-hour cycle (0.25 days):

$$\begin{aligned} F_o &= (0.087 * 0.25) / 0.0542 = 7.3 \\ G &= 0.0756 \times 2.3 \times \lg 7.3 + 0.0927 = 0.242 \\ R_{gd} &= 0.242 / 2.076 = 0.117 \text{ m} \cdot \text{K} / \text{W} \end{aligned}$$

The glycol temperature at the inlet to the VGHE is determined by the formula (3):

$$T_{I2} = (4.0 + 0.0755 \cdot 35 - 7.175) / (0.1729 - 0.0026 \cdot 35) = -6.5 \text{ }^\circ\text{C}$$

The glycol temperature at the outlet of the VGHE is assumed to be 5°C higher:

$$T_{I1} = -6.5 + 5 = -1.5 \text{ }^\circ\text{C}$$

The total length of the wells is determined by the formula (6): The glycol temperature at the outlet of the VGHE is assumed to be 5°C higher:

$$LC = [15796 \cdot 0.466 + (500000 - 125000) \cdot (0.069 + 0.44 \cdot 0.291 + 0.117 \cdot 1.04)] / [10 - 0.5 \cdot (-1.5 - 6.5)] = 9055 \text{ m}$$

The total length of the wells is determined by the formula (6):

The heat flow from the ground to the VGT is determined by the difference in the values of the thermal and electrical power of the heat pump, that is:

500000 - 125000 = 375000 W, and the specific value of the heat flux, referred to one meter of the VGHE, is equal to: 375000/9055 = 41.4 W / m.

The specific thermal power of the heat pump, referred to one meter of WHC, is: 500000/9055 = 55.2 W/m.

As we can see, the result is close to the expected one, which makes it possible to treat this technique with confidence, despite the fact that some of its provisions do not follow directly from the structure of simple concepts formed by primitive logic.

2.2. Influence of initial data on the calculation result

Let us consider how its thermal conductivity affects the magnitude of the heat flux to the VGHE from the soil [32].

Our calculation example was performed for soil with thermal conductivity $\lambda = 2.076 \text{ W}/(\text{K} \cdot \text{m})$, and the specific heat flux was $q_{yd} = 41.4 \text{ W}$. On shows the function $q_{yd} = f(\lambda)$ with other calculation conditions unchanged.

When using VGHE in summer in the mode of removing heat from the refrigerating machines of the air conditioning system, the efficiency of ground heat exchangers operating in winter together with a heat pump increases. The curve in Fig. 3 shows the nature of the dependence of the specific heat flux from the ground to the VGT in winter on the ratio of the building's annual need for cold to its annual need for heat for heating [33].

In practice, in the construction of ground source heat pumps, a VGHE with two U-shaped polyethylene pipes installed in one well is usually used. The mathematical model makes it possible to evaluate the effectiveness of such a technical solution (Fig. 4). The values of the specific heat flux in the left and right columns of the diagram are calculated for the values of the equivalent diameter of the VGHE, corresponding to the design of the heat exchanger with one and two U-tubes [34].

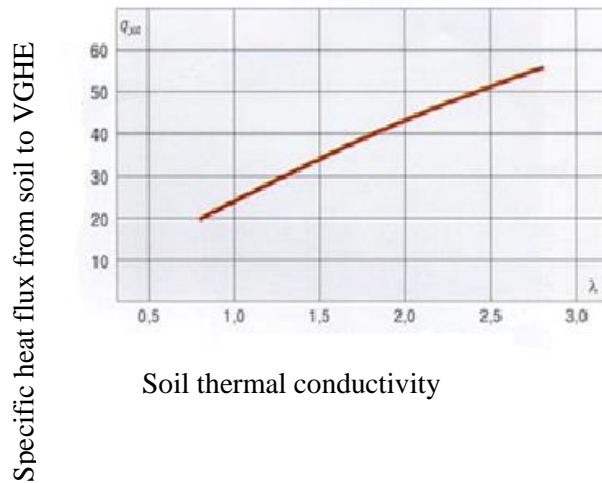


Figure 3: The nature of the change in the value of the specific flux to the from soils with different thermal conductivity

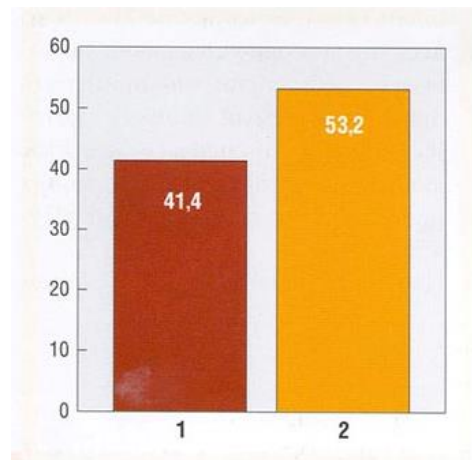


Figure 4: The nature of the change in the value of the specific heat flux, W / m, from the number of U-shaped pipes installed in the VGHE: 1 - one U - shaped pipe; 2 - two U - shaped pipes

It should be noted that Figures 3-4 do not display the absolute values of the specific heat flux from the soil to the VGHE, but the nature of the change in these values from one of the arguments. It is recommended to determine the length of vertical ground heat exchangers using formula (3).

Carrying out a comparative analysis of the use of dual-use VGHE with the use of renewable energy sources with the existing power supply system of a remote pilot facility, assessing the effectiveness of using

dual-use VGHE [35].

3. References

- [1] G. V. Safonov, B. K. Yesekina, Sh. Tuebekova, Decarbonization of the national economy: strategies and scenarios. Proceedings of the National Academy of Sciences of the Republic of Kazakhstan. Social Sciences and Humanities Series.N.3: pp. 13–22. 2017.
- [2] Decarbonization of Economy's Extractive Sectors of the Republic of Kazakhstan. Under edition Academician of the National Academy of Sciences of the Republic of Kazakhstan, Doctor of Geological and Mineralogical Sciences Daukei, S.: Bi-PRINT: 265 p. 2021.
- [3] K. H. Moldamurat, S. Akhmejanov, K. Kariyeva, Z. Omarov, D. Kalibekov, N. Sayasat, Design and optimization of the parameters of a hybrid unmanned aerial vehicle in the Solid Works complex. I2022 International Conference on Smart Information Systems and Technologies, pp. 28-30, April 2022.
- [4] G. Heinrich, et al. Heat pump installations for heating and hot water supply / per. With him.N. L. Korableva, E. Sh. Feldman; ed. B. K. Yavnel. Stroyizdat: p. 351, 1985.
- [5] Market overview of heat pumps in Sweden, Finland (2002): ABOK.N.1: p. 40-41.
- [6] A. P. Burdukov, Yu. M. Petin, Heat pumps for Russia: technology for the use of geothermal and waste heat by enterprises. Equipment. Developments. Technology.N.7: pp. 27-32, 2007.
- [7] E. Bubalis, K. Marcinauskas, R. Shkema, Opportunities and prospects for the use of heat pumps in the production of low-grade heat. Industrial Energy. V.22, N. 3: pp. 15-18, 2000.
- [8] V. V. Danilov, Improving the efficiency of the district heating system based on the use of heat pump technology. Energy saving and water treatment. N. 2: pp. 5-14, 2000.
- [9] Yu. M. Petin, Experience of a decade of production of heat pumps in CJSC Energia. Energy policy. V.3: pp. 28-33.
- [10] A. V. Baranenko, L. S. Timofeevsky, A. G. Dolotov, A. V. Popov, Absorption heat converters: Monograph. St. Petersburg: SPbG UNIPT: p. 338, 2005.
- [11] V. N. Romanyuk, A. A. Bobich, D. B. Muslina, N. A. Kolomytskaya, S. V. Malkov, T. V. Bubyr, Absorption heat pumps in the heat circuit of a thermal power plant to increase its energy efficiency. Energy and Management. N. 1: pp. 14–19, 2013.
- [12] W. Wei, W. Baolong, Sh. Wenxing, L. Xianting, Absorption heating Technologies: A review and perspective. Applied Energy 130: pp. 51–71, 2014.
- [13] S. Jian, F. Lin, Zh. Shigang, Experimental study of heat exchanger basing on absorption cycle for CHP system. [Applied Thermal Engineering. V. 102.](#): pp. 1280-1286, 2016.
- [14] X. Xiaoyun, J. Yi, Absorption heat exchangers for long-distance heat transportation. [Energy. V. 141.](#): pp. 2242-2250, 2017.
- [15] Z. Y. Seitbattalov, S. K. Atanov, Z. S. Moldabayeva, An Intelligent Decision Support System for Aircraft Landing Based on the Runway Surface. SIST 2021. 2021 IEEE International Conference on Smart Information Systems and Technologies, 2021.
- [16] Zhiqiang, Liu, Nan, Xie, Sheng, Yang, Thermodynamic and parametric analysis of a coupled LiBr/H₂O absorptionchiller. Kalina cycle for cascade utilization of low-grade waste heat: Energy Conversion and Management. [Volume 205](#), February 1: 112370, 2020.
- [17] A. Sh. Alimgazin, A. N. Berguzinov, Application of the "Green Heating" technology for energy supply of the "Energy Research Center" facility of the international exhibition "EXPO-2017".Bulletin of the PSU named after S. Toraigyrov, series "Energy".N. 1.: pp. 21-28, 2017.
- [18] A. Sh. Alimgazin, S. G. Alimgazina, Development of technologies and implementa- tion of heat pump systems for heat supply of residential, public and industrial buildings in the Republic of Kazakhstan using non-traditional and renewable energy sources.Astana: Artprint Publishing House: p. 171, 2010.
- [19] S. O. Filatov, Thermal calculation of vertical ground heat exchangers. News of higher educational institutions and energy associations of the CIS. Energy: Intern. sci.-tech. magazine.N. 4.: pp. 81-91, 2013.

- [20] A. Sh. Alimgazin, S. G. Alimgazina, M. G. Zhumagulov, Heat pump in a new modular configuration to recover low-grade heat emissions at enterprises. *E3S Web of Conferences*. 2020, p. 178. - 01003. <https://doi.org/10.1051/e3sconf/202017801003>.
- [21] A. Sh. Alimgazin, S. A. Prishchepova, I. A. Sultanguzin, A. V. Fedyukhin, Yu. V. Yavorovsky, A. I. Bartenev, The use of heat transformers for the low-temperature secondary energy resources recovery in non-ferrous metallurgy enterprises. *E3S Web of Conferences*. – 2020, Vol. 178. 01017. <https://doi.org/10.1051/e3sconf/202017801017>.
- [22] Report on the results of a military scientific study of a specialized International Exhibition EXPO-2017 (Astana) during the period of the exhibition from 8 to 11 August 2017.
- [23] S. Brimzhanova, S. Atanov, K. Moldamurat, K. Brimzhanova, A. Seitmetova, An intelligent testing system development based on the shingle algorithm for assessing humanities students' academic achievements. *Education and Information Technologies*, 2022.
- [24] E. Zh. Akimbaev, A. B. Baktibaev, The use of energy-saving technologies in the Republic like Kazakhstan. *Askeri gylym akademiy synnyn khabarshysy*. Astana, N. 4.: pp. 8-11, 2016.
- [25] A. S. Utegen, K. Moldamurat, M. Ainur, A. G. Amandykuly, S. S. Brimzhanova, Development and modeling of intelligent control system of cruise missile based on fuzzy logic. *Proceedings - 2021 16th International Conference on Electronics Computer and Computation, ICECCO 2021*, 2021.
- [26] V. V. Gruzin, M. E. Shleiko, A. U. Shoynbaev, Development of a structural diagram of a hybrid power plant. *Askeri gylym akademiy synnyn khabarshysy*. Astana. N. 3.: pp. 31-38, 2014.
- [27] I. S. Asanov, Rational technical appearance of the alternative energy system of the units of the Border Service of the KNB of the Republic of Kazakhstan. *Askeri gylym akademiy synnyn khabarshysy*. Nur-Sultan. N. 4.: pp. 30-37, 2019.
- [28] D. B. Baikenov, G. N. Zhampeisov, Alternative energy sources as an element of increasing the autonomy and energy independence of the armed forces. *Askeri gylym akademiy synnyn khabarshysy*. Nur-Sultan. N. 4.: pp. 41-47, 2019.
- [29] Y. Z. Lu, *Industrial intelligent control: fundamentals and applications*. New York: Wiley: p. 346, 1996.
- [30] K. M. Hangos, R. Lakner, M. Gerzson, *Intelligent control systems: an introduction with examples*. New York: Kluwer academic publishers.: p. 301, 2001.
- [31] S. K. Atanov, Z. Y. Seitbattalov, Z. S. Moldabayeva, Development an Intelligent Task Offloading System for Edge-Cloud Computing Paradigm. *Proceedings. 2021 16th International Conference on Electronics Computer and Computation, ICECCO 2021*, 2021.
- [32] A. E. Kyzyrkanov, S. K. Atanov, S. A. R. Aljawarneh, Formation control and coordination of swarm robotic systems. *ACM International Conference Proceeding Series*, 3492704, 2021.
- [33] D. Ray, D. McMichael, Heat pumps /per. from English.: *Energoizdat*, - p. 224, 1982.
- [34] D. Keppler, Absorption chillers as a contribution to a climate-friendly refrigeration supply regime. Factors of influence on their further diffusion: *Journal of Cleaner Production* 172: pp.1535-1544, 2018.
- [35] S. S. Brimzhanova, S. K. Atanov, M. Khuralay, D. M. Kalmanova, T. Tabys, Problems of detecting fuzzy duplicates *ACM International Conference Proceeding Series*, 2019, 23.

Optimization of Launch Vehicles with Using Composite Materials

Sayat Akhmejanov¹, Valeriy Dzhundibayev¹, Marat Nurguzhin², Aibek Moldamurat¹,
Almas Idrissov¹, and Galia Mukhamedrakhimova¹

¹ *L.N Gumilyov Eurasian National University, Astana, Kazakhstan*

² *Daukeyev G. AUPET, Almaty, Kazakhstan*

Abstract

This article discusses the use of composite materials in the design of ultralight launch vehicles using the example of the «Pegasus launcher» «air-to-air» cruise launch vehicles. Using CAD «SolidWorks», dynamic and statistical calculations of the rocket fairing were carried out, presumably made of a traditional material – aluminum alloy 6063-T1 and CM based on carbide-silicon fiber and titanium matrix, which made it possible to visualize the advantages of CM for stress, deformation and displacement in the stress-strain state of the head fairing.

Keywords

Launch vehicles, existing fairings, composite materials, payload optimization, design

1. Introduction

Modern aircraft tend to decrease in weight and strength, for this purpose modern technologies, composite materials for their production are used. Pegasus-XL is an American light-class cruise launch vehicle developed by Orbital Sciences Corporation. The launch is carried out using a specially equipped L-1011 Stargazer aircraft from Lockheed Corporation. The separation of the launch vehicle from the carrier aircraft occurs at an altitude of 12 CM. The launch vehicle consists of three solid-fuel stages, in the Pegasus HAPS variant, the launch vehicle is also equipped with a maneuvering unit powered by hydrazine. The mass of the payload launched into a sun-synchronous orbit with a height of 500 CM ~ 250 kg.

This work implies the use of the software "SolidWorks" to improve and optimize the geometries and topologies of the aircraft, the formation of comparative calculations to demonstrate the capabilities and results of the elective method.

Software "SolidWorks" to conduct a study of methods, we use composite material for the calculation of the Pegasus XL aircraft.

Modern aerospace technology is unthinkable without polymer CM. New CM for the space industry can withstand the loads of space flights (high temperatures and pressures, vibration loads at the launch stage, low temperatures of outer space, deep vacuum, radiation exposure, exposure to microparticles, etc.) and have a fairly low specific density. Most carbon CM are lighter and stronger than the most suitable metal (aluminum and titanium) alloys in their physical properties.

The result of the study of the Pegasus XL aircraft and the integration of changes will lead to improvements in the form of:

1. reduce the weight of the final products;
2. reduce fuel consumption;
3. improve flight safety;
4. reduce operating costs.

2. Literature review

For the design of the Pegasus XL air-to-air launch vehicle, this project used the capabilities of virtual

calculation and SolidWork software, as well as add-ons such as Solidworks Flow Simulation, Solid Simulation Premium, which includes such calculation tools as:

- Statistical calculation;
- Aerodynamic calculation;
- Optimization of the product topology.

In this work, a system computer simulation of the "Pegasus launcher" launch vehicle has been performed. The purpose of this calculation was to demonstrate the great possibilities of virtual calculation and its advantage in the field of designing and improving existing structures to use improved components and materials for specified purposes.

For the design of the LV in this project, the software "SolidWorks" was used, as well as additions such as "Solidworks Flow Simulation", "Solidworks Simulation Premium", which includes such calculation tools as "Static Calculation", "Optimization of product topologies" and "Aerodynamic calculation".

3. Methods and technologies

The algorithm of actions for performing this task is presented in the following sequence:

1. Designing the "Pegasus Launcher" PH in a virtual CAD environment using the solid-state modeling method.

2. Using all available tools for the analysis of this assembly, the calculation was carried out in the "SolidWorks Flow Simulation" environment. By entering the input data, the required results are obtained at the output, such as pressure, force and temperature from the effects of friction.

3. Next, using the output data, we go to the tool called "Optimization of product topologies". In this analysis tool, an analysis of the combination of mass for strength was carried out. Thus reducing the mass while the required strength remains unchanged.

4. To verify the accuracy of the designed product in terms of strength characteristics, another operation was performed in the "SolidWorks Simulation Static Calculation" environment based on the data obtained during the calculation of "SolidWorks Flow Simulation".

This package allows you to build an aircraft model and calculate aerodynamics using "Flow Simulation", which is a hydro-gas dynamic analysis module in the "SolidWorks" environment, minimizing errors that depend on the human factor.

Thus, a comparative analysis of the product with different materials used was carried out by visualizing all the data of plots, graphs, etc.

3.1. 3D modeling method in the SolidWorks virtual environment on Pegasus XL

These results are presented below in the form of tables, graphs and illustrations.

For the first calculation, using data obtained from Ukrainian sources about the PH "Pegasus Launcher", a 3D modeling process of this product was carried out, which was carried out according to the drawings presented (Fig.1.), computer-aided design methods were taken from this source [5,12], the results are given below:

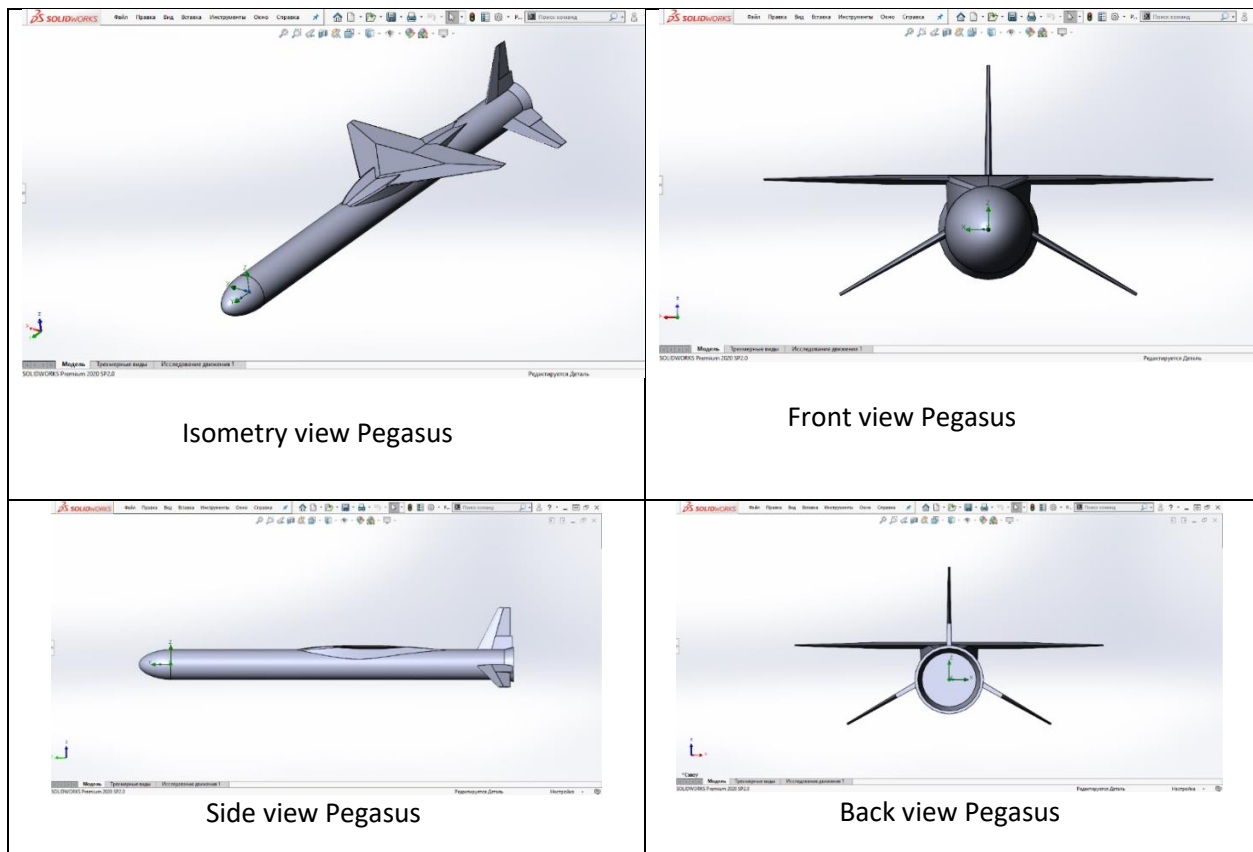


Figure 1: The PH parameters of the "Pegasus Launcher" used in the calculation

The method of solid-state modeling and assembly/combination of bodies in the SolidWorks modeling environment is used.

3.2. Method of aerodynamic calculation on Pegasus XL

To calculate the flow and obtain data on the received loads at this PH, the following input data were used.

Table 1

External conditions

Thermodynamic parameters	Speed Parameters
	Velocity vector
	Speed in the direction of X: 0 m/s
	Speed in the direction of Y: (-240.000) – (-2800) m/s
Speed in the direction of Z: 0 m/s	Turbulence Parameters
	Intensity and scale of turbulence
	Intensity: 0.10 %
Length: 0.019 m	

Calculation results. The following parameters are accepted within their limits Min/Max.

Table 2
 Min/Max values

Name	Minimum	Maximum
Pressure [Pa]	13183.51	48262.64
Density (fluid environment) [kg/m ³]	0.19	0.74
Speed [m/s]	0	314.115
Speed (X) [m/s]	-177.615	179.328
Speed (Y) [m/s]	-311.109	104.643
Speed (Z) [m/s]	-138.102	124.781
Temperature [°C]	-76.33	-27.63
Temperature (fluid environment) [°C]	-76.33	-27.63
Vorticity [1/s]	0.02	23793.70
Velocity in a rotating coordinate system [m/s]	0	314.115
Velocity in a rotating coordinate system (X) [m/s]	-177.615	179.328
Velocity in a rotating coordinate system (Y) [m/s]	-311.109	104.643
Velocity in a rotating coordinate system (Z) [m/s]	-138.102	124.781
Mach number []	0	1.11
Tangential stress [Pa]	0	268.59
Relative pressure [Pa]	-6215.77	28863.37
Indicator of non-collinearity of heat flow []	3.1857118e-13	1.0000000
Thermal resistance indicator []	5.2437495e-14	1.0000000
Acoustic power [W/m ³]	0	111.524
Acoustic power level [dB]	0	140.47

The pressure result in the "Flow Simulation" was visualized in a gradient of colors and a time-based visualization of the flow movement was obtained, for example, Figure 2 shows for a time of 4.1 seconds. The calculation of the flow was in dynamic terms, since the "SolidWorks" software allows you to enter dynamic input data with the ratio of height to time. So, for the calculation of this project, data from Ukrainian studies were used as input data. The PH "Pegasus" of the air-to-air class rises and starts from 12 kilometers and rises to 100 kilometers, respectively, the speed is from 240 meters per second to 2,800 meters per second. The results are presented in the tables below. The methods of aerodynamic calculation for this work were taken from the list of references [2, 14].

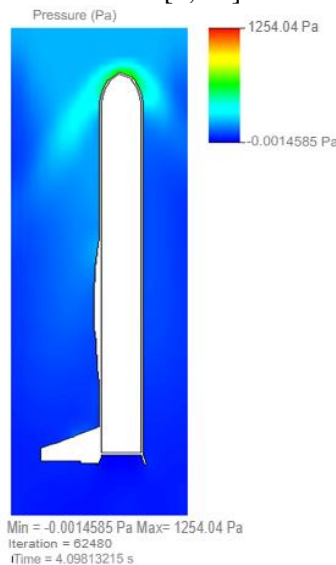


Figure 2: Results of visualization of the flow of the virtual environment at 4.1 seconds

Material - Aluminum, Path: Material Predefined\Metals; Density: 4505.00 kg/m³

Specific heat capacity

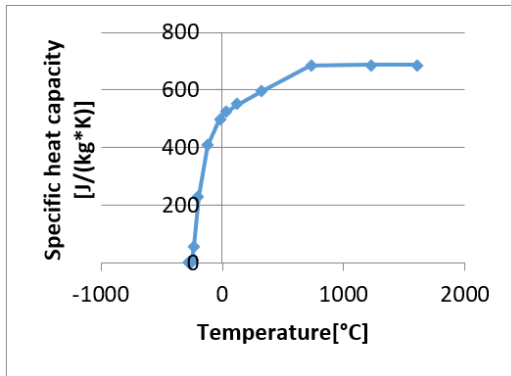


Figure 3: Type of Conductivity: Isotropic

Coefficient of thermal conductivity

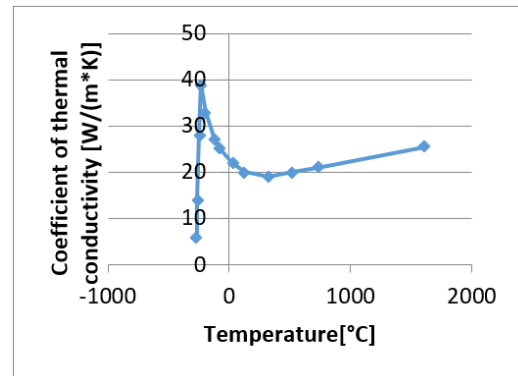
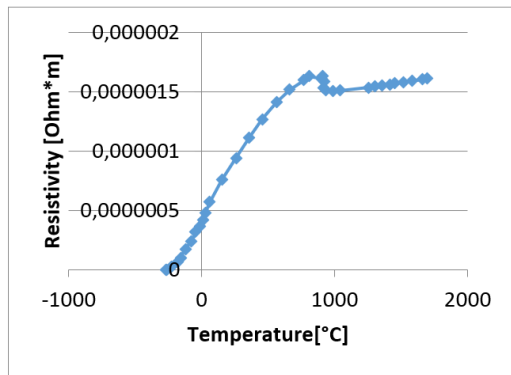


Figure 4: Electrical Conductivity: Conductors



Radiation properties: No, Melting Point: Yes
 Temperature: 1608.05 °C

Figure 5: Resistivity

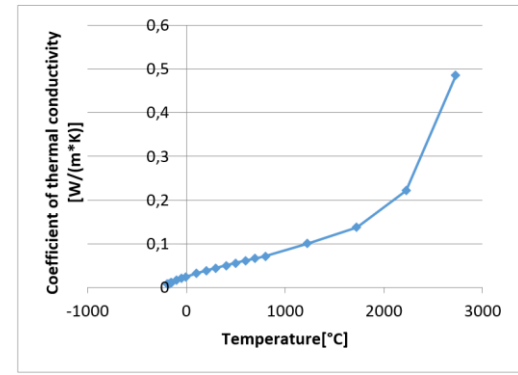


Figure 6: Coefficient of thermal conductivity

Gases-Air, Path: Gases are Predefined; Adiabatic index (Cp/Cv): 1.399, Molecular weight: 0.0290 kg/mol

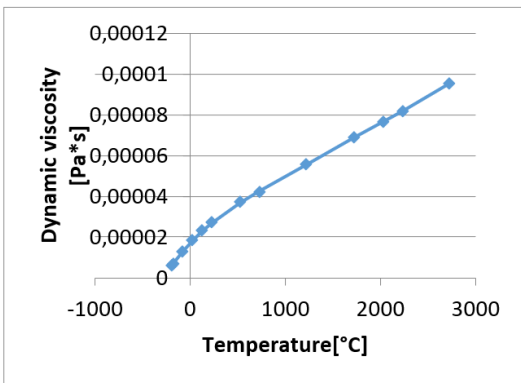


Figure 7: Dynamic viscosity

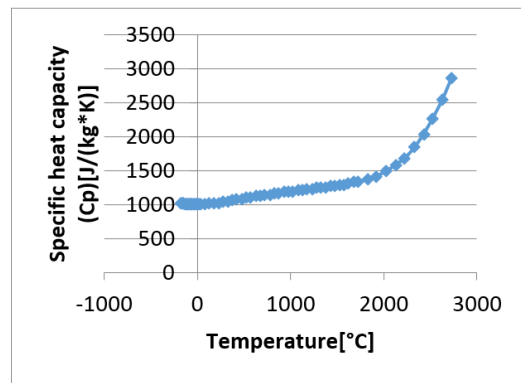


Figure 8: Specific heat capacity (Cp)

Further, based on the data obtained from "Flow Simulation", in particular, the result of pressure in Pa. The maximum value was equal to $P_a(\max) = 48262.64$; This value is equal to the data presented in the research papers of Ukraine.

3.3. Method of static calculation in the CAE environment of SolidWorks

Based on these data, work was carried out in the "Solidworks Simulation" environment, static calculation and comparison of materials.

Static calculation in this software makes it possible to virtually calculate the product for stress, displacement and deformation. Using the data obtained, we will be able to optimize the topology of the product-structures to obtain the optimal ratio of mass to strength. From this literature, design and calculation methods were used [10,13].

Below are the input and output data from the calculations:

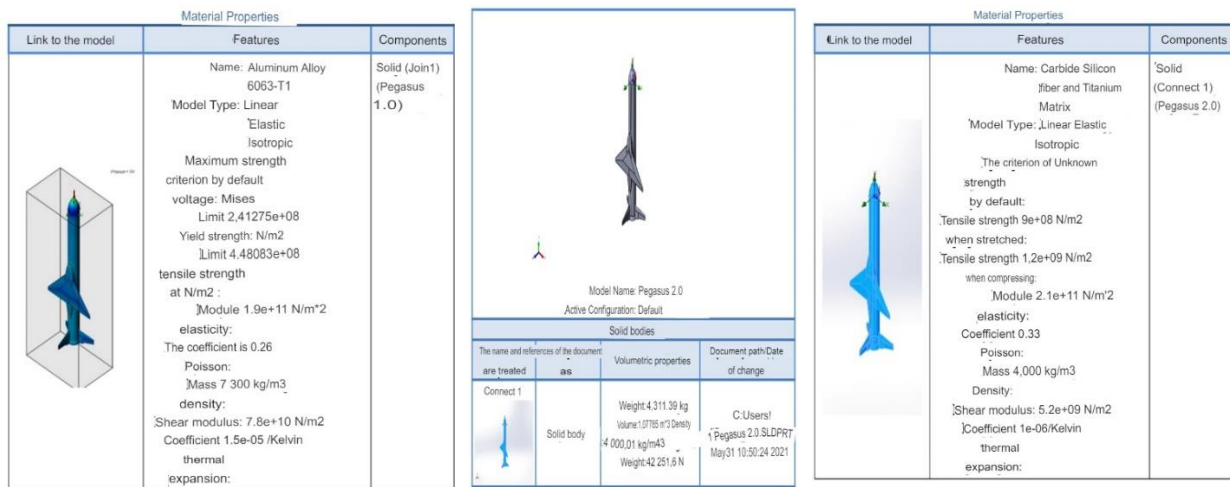


Figure 9: Composite material input data

The above shows the properties of the 6063-Ti aluminum alloy material and the input data.

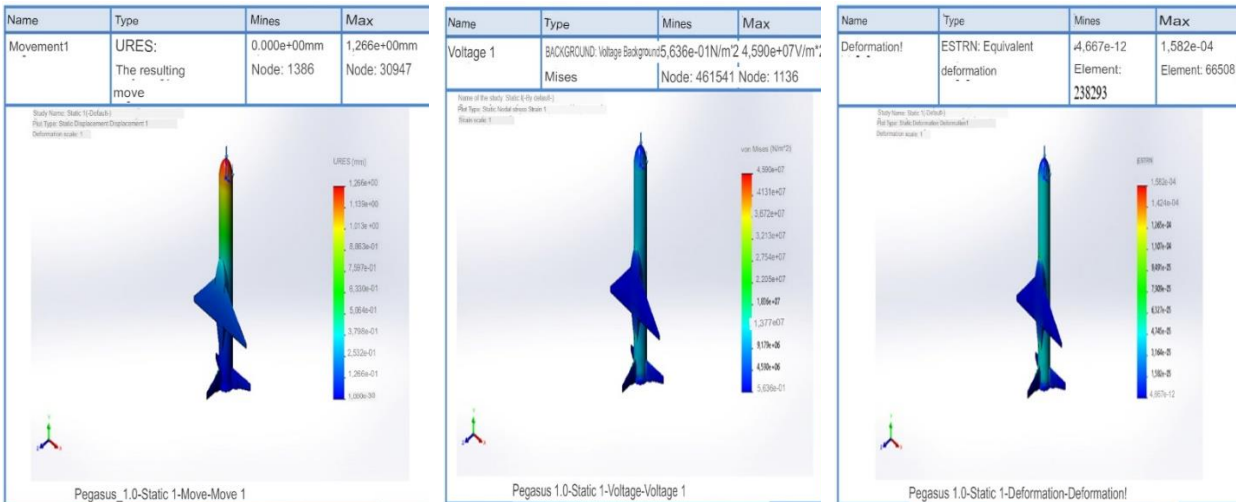


Figure 10: The result of the static calculation

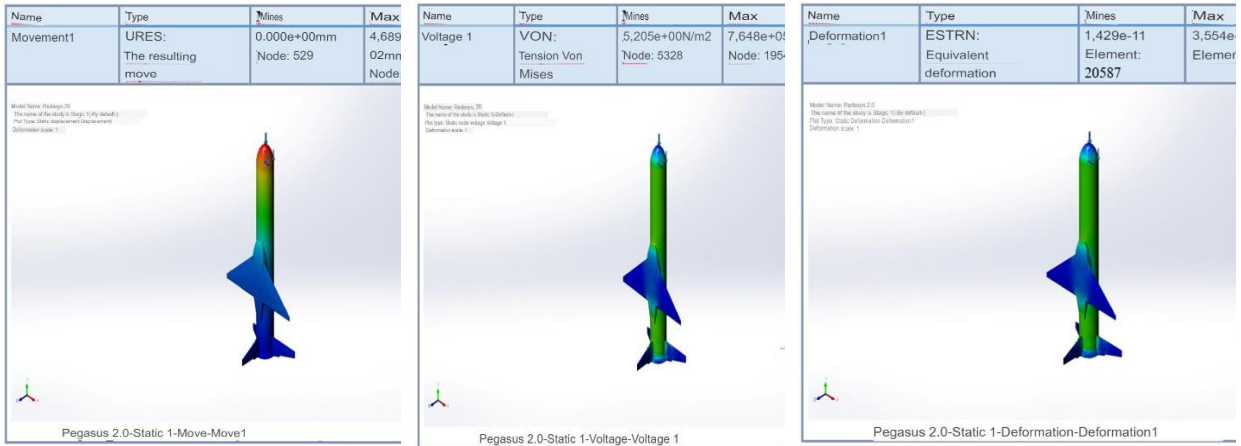


Figure 11: Output data from the composite material study

Comparative analysis of the above static calculation results.

4. Results

This calculation makes it possible to maintain the conditions of external VAT with additional loads, update and improve the design of the aircraft. Due to the exclusion of excessive technical characteristics, the efficiency of the aircraft increases to exorbitant coefficients.

Table 3
 Comparison table

	Designations	Aluminum Alloy 6063-T1	Silicon carbide fiber and titanium matrix
Voltage	max	4,590e+07N/m ² Knot: 1136	7,648e+05N/m ² Knot: 19545
	min	5,636e-01N/m ² Knot: 461541	5,205e+00N/m ² Knot: 5328
Deformation	max	1,582e-04 Element: 66508	3,554e-06 Element: 509
	min	4,667e-12 Element: 238293	1,429e-11 Element: 20587
Weight	mid	11 158 kg	4 311,39 kg
Ultimate strength	mid	4,48083e+08 N/m ²	9e+08 N/m ²

The results of comparing the output data from the static calculation.
 To optimize topologies, the "Topology Research" supplement was used in this software.

4.1 Pegasus XL topology optimization method in the SolidWorks environment

Topology research implements nonparametric optimization of the topology of parts. Starting from the maximum space of the original project (which is the maximum allowed size of the component) and taking

into account all the applied loads, fasteners and production constraints, topology optimization is looking for a new layout of the material within the boundaries of the maximum allowable geometry due to the redistribution of the material. The optimized component meets all the required mechanical and manufacturing requirements. The literature indicates the source that was used to test the optimization method [7].

Input data:

- Material: Silicon carbide fiber and titanium matrix;
- Loads: 0,6 N/mm² (MPa).

Goal:

- Mass limitation;
- Optimal weight-to-strength ratio.

According to the results of this analysis, the following were obtained:

As a result of the entire analysis, it was calculated that the optimal thickness of this fairing is 35 mm.

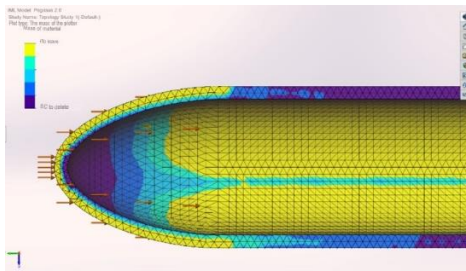


Figure 12.1: Optimization of topologies input data

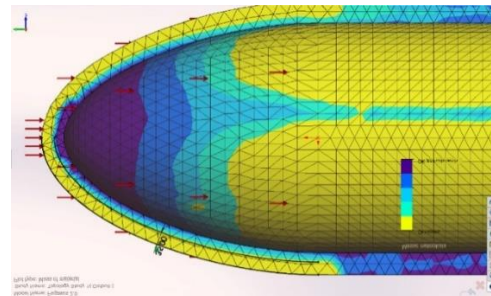


Figure 12.2: Topology optimizations visualization of the result

5. Discussion

Topology research implements nonparametric optimization of the topology of parts. Starting from the maximum space of the original project (which is the maximum allowed size of the component) and taking into account all the applied loads, fasteners and production constraints, topology optimization is looking for a new layout of the material within the boundaries of the maximum allowable geometry due to the redistribution of the material. The optimized component will meet all the required mechanical and manufacturing requirements.

6. Conclusion

Using the above research methods, the improvement and optimization of all parameters of the Pegasus XL aircraft in the SolidWorks design environment was demonstrated. The data obtained were used to demonstrate the capabilities of the SolidWorks software as a recommended CAD system for further product design.

Summing up the consideration of the issue of the use of CM in ultralight class rockets based on the analyses carried out in the SolidWorks software, we can say that CM, in many cases, are the best replacement for traditional materials in the modern space industry, because:

- CM based on silicon fiber carbide and titanium matrix, with a lower weight and a greater margin of safety exceeds the performance of aluminum alloy 6063-T1;

- with the same input data, CM is on average stronger and lighter by almost 5 tons compared to the initial materials, which allows a reasonable increase in payload;
- nominal values of stress, deformation and displacement exceed, on average, by 98% compared to those used by aluminum alloy;
- the CM structure is not susceptible to destruction when mechanical loads are applied to the fairing at sufficiently high pressures arising from the influence of turbulent flows and other possible conditions, given that the loads were taken with a large margin to exclude other factors;
- the calculations carried out showed the prospects of using CM in the field of building spacecraft, both for experimental study of the technology of constructing structures from such materials, and for expanding the scope of application of CM and software "SolidWorks";
- based on the above results of the optimization of the product topologies, using all the data obtained, a calculation was carried out to optimize the mass-strength ratio. Thus, it was possible to reduce the specific thickness to 35 mm. Keeping all priority assigned loads.

According to the results of the study, two materials were used in the SolidWorks software in the form of "Aluminum alloy 6063-T1" and "Silicon fiber carbide and titanium matrix". The table below shows the minimum and maximum values of the analysis performed. The difference is visible in the stress graph, where the values of the composite material significantly exceed the alloy, as well as in other sections. A significant difference is shown in the mass column, almost 3 times the reduced mass will allow this device to be more aggressive and the ability to load a larger payload. Also, the graph of the ultimate strength indicates that the composite material has a large margin of safety compared to aluminum alloy. This proves that the use of CM is advisable to use for the replacement of the housing and non-supporting structures.

This software makes it possible to explore more complex designs to improve design and reduce factors for errors. Also, demonstration at the design stages of all possible design errors and improvements. Demonstrating the capabilities and skills of designing and operating this software allows you to better prepare future design engineers and designers.

7. References

- [1] Gusynin V. P. Aviation and space system "Pegasus". Review based on the materials of the open foreign seal for 1988-1896. 1. Project "Pegasus" // Space Science and technology. -1998. T4.,1/2.-c.113-119. <https://doi.org/10.15407/knit1998.01.113>.
- [2] Conference Paper, Development and modeling of intelligent control system of cruise missile based on fuzzy logic Utegen, A.S., Moldamurat, K., Ainur, M., ...Amandykuly, A.G., Brimzhanova, S.S. Proceedings - 2021 16th International Conference on Electronics Computer and Computation, ICECCO 2021, 2021.
- [3] 1.Gusynin V. P. Aviation and space system "Pegasus". Review based on the materials of the open foreign seal for 1988-1896. 1. Project "Pegasus" // Space Science and technology. -1998. T4.,2/3.-c.119-125. <https://doi.org/10.15407/knit1998.02.119>.
- [4] Gusynin V.P. The Pegasus Aerospace system. Review based on the materials of the open foreign press for 1988-1896. 3. Modification, flight tests and operation. // Cosmic science and Technology.-1998. T4.,(5).-c.148-155. <https://doi.org/10.15407/knit1998.05.148>.
- [5] Development of a software simulator for small satellite swarm control, Moldamurat, K., Utegen, A.S., Brimzhanova, S.S., Kalmanova, D.M., Yrskeldi, N.G. Proceedings - 2021 16th International Conference on Electronics Computer and Computation, ICECCO 2021, 2021.
- [6] Gunyaeva A.G., Kurnosov A.O., Gulyaev I.N. High-temperature polymer composite materials developed at FSUE "VIAM" for aerospace engineering: past, present, future (review). Electronic scientific journal "PROCEEDINGS of VIAM". dx.doi.org/10.18577/2307-6046-2021-0-1-43-53.

[7] Conference Paper, Hardware Implementation of Pseudo-Random Numbers on CPLD, Maidanov, A., Atanov, S., Tailak, B., Proceedings - 2021 16th International Conference on Electronics Computer and Computation, ICECCO 2021, 2021.

[8] Application of composite materials for aerospace objects.//Sereda A.G. Scientific hand. S.N.Fedoseev// Progressive technologies and economics in mechanical engineering: Proceedings of the VIII All-Russian Scientific and Practical Conference for students and students. April 6-8, 2017, Yurga-Tomsk: Изд.ТПУ, 2017-с.10-12. Conference.tpu-2017-с.57_p10-12, pdf.

[9] UDC 004.94:533.68 Tkachenko E.D. Determination of aerodynamic coefficients of a surface-to-air rocket by computational fluid dynamics methods in Solidwork flow simulation».

[10] Moldamurat Khuralay, Akhmejanov Sayat, Kariyeva Kamila, Omarov Zhanggir. Kalibekov Dias, Sayasat Nurbakytbek Design and optimization of the parameters of a hybrid unmanned aerial vehicle in the SolidWorks complex, In recognition of outstanding presentation on 2022 International Conference on Smart Information Systems and Technologies, 28-30 April 2022.

[11] Nurguzhin M.R., Yavorsky V.V. Computer modeling of systems. Karaganda: Proceedings of KarSTU, 2006. №3(24), с.74-86.

[12] Book Chapter, Computer modeling of residual stresses and strains at arc welding by modulated current, Nurguzhin, M., Danenova, G., Akhmetzhanov, T., Lecture Notes in Mechanical Engineering, 2019, 0(9783319956299), стр. 2453–2460.

[13] Conference Paper, Computer modeling of the stress-strain state of welded construction, Nurguzhin, M., Danenova, G., Akhmetzhanov, T., AIP Conference Proceedings, 2017, 1899, 060008.

[14] Article, Development of effective methods of stabilizing geometric parameters and increasing the load-carrying capacity of welded metal structures, Alter, I.M., Nurguzhin, M.R., Sagalevich, V.M., Nasyrov, G.Kh., Welding and Surfacing Reviews, 1997, 8(1), стр. 19–26.

Prototyping of Unmanned Aerial Vehicles Using Computer Software

Fariza Moldamurat¹, Tattigul Samuratova¹, Karlygash Otyzbayeva¹, Dastan Yergaliyev¹,
Olga Bizhanova², and Kamila Kariyeva¹

¹ L.N. Gumilyov Eurasian National University, Astana, Kazakhstan

² NPLC A. Baitursynov KRU, Kostanay, Kazakhstan

Abstract

This article discusses the methods of creating a drone against a drone using a computer program. The article provides a picture of the virtual programs used and the dimensions of the aircraft, as well as hardware and software systems and launch tests. CRITICISM: A 3D model of an unmanned aerial vehicle was developed, the effect of aerodynamic forces on the wings was calculated in a virtual program, and a special accurate compact model was obtained by studying the animation model of the aircraft. Then the program was written in a computer program with a microcontroller control software system. The frame of the unmanned aerial vehicle was prepared by hand: the written software code was transferred to the microcontroller, a special flight test of the complete aircraft was conducted in the field, the results of examinations and tests were discussed and the application environment was determined.

Keywords

Unmanned aerial vehicle; 3D modeling; microcontroller control system; prototype; aerodynamic forces; wing pattern; computer software complex; simulation

1. Introduction

In the process of training a model of unmanned aerial vehicles in the learning process in a set of computer programs - 3D modeling, sampling of the wings of the aircraft in question, programming of the microcontroller system in the development of the onboard system of the aircraft. When designing a drone, using 3 different virtual programs, we were able to see from simulation to animation and visualization 3D images, microcontroller programming and GPS flight of the aircraft on central control computers. The results obtained in the computer software were used in the manual assembly of a special aircraft. In the design of unmanned aerial vehicles, effective samples of the wings were obtained to determine the endurance and flight flexibility of the wings under the influence of aerodynamic forces and 3D modeling complexes. In addition, a prototype model of the aircraft was taken and special launch experiments were performed.

2. Obtaining a geometric model of the wings of an unmanned aerial vehicle

The cross section of an aircraft wing is the most important part of an aircraft. The cross-section of the wing of the aircraft consists of geometric parameters such as front edge, rear edge, maximum thickness, circumference (chord) and curvature [1]. The main part of the aircraft wing and the parameters of the aircraft will depend on the choice of its geometrically efficient model. The geometry of the wings depends on the following parameters: wing area-S, cover-I, chord -C, constriction- η , relative thickness-b we calculate the model of the wings of the aircraft [2, 3]. In a special virtual complex, as you can see in Figure 1 below, we modeled the arrow-shaped wings on the drone we wanted to make. The wings have been shown solely to give a sense of proportion and speed.

If the technical task requires good take-off and landing performance to achieve speed, the following

types of wing landing mechanisms should be used. These include the closed wing, the front wing and the fan wing. Closed wings can be simple, single-hole, and multi-hole, movable. Ventilation covers on small light aircraft are not used due to sudden changes in the aerodynamic properties of the wings when the wing lift is relatively low.

This is good for maneuvers such as lifting and braking, but increases the weight of the controls and is often unsuitable for operator control. The above are some examples of common wings in a virtual program.

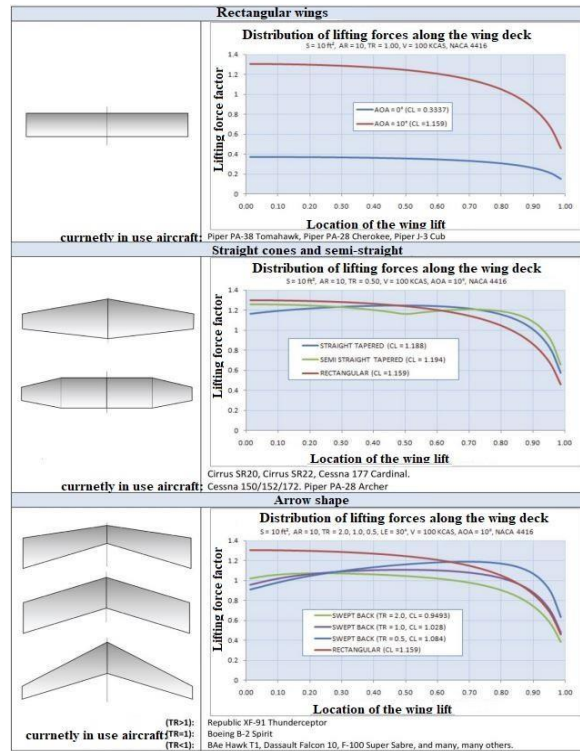


Figure 1: Parametric calculations of wing samples in a virtual program

2.1. Calculate the center of gravity

The center of gravity of the aircraft plays an important role in balancing the direct flight and maneuvering in the air. Flight models and small drones adjust the center of gravity to no more than 25% of the leading edge of the wing section. Because the center of gravity cannot find the most suitable location, there is a risk of increased efficiency, increased energy consumption, and loss of control.

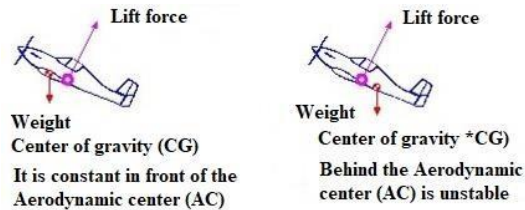


Figure 2: Gravity balancing center for unmanned aerial vehicles

The stability of the aircraft depends on its center of gravity and how far the stabilizer is from the main

wing. Many aircraft are unstable without a horizontal stabilizer [4, 5]. Asymmetrical aerodynamic surfaces have a sufficient lifting factor, but have the disadvantage of directing the tip of the plane downwards, which makes it statically unstable. Vertical stabilizers are required for sufficient stability. A symmetrical aerodynamic surface occurs during normal motion, and as a result of stability, the plane flies to the location you specify [6, 7].

The upward sloping wing has the right movement, stabilizes it and is used for flying wings (without vertical stabilizer). It is important that the center of gravity (CG) of the aircraft be in the correct position. This can lead to stable and manageable flight results. The center of gravity (CG) must be in front of the neutral point to ensure stability. The neutral point (NP) is the aerodynamic center (AC) of the entire aircraft.

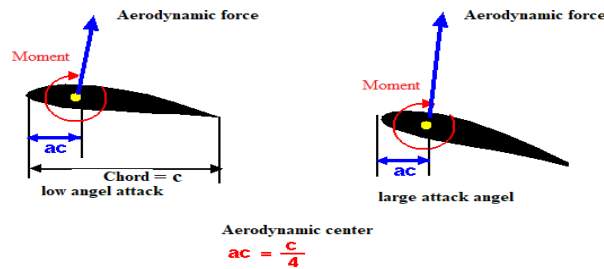


Figure 3: You can see that the torque and attack angles of the aerodynamic point and the aerodynamic center are not excavated

The angle of the body in the direction of flight affects its endurance, but if the angle of projection of the body and the angle of its direction is not large, the balancer has little effect. The tail is sensitive and unstable when a heavy aircraft lands at low speeds. The tip is that heavy planes rise from the ground and are difficult to reach, and when the control is lowered, the nose of the aircraft lowers. It also requires high speed to land safely. The angle between the wing strap and the 2 lines of the stabilizer is called the Longitudinal Dihedral (LD), otherwise known as the decalage. Velocity and altitude change as the LD angle increases and decreases [8,9,10].

At normal speed of sound, there is an aerodynamic force point at a distance $\frac{1}{4}$ from the front edge of the wing, and the aerodynamic moment does not change when the angle of attack changes. This has been proven experimentally and theoretically [11]. This position is called the wing aerodynamic center. (At high speed of sound, the wing has $\frac{1}{2}$ at the aerodynamic center point). For wings other than rectangles (triangular, trapezoidal, etc.), the Mean Aerodynamic Center (MAC) is the center of the wing. We need to find the average aerodynamic MAC center of all wing types.

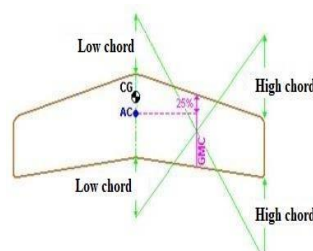


Figure 4: The center of gravity, as shown above, shows the location of the aerodynamic point of the wing of the aircraft in front of the AC 10% center of gravity CG

MAC is calculated mathematically [12, 13]. This calculation is called 'Geometric Mean Chord' GMC or 'Standard Mean Chord' SMC as shown in the figure below. For arrow-shaped wings, MAC differs from GMC, Taper ratio = Low chord / High chord.

Table 1

Parametric dimensions of the MAC model for arrow-shaped wings are given

Technical characteristics	Size
Chord - c	0.25 m
Cover - b	1.2 m
Wing area - S	0.3 m ²
Aspect Ratio - The ratio of the square of the wing to the area of the wing - AR	4.8
Lifting force factor - Cl	1.15
Attack angle - i_w	$10.25^0 = 0.263$ rad
Density - ρ	1,225 kg/m ³
Speed - V	16.58 m/s

2.2. Designing the wings of unmanned aerial vehicles

The first step is to make the surface of the wings and other static and analytical calculations to select the engine.

The second step is to combine the final calculations of the above elements and determine other parameters of the fan diameter relative to the engine power [14, 15].

The third step is to calculate the wings and determine the aerodynamic properties of the hull fasteners, cross-sections and surface sections. The fourth step is to determine the properties and dimensions of the horizontal stabilizer and perform calculations. The general design of the device was made using the following information. Depending on the role of unmanned aerial vehicles (UAV), it is necessary to determine whether it is stable or unstable and to obtain the exact dimensions required for the model. These include the position of the wings, the fuselage, the type of wings, the position of the center of gravity, and the general shape of the aircraft. When designing the model, it is necessary to theoretically study the stability that must be present in the aircraft and the direction of movement that occurs when the main control surface changes [16, 17, 18].

2.3. Simulation results in computer software complex ANSYS

Recent trends in research have led to a culture of analysis and inference using scientific methods using various computer simulation programs before the model was invented [19].

We observed the results of modeling an unmanned aerial vehicle (UAV) used to calculate pressure, flow dynamics and lift in the wing section. The simulation simplifies the design of unmanned aerial vehicles, taking into account the deformation of the body and the stiffness of the material [20].

Airflow was modeled and turbulent flow in the fuselage and wings was calculated. From the simulation results, it can be seen that the airflow is uniform and the turbulent flow is relatively small. This demonstrates the excellent aerodynamic properties of a UAV.

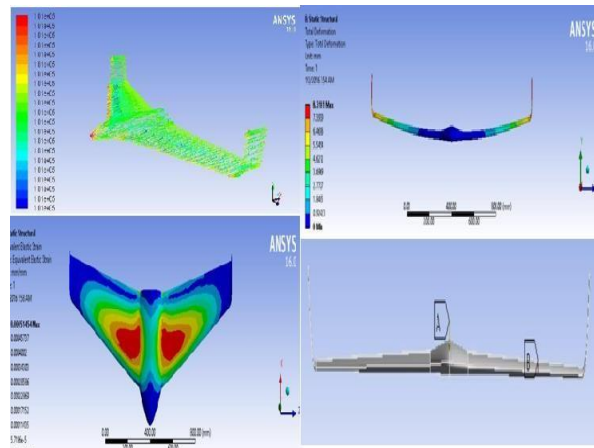


Figure 5: Results of the analysis of deformation and refraction in determining the effect of aerodynamic forces in the software complex simulation ANSYS

Deformation modeling was performed to see the most loaded part of the unmanned aerial vehicle [21, 22]. From the simulation, it can be seen that the maximum load on the wing unit is applied, so the wing lock must be good. When selecting a fan, the MAX determines the RPM value according to the following formula:

$$maxPRM = \frac{105000}{d} = 175000 \quad (1)$$



Figure 6: Trunk engine shaft and wings

Table 2

Parametric dimensions of the prototype model of unmanned aerial vehicles are shown

No	Name	Size
1	Diameter	20.32 mm
2	Edge	2
3	Width	6E
4	Weight	28.06 rp
5	Maximum turnovers	10335 RPM
6	Lifting force factor - CT	0.0687
7	Power factor – CP	0.0389

Unmanned aerial vehicle microcontroller system AutoDesk, we develop Tinkercard software and implement Arduino UNO microcontroller. We perform launch tests by connecting the drone to the central

control system [23].



Figure 7: Unmanned aerial vehicle prototyping and field launch and remote control

3. Conclusion

The results of the analysis of the design and launch of unmanned aerial vehicles, as well as remote control, determined the scope and environment of application. According to the results of the above virtual and realistic expert calculations and studies, the drone model is fully resistant to aerodynamic forces, and the wings of the manned aircraft model had high brittleness and flexibility, material density of the wings when maneuvering.

The Republic of Kazakhstan has developed a fully unmanned aerial vehicle model suitable for extreme climates. It can be used in cold temperatures - up to 25-45 0C and is designed with the need to maneuver in winds of 4-8 m / s. In order to determine the most commonly used unmanned aerial vehicle model in Solidworks software and computer software simulation ANSYS, AutoDesk, Tinkercard and Arduino UNO microcontrollers were developed.

4. References

- [1] S. Manas, B. Erdenebat. Travel in a short time without adding fuel ways to build capabilities in unmanned aerial vehicles. / Khurel Togoot 2010 / Ulaanbaatar 2010.
- [2] B. Erdenebat. Use of NNA and opportunities for its development in Mongolia. / Military reform /Ulaanbaatar 2010. E.Batzorigt, V.A. Lebiga. Problems and goals of application of unmanned low-sized aviation for national economy of Mongolia./ International conference on the methods of aerophysical research/ Novosibirsk Parallel 2010.
- [3] Yemelyev, A.K., Moldamurat, K., Seksenbaeva, R.B. Development and Implementation of Automated UAV Flight Algorithms for Inertial Navigation Systems, SIST 2021 - 2021 IEEE International Conference on Smart Information Systems and Technologies, 2021, 9465965.
- [4] Yergaliyev, D., Tulegulov, A., Zhumabayeva, A., Yussupov, A., Zhauyt, A. Study of stress-strain state of the roller conveyor Metalurgija, 2022, 61(2), pp. 347–350.
- [5] Atanov, S.K., Bigaliyeva, A.Z., Apachidy, N.K., Rusak, A.V. Process control issues of fine grinding in a planetary mill, Vestnik Sankt-Peterburgskogo Universiteta, Prikladnaya Matematika, Informatika, Protsessy Upravleniya, 2020, 16(3), pp. 277–292.
- [6] Bekmanova G., Ongarbayev Y. Somzhurek B. Mukatayev N. Personalized training model for

organizing blended and lifelong distance learning courses and its effectiveness in Higher Education // *Journal of Computing in Higher Education* (2021) 33:668–683.

[7] Kyzyrkanov, A.E., Atanov, S.K., Aljawarneh, S.A.R., Formation control and coordination of swarm robotic systems, *ACM International Conference Proceeding Series*, 2021, 3492704.

[8] Tomislav P., Krunoslav K., Danijel R., Alen B., Marin L., Vladimir M. and Mladen C. Cognitive Model of the Closed Environment of a Mobile Robot Based on Measurements // Basel, Switzerland – 2021.

[9] Akhmediya A. A., Moldamurat Kh., Mo Jamshidi., Brimzhanova S., Nabiyeu N., & Kismanova A. Application of Sentinel-1 SAR Data for Detecting a Nuclear Test Location in North Korea Application de données SAR de Sentinel-1 pour détecter un lieu d'essai nucléaire en Corée du Nord Received 17 Jul 2021, Accepted 28 Dec 2021, Published online: 13 Jan 2022.

[10] Moldamurat Kh, Mobile firefighting robot, patent for inventions - barcode No. 2332114. Reg. application number 2020/0819.1, dated November 26, 2020.

[11] Klyuev, S.V., Klyuev, A.V., Grishko, A.K., Trukhanov, S.V. Management of the design parameters in optimal design problems. *Materials Science Forum*, 2019, 974, pp. 723–728.

[12] Baimukhamedov M.F., Moldamurat K., Akgul M.K., Optimal control model of the automobile transport, *Transport Means - Proceedings of the International Conference*, 2019, 2019-October, pp. 1312–1316.

[13] Adilzhan K.K., Sabyrzhan A.K., Timur T.Z., The Usage of Extended Kalman Filter to Increase Navigation Accuracy of Mobile Units in Closed Spaces, *SIST 2021 - 2021 IEEE International Conference on Smart Information Systems and Technologies*, 2021, 9465903.

[14] Jiawen Y. Design and Optimization of Wing Structure for a Fixed-Wing Unmanned Aerial Vehicle (UAV) // *Modern Mechanical Engineering*, 2018, 8, 249-263.

[15] Kereyev, A.K., Atanov, S.K., Aman, K.P., Kulmagambetova, Z.K., Kulzhagarova, B.T., Navigation system based on bluetooth beacons: Implementation and experimental estimation, *Journal of Theoretical and Applied Information Technology*, 2020, 98(8), pp. 1187–1200.

[16] Moldamurat Kh., Utegen A.S., Brimzhanova S.S., Kalmanova D.M., Yrskeldi N. Development of a software simulator for small satellite swarm control, *The 16th International Conference on Electronics Computer and Computation (ICECCO 2021)*, <https://www.scopus.com/authid/detail.uri?authorId=57209971029>.

[17] Melnichuk, A., Kuzina, E.A., Yurkov, N.K. Conference Paper. Methods and means for countering unmanned aerial vehicles. *Proceedings - 2020 International Conference on Industrial Engineering, Applications and Manufacturing, ICIEAM 2020*, 2020, 9112082.

[18] Utegen A.S., Moldamurat Kh., Mukhanbetkaliyeva A.K., Talgat A., Anuar G., Brimzhanova S.S. Development and modeling of intelligent control system of cruise missile based on fuzzy logic, *The 16th International Conference on Electronics Computer and Computation (ICECCO 2021)* <https://www.scopus.com/authid/detail.uri?authorId=57209971029>.

[19] Karbetova, Z., Karbetova, S., Otyzbayeva, K., Daribayeva, A., Zhanakova, N. Competitive strategy priorities for insurance businesses in Kazakhstan // *Life Science Journal*, 2014, 11(9), pp. 57–65, 9.

[20] Karbetova, Z., Karbetova, S., Otyzbayeva, K., Dulatbekova, Z., Tastanbekova, K. Strategic priorities and challenges of environmental management in Kazakhstan // *Journal of Advanced Research in Law and Economics*, 2016, 7(5), pp. 1058–1065.

[21] Samuratova T.K., Kaliyeva Z.E., Makhanov., M., Yermekova Z.K. Energy efficient environment in architecture E3S *Web of Conferences*, 2019, 116, 00031.

[22] Brimzhanova, S., Atanov, S., Moldamurat, K., Brimzhanova, K., Seitmetova, A. An intelligent testing system development based on the shingle algorithm for assessing humanities students' academic achievements // *Education and Information Technologies*, 2022.

[23] Samuratova, T., Akhmetova, G. The symbolic image of the yurt in Kazakh applied arts // *Acta Histriae*, 2016, 24(2), pp. 427–450.

Development of a Computer Model of the Movement of a Vertical Launch Rocket

Dinara Kalmanova¹, Kamila Kariyeva¹, Nazerke Yryskeldi¹, Niyaz Belgibekov², and
Kanat Kazhibayev²

¹ Space Engineering and Technology, L.N Gumilyov Eurasian National University, Astana, Kazakhstan

² Department of military-technicians research and development work Project R&D centers Kazakhstan engineering,
Astana, Kazakhstan

Abstract

The article considered the movement of the rocket in the starting part of the trajectory. In the course of the work, motion parameters were studied and a calculation program was created. The generated program is used to ensure the passage of the aircraft's trajectory from initial violations and deviations, or to ensure the programmatic rotation (deviation) of the aircraft in the trajectory during Vertical Takeoff

Keywords

Mechanical system, trajectory, aerodynamic forces, ballistic missiles, vertical launch

1. Introduction

Ballistic missiles are launched vertically above the missile table. The purpose of control in the launch compartment is to maintain the missile's vertical position and not violate its trajectory's straightness. In contrast to guided flight, which, according to a certain law, provides for changes in trajectory parameters over a wide range, trajectory correction is used to ensure deviations of the trajectory of unmanned missiles from calculated missiles resulting from initial violations, aerodynamic asymmetry of the missile, or to ensure the software rotation (deviation) of the aircraft in the trajectory during vertical launches, often used in anti-aircraft missile complexes.

The article aims to describe mathematical and physical models of a vertically launched rocket. Preparation of a program for calculating the flight trajectory of the aircraft. This calculation program was solved for a rocket with a mass of 470 kg and 350 kg.

2. Forces acting on a guided missile

We consider the rocket as a mechanical system, that is, a set of masses contained in a volume limited by the outer surface of the hull, the plane of the output cross-section of the rocket rudders and the engine nozzle. When studying the movement of a rocket with its engine turned on, 3 groups of forces are considered. These are: reactive forces; mass forces; surface forces. As a result of the action of all these forces, acceleration occurs. At the same time, there is a concept of volumetric forces. Calculations of the flight trajectory indicated in the list of references were obtained [1]. These forces affect the entire volume of the rocket, that is, each point (molecule and Atom). As a result of the action of all these forces, acceleration occurs. At the same time, there is a concept of volumetric forces. These forces affect the entire volume of the rocket, i.e. each point (molecule and Atom).

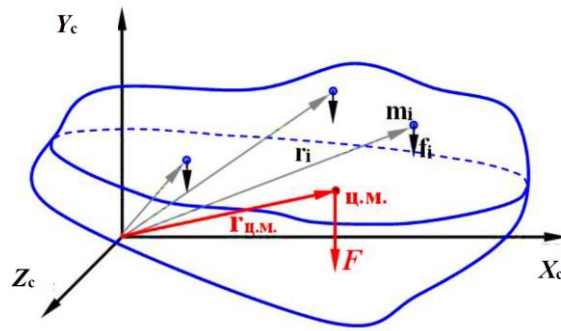


Figure 1: Location of the center of mass

The following are aerodynamic forces. They affect the rocket, as a rule, as three components. A description of the components of aerodynamic forces is obtained from the article in the list of references [2]:

Direct resistance force

$$X = c_x Sq \quad (1)$$

Lifting force:

$$Y = c_y Sq \quad (2)$$

Lateral force:

$$Z = c_z Sq \quad (3)$$

2.1. Starting part of the trajectory

There are two main parts of the trajectory: active and inactive. Figure 2 shows the active OcK and the inactive KC.

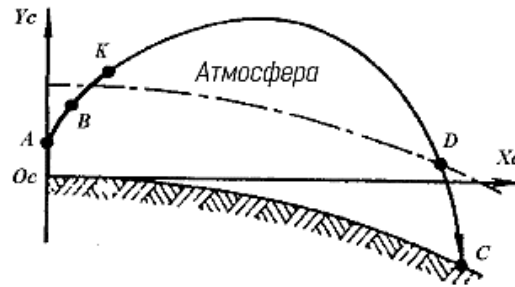


Figure 2: Flight trajectory of the rocket

Part of the trajectory we need is the active part. It breaks it down into smaller, more important parts. These are start (OcA), program turn (AB) and guidance parts (BK). Taken from the article in the list of references on the main parts of the trajectory [3].

Ballistic missiles are launched vertically above the missile table. The purpose of the control in the launch compartment is to maintain the vertical position of the rocket and not violate the straightness of its trajectory features of the trajectory of a vertical launch rocket are obtained in the article in the list of References [12].

There are reasons for choosing the vertical high launch method.

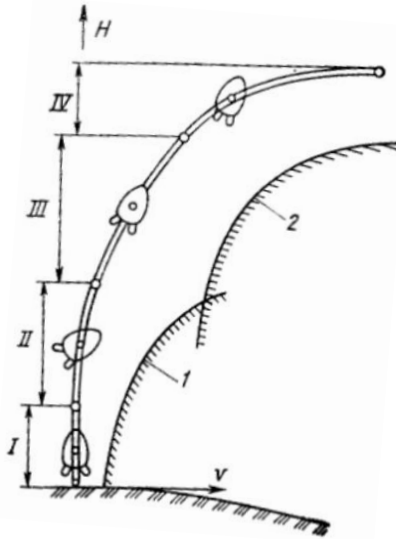
First, vertical launch allows the rocket to pass through the densest layers of the atmosphere at relatively

low speeds over short distances, which reduces the aerodynamic resistance and heating of the rocket. In addition, during vertical launch, the lateral movement of the rocket decreases, which can occur during inclined start-ups in the first seconds of flight. The advantages and disadvantages of inclined start are obtained in the article in the list of References [7].

Secondly, the vertical start of the rocket is mainly accompanied by axial loads on the structure, so the structure of the rocket does not have a large horizontal rigidity, and this helps to reduce its mass. The importance of fuel consumed on a vertical launch rocket in the article in the list of references is taken [10].

Third, it is simplified to design and manufacture a launch device that holds the rocket before launch only with the help of supports on the back.

Fourth, during an inclined start, a very powerful engine unit will be required, since the vertical component of the thrust force, being the supporting force, must be greater than the force of gravity acting on the rocket. Figure 3 shows the parts of the trajectory of the vertical launch of the trihu apparatus.



The 1-permissible speed limit in the coordinates of speed and altitude; 2-permissible heat flow limit

Figure 3: Parts of the trajectory of a vertical launch aircraft

In part I of the trajectory - in the vertical ascent part – the height is raised to a height of about 100 meters, which is necessary for maneuvering outside the starting unit. During the flight up to the speed of sound – in Part II – the curvature of the trajectory begins. It determines the movement of the active part of the aircraft in the atmospheric area in parts I-III. The speed limit reaches its maximum in Part III. Here the movement is carried out at a zero angle of attack. The description of the impact of the angle of attack on the trajectory is taken from the textbook in the list of References [4-6]. Although there are many requirements for the movement of the aircraft in the atmospheric area of the active part, the bending of the velocity vector θ and the bending of the attraction vector θ can be approximated by this dependence:

$$\theta \approx \mathcal{G} = \arcsin \mu \quad (4)$$

2.2. Turning methods

For the rocket to gain a certain altitude and enter orbit, it is necessary to make a programmatic turn. During the vertical launch, the rocket gains a speed of 30-40m/s. at this point, the angle of attack remains zero. at the time of t_1 , the program rotation begins.

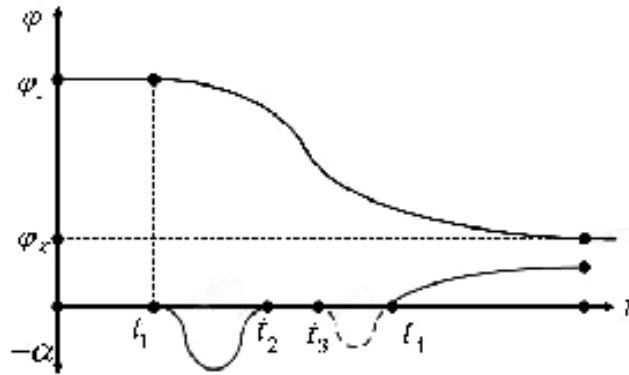


Figure 4: Change in the flywheel angle and tangage angle over time

In order to implement the program, turn, it is necessary to organize a negative value of the angle of attack. It leads to the emergence of normal forces. BL forces: component of the force of attraction and lifting force.

Component of the force of attraction:

$$P' = P \sin \alpha \quad (5)$$

Lifting force:

$$Y = C_y q S \quad (6)$$

where

q – speed pressure;

S – characteristic area;

C_y – aerodynamic coefficient.

2.3. Algorithm for calculating the trajectory of a vertical launch rocket

Let us divide the flight trajectory of the sign into 3 stages. This:

I – vertical launch part;

II – torque turning part;

III – part of the descent to the ballistic ground. It is shown in Figure 5.

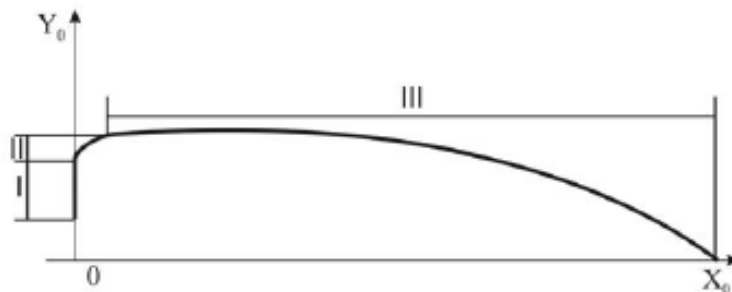


Figure 5: The trajectory of the aircraft's movement

In the active part of the trajectory, the rocket is affected by the force of attraction, aerodynamic force and gravity. The process of modeling forces was discussed in the article in the list of references [13]. The

force of attraction coincides with the velocity vector, and it is also directed indirectly along the trajectory. And the aerodynamic force is directed indirectly along the trajectory opposite to the velocity vector.

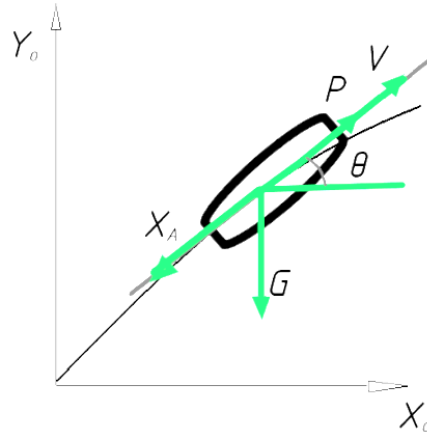


Figure 6: Force diagram in the ballistic part

It is necessary to obtain projections drawn on the axes of the moving earth coordinate system of forces.

$$\begin{aligned}\ddot{x} &= \frac{P}{m} \cos \theta - \frac{X_a}{m} \cos \theta, \\ \ddot{y} &= \frac{P}{m} \sin \theta - \frac{X_a}{m} \sin \theta - g.\end{aligned}\quad (7)$$

Where

\dot{x} - the derivative of the V_x speed obtained over time;

\dot{y} - the derivative of the V_y speed obtained over time;

P - traction force;

X_a - aerodynamic force;

θ - angle of inclination of the trajectory;

m - rocket mass.

Aerodynamic force:

$$X_a = C_x S q \quad (8)$$

C_x - is the coefficient of direct resistance force.

S - is the midline cross-sectional area. The midline section is the largest cross section of a body with a plane perpendicular to the direction of movement

q - speed ratio. Formula:

$$q = \frac{\rho V^2}{2} \quad (9)$$

where

V - speed:

$$V = \sqrt{V_x^2 + V_y^2} \quad (10)$$

ρ - air density:

$$\rho = \rho_0 H(y) \quad (11)$$

And the angle of inclination of the trajectory:

$$\theta = \arcsin \frac{V_y}{V} \quad (12)$$

The torque is determined by the following formulas:

$$\begin{aligned} \frac{dV}{dt} &= -\frac{X_a}{m} \cos \alpha - \frac{Y_a}{m} \sin \alpha - g \sin \alpha, \\ \frac{d\theta}{dt} &= -\frac{P_y}{mV} \cos \alpha + \frac{X_a}{mV} \sin \alpha - \frac{g}{V} \cos \alpha, \end{aligned} \quad (13)$$

Using these equations, the program is written in the Matlab program environment. In the next chapter, the results will be analyzed.

3. Creating a program in Matlab

A system of differential equations implemented in the MATLAB system:

$$\begin{aligned} \dot{V} &= \frac{(P - X_c) \cos \alpha - X_a - Y_c \sin \alpha}{m} - g \sin \theta; \\ \dot{\theta} &= \frac{(P - X_c) \sin \alpha + Y_a + Y_c \cos \alpha}{m \cdot V} - \frac{g \cos \theta}{V}; \\ \dot{x} &= V \cos \theta; \\ \dot{y} &= V \sin \theta; \end{aligned} \quad (14)$$

This system of differential equations is solved by the Runge-Kutta method.

The following values were used in the calculation:

$P = 7500$ N – engine traction force;

$r = 6356767$ m – Conditional radius of the Earth.

$Y_a = 28$ N – lifting force;

$Y_c = 5$ N;

$X_c = 15$ N;

$\dot{m} = 0.23$ kg/sec;

$\rho_0 = 1.29$ kg/m³;

$v_0 = 90^\circ$

$c_x = 0.07$.

Initial values:

$x_0 = 0$;

$y_0 = 0$;

$V_0 = 10$;

$\theta_0 = 90^\circ$.

3.1. Mathematical model of the computational process

The calculation process is stopped as soon as the angle of inclination of the trajectory reaches 25°. Methods of computer modeling and aerodynamic research are obtained in the article listed in the literature [8]. The program executed in the Matlab environment is provided in Appendix A. The calculation was made by the Runge-Kutta method. The program resulted in these graphs:

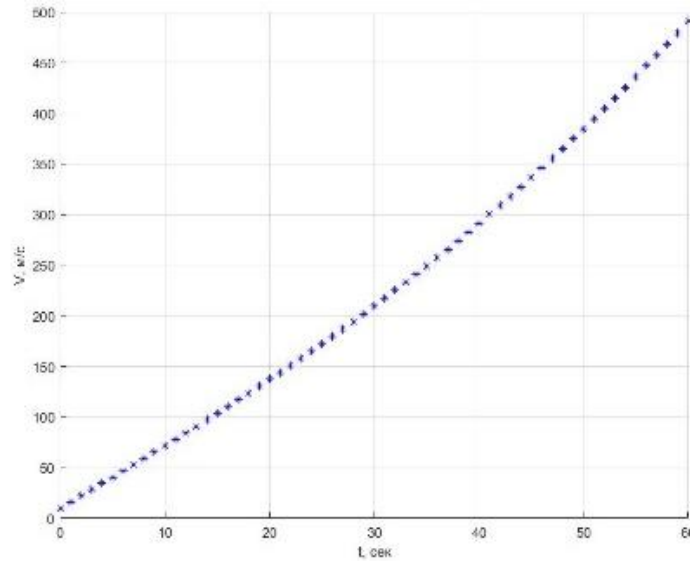


Figure 7: Change in the speed of the launch part of the rocket over time

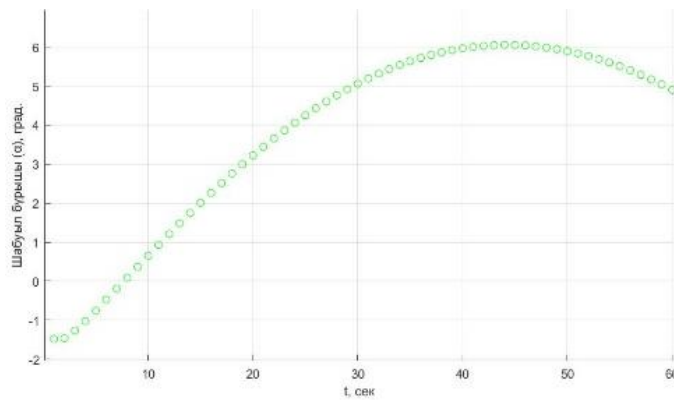


Figure 8: Changes in the angle of attack on the launch part of the missile over time

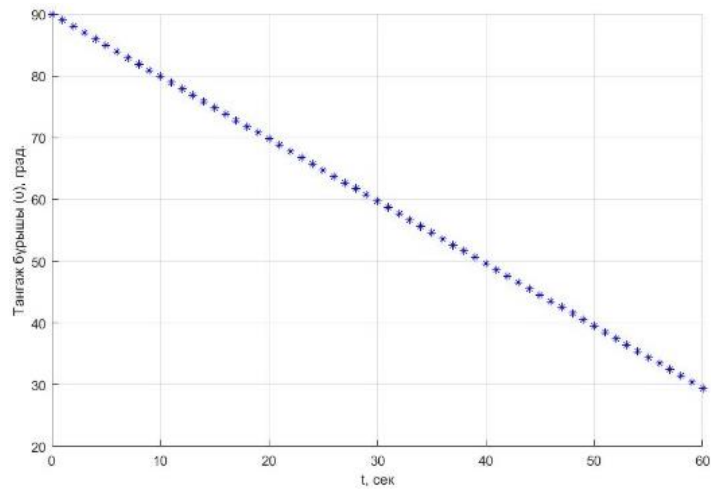


Figure 9: Change in the tangage angle in the launch compartment of the rocket over time

Lower graphs are constructed to see the degree of deviation:

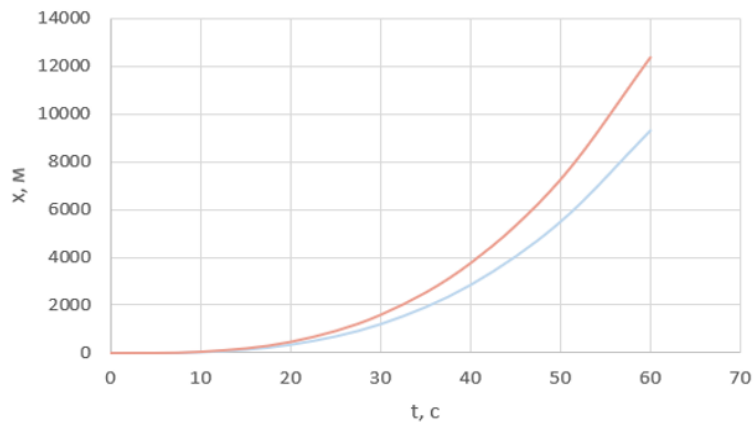


Figure 10: Change in the X coordinate of the rocket at different masses over time

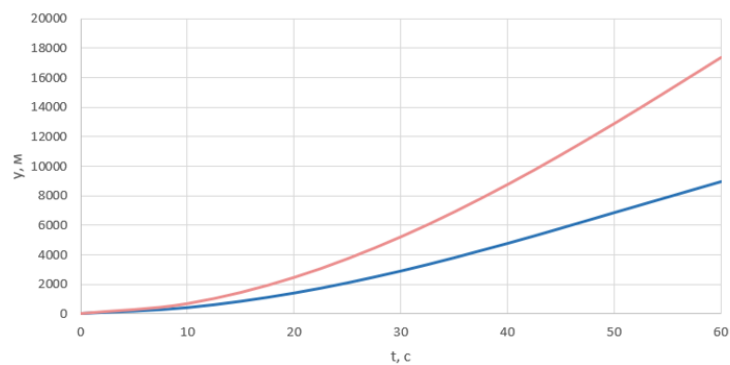


Figure 11: Change in time of the Y coordinate of the rocket's trajectory at different masses

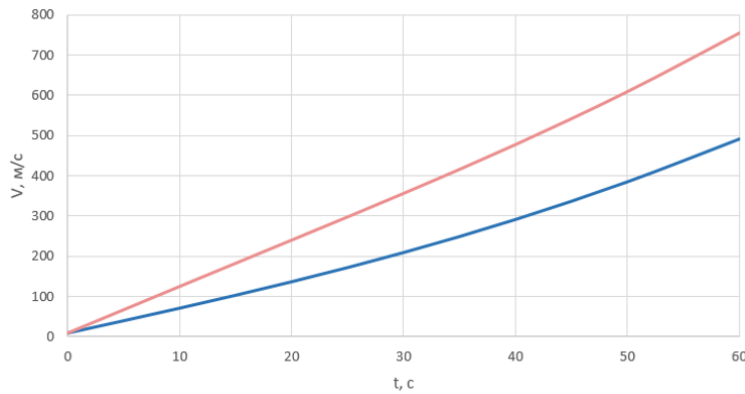


Figure 12: Changes in the speed of a rocket over time at different masses

These results prove that the mathematical model for calculating the motion parameters of a vertical launch rocket works correctly and systematically. The main methods of the simulation were obtained in the article in the list of References [11]. The program can be used to simulate various launch modes. At the same time, it can be used to design the operation of a rocket on a trajectory. Thus, the advantages of the vertical launch were noted.

1. Vertical launch allows the rocket to pass the densest layers of the atmosphere over short distances at relatively low speeds, which reduces the aerodynamic resistance and heating of the rocket.

2. During a vertical launch, the lateral movement of the rocket decreases, which can occur during an inclined start in the first seconds of flight. Possible errors were taken into account from the article in the list of references [14].

3. Vertical launch of the rocket is mainly accompanied by axial loads on the structure, so the structure of the rocket does not have a large horizontal rigidity, and this helps to reduce its mass. From the article taken from the list of references, coffee filters for verification errors were obtained [9]. The design and manufacture of the launch device, which holds the rocket before launch only with the help of supports on the back, is simplified.

The generated program is used to ensure the passage of the aircraft's trajectory from initial violations, and deviations, or to ensure the programmatic rotation (deviation) of the aircraft in the trajectory during Vertical Takeoff.

4. Conclusion

By introducing a system of differential equations describing the movement of an aircraft, a numerical solution program was written in the MATLAB software environment, and a rocket with a numerical calculation mass of 470 kg and 350 kg was taken as an example. But the prepared computer code can be used for any aircraft. It is only necessary to enter a particular aircraft's technical parameters and dimensions. We analyzed the changes in the parameters of the aircraft's movement V , θ , x and y over time with changes in air density, mass, and tangent angle. Comparing the two missiles, the results of such calculations were obtained:

- The change in the projection of the trajectory x , y over time makes a difference of 15% ;
- The change in velocity projection over time makes a difference of 11.5% ;
- Changing the angle of inclination of the trajectory over time creates a difference of 6.9% ;
- The tangent angle fluctuates by 2.5 times;
- The angle of attack varies by 1.2 times.

The prepared computer code can be used for any aircraft. It is only necessary to enter a particular aircraft's technical parameters and dimensions.

5. References

- [1] I.K. Romanova. "Flight trajectories of aircraft: a textbook" I. K. Romanova. — Moscow: Bauman Moscow State Technical University, 2017. — 149 p.
- [2] R.F. Appazov, O.G. Sytin. Methods of projecting trajectories of carriers and satellites of the Earth. — M.: Nauka, 1987. — 440 p.
- [3] S.V. Belov. A₃ and dynamics flight: school work / s. V. Belov, A. V. Gordienko, V. D. Proskurin. - Orenburg: Ogu, 2014. - 109 s. 4.
- [4] V. N. Kobelev. Fundamentals of rocket flight theory (lectures). – M., 2020 – 99c.
- [5] N. A. Testoedov. Design and construction of ballistic missiles and carrier rockets / N. A. Testoedov, Kolga, L. A. Semenova ; Sib. gos. aerospace. unt. Krasnoyarsk, 2014. 308 p.
- [6] V.V. Volotsuev, I.S. Tkachenko. Introduction to the design, construction and production of missiles: textbook. stipend. Samara: Publishing House of Samara University, 2017. 88 p.
- [7] H.M. Nguyen. "The influence of wind action on the dynamics of the movement of corrected ammunition" Bulletin of the Bauman Moscow State Technical University. Ser. Mashinostroenie. 2008. №3.
- [8] A.S. Utegen, K. Moldamurat, M. Ainur, A.G. Amandykuly, S.S. Brimzhanova. "Development and modeling of the intelligent control system of cruise missile based on fuzzy logic." Proceedings - 2021 16th International Conference on Electronics Computer and Computation, ICECCO 2021.
- [9] K. Moldamurat, A.S. Utegen, S.S. Brimzhanova, D.M. Kalmanova, N.G. Yrskeldi. "Development of a software simulator for small satellite swarm control." Proceedings - 2021 16th International Conference on Electronics Computer and Computation, ICECCO 2021, 2021.
- [10] A.S. Askarova, S.A. Bolegenova, V.Yu. Maximov, K.S. Baktybekov, A.B. Syzdykov. "Investigation of the different Reynolds numbers influence on the atomization and combustion processes of liquid fuel." Bulgarian Chemical Communications, 2018, 50, стр. 68–77.
- [11] K. Baktybekov, I. Vasil'eva. "The simulation of the interaction of dielectric materials with soft space radiation." European Space Agency, (Special Publication) ESA SP, 2003, (540), стр. 719–721.
- [12] A. Kyzrkanov, S. Atanov, S. Aljawarneh. "Coordination of movement of multiagent robotic systems." Proceedings - 2021 16th International Conference on Electronics Computer and Computation, ICECCO 2021.
- [13] A.K. Kereyev, S.K. Atanov, K.P. Aman, Z.K. Kulmagambetova, B.T. Kulzhagarova. "Navigation system based on Bluetooth beacons: Implementation and experimental estimation." Journal of Theoretical and Applied Information Technology, 2020, 98(8), pp. 1187–1200.
- [14] Kh. Moldamurat, K. Akhmetov, A. Otegen, S. Brimzhanova, K. Otyzbayeva, A. Zhiyenbek, Computer simulation of intelligent control systems for high-precision cruise missiles.
- [15] K. Moldamurat, S. Brimzhanova, B. Baizhumanova O. Bizhanova, K. Akhmetov, A. Moldamurat. Computer simulation of the path and control of an intelligent mobile robot in Python
- [16] K. Moldamurat, K. Akhmetov, A. Otegen, S. Brimzhanova, K. Otyzbayeva, A. Zhiyenbek. Computer simulation of intelligent control systems for high-precision cruise missiles.

Applying of the Developed Mathematical Methods and Models for the Diagnosis of Diseases of Internal Organs Using Statistical Data of People of Kazakhstan

Alua Myrzakerimova¹, and Mugulsum Nurmaganbetova²

¹International Information Technology University, Almaty, Kazakhstan

²Kazakh National Medical University named after S.D. Asfendiyarov, Almaty, Kazakhstan

Abstract

Sustainable and stable growth in the well-being of the population in Republic of Kazakhstan is the development of the healthcare industry – is one of the main priority. In Kazakhstan, the digitization of the healthcare system and the use of AI elements within the framework of the Digital Kazakhstan program were already underway [1]. Moreover, certain elements of AI have already been introduced and are working in the field of medicine, and some have just begun to be tested in the field of medicine. The object of the study is an automated system for diagnosing diseases of internal organs. The subjects of research are the methods and algorithms of the theory of decision making. Particularly, the study carried out have shown that for the differential diagnosis of benign and malignant gastric ulcers, a mathematical model, previously developed, is applicable, based on a decision-making method with qualitative and probabilistic uncertainty.

Keywords

IT in medicine, automated system for diagnosing diseases, theory of decision making, math modeling

1. Introduction

Nowadays, there is a global move from the treatment of consequences to a preventive health care system based on early diagnosing. Each medical protocol and history of the patient contains information that allows doctor to accurately diagnose and prescribe treatment. But sometimes unfortunately, even experienced treatment center does not always see the full picture of the disease, because the data in the medical documentation is not structured, and the medical history can be too large. Medicine is a very important part of the life of our entire society. Unfortunately, every day a person is in danger and associated with a threat to their fate. Most often, such cases are associated with a medical issue. In essence, all life is under some kind of protection by people in white coats. But the work for medical staff is equally important to properly building communication with patients.

Their performance is also affected by fatigue and, in some cases, lack of knowledge in narrow areas. Some diseases, for example, oncological ones, can be defeated if non-obvious symptoms are recognized in time and treatment is started. In Kazakhstan, the digitization of the healthcare system and the use of AI elements within the framework of the Digital Kazakhstan program were already in progress.

"Digital Kazakhstan" is very vital project which aims to improve the standard of living of every person [1]. Program has major goals, which are to accelerate the development of the economy of the Republic of Kazakhstan and improve the quality of life of the population, as well as to create conditions for the transition of the economy to a fundamentally new trajectory - the digital economy of the future [1].

Digitalization in the healthcare system of Kazakhstan has been going on since 2005. Today, since 2005, the information systems of the ministry have accumulated 14 terabytes of data, which is comparable to 5.8 billion pages of text. This is a significant amount of data that needs to be processed using Big-data technologies and artificial intelligence, which allows deep machine analysis of the problems and needs of the healthcare system [1].

In Kazakhstan, certain elements of AI have already been introduced and are working in the field of medicine, and some have just begun to be tested in the field of medicine. Moreover, both with global corporations and with domestic developers. According to on statistical data reports collected by the Ministry of Health of Kazakhstan from 2009 till 2020, namely “Statistical digest” Health of the population of the Republic of Kazakhstan and the activities of healthcare”, there was an estimated 18 million people [3]. Data reported by rate per 100 000 populations per year. The bar chart below represents how data has changed over two years’ period among main regions of Republic of Kazakhstan (see Fig. 1).

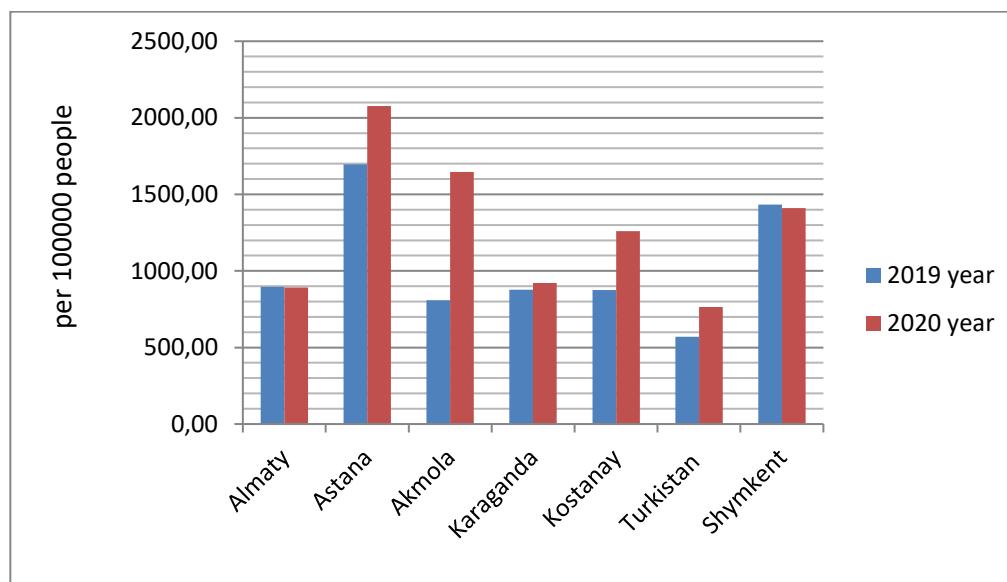


Figure 1: Rate of illnesses of internal organs in Kazakhstan by region

There is a rate (average number of people) per 100 000 person for all regions about all diseases among country. By the graph it is visible that in Astana region general incidence rate is highest, and the trend is increasing for 11%. The lowest average number of people seems to be in Shymkent and Almaty region and trend is relatively stable compared with others. Regarding to the bar graph sharpest tendency observed in Kostanay region, for the two years increased for 18%. It might show the epidemic of some kind of disease during this period.

2. Role of IT in medicine

It has been proved that the use of IT in the tasks of medical diagnostics can reduce the examination time. When making a diagnosis, the doctor has to process a large array of biomedical information: examination data, individual characteristics of each patient (past diseases, hereditary reactions). Along with this, the increasing increase in the information load leads to physical and psychological fatigue of the doctor, an error in the choice and implementation of treatment and diagnosis [4]. However, it is known that making an accurate diagnosis at an earlier stage of the development of the disease and initiating treatment of the disease will help to avoid complications that can harm the body. Therefore, today there is a tendency of increasing the number of developed diagnostic medical automated systems.

Most of the existing modern systems are narrowly focused. In this regard, the development of an easily customizable system aimed at improving the accuracy and efficiency of obtaining a diagnostic solution is relevant and in demand in the modern medical technology market.

The object of the study is an automated system for diagnosing diseases of internal organs. The subjects

of research are the methods and algorithms of the theory of decision making. The aim of the work is to improve the accuracy and efficiency of diagnosing a patient using an automated system for medical diagnosis of diseases of internal organs. Due to the processing of a large amount of medical biological information processed by the system according to algorithms and methods based on decision theory. More specifically, the purpose of this article is

- Application of developed mathematical methods and models for diagnosing diseases of internal organs;
- Formulation of the problem of medical diagnosing;
- Determine the requirements for methods of constructing models for describing the object of diagnostics of execution, which will ensure the achievement of objectivity and accuracy of decisions made;
- An approach to building a system based on a patient's health state model and a diagnostic model was formulated using a multilevel model for describing all possible diseases of the patient.

It should be noted that in practice, the diagnosis significantly depends on taking into account the coherent features of the patient's health status. While most intelligent diagnostic systems are focused on the "average" patient. Informative variables for the formation of a model of the patient's state of health suggest taking two variables[2]:

- Patient's medical records;
- Questioning the patient in order to identify their individual characteristics.

Recent years, the use of electronic patient records in hospitals has been actively developing in the Republic of Kazakhstan. Thanks to such records, the time for generating data is significantly reduced [5].

2.1. Features of medical diagnosing

Human - is a complex organism in which many processes take place. According to the International Classification of Diseases [2], over 20,000 diseases and over a million symptoms are currently identified. Symptoms characterize a particular disease. Therefore, it is very important that modern diagnostic systems can work with a large data set. And moreover, they gave the correct solution to the task of diagnosing diseases.

Furthermore, diagnosing and making a correct diagnosis is a complex process even for the most experienced doctor. Many different factors must be taken into account:

- External symptoms body temperature, pressure, coughs, etc.;
- Complete examination in the form of X-ray tomography analyzes, etc.;
- It is also important to take into account previous diseases, genetically transmitted diseases;
- Blood type and heredity.

Taking into account the above will allow achieving a more accurate result. Therefore, the patient's recovery period will be much reduced and additional harm to the body caused by improper treatment will not be caused. The diagnostic object is characterized by a large set of properties (symptoms). This leads to the fact that the object has to be considered as a complex system [3].

We can distinguish the following main properties, specific for complex systems:

1. The system consists of subsystems;
2. Data diversity. Data can be quantitative, fuzzy, interval, etc.;
3. Some parameters are not available for measurement or evaluation;
4. The structure of the system is multi-connected (many-to-many connection);
5. The constant impact of the environment leads to the fact that the state of the object is constantly

changing.

Based on the analysis above, it can be concluded that the main problem of medical diagnostics is to achieve the accuracy of the diagnosis. As well as reducing the time and material costs of the patient. And give the doctor better tools, for example, a system for diagnosing diseases. One of the most effective ways

to solve problems is the create algorithm for the process.

Algorithm for determining the most probable state of the patient according to a given symptoms:

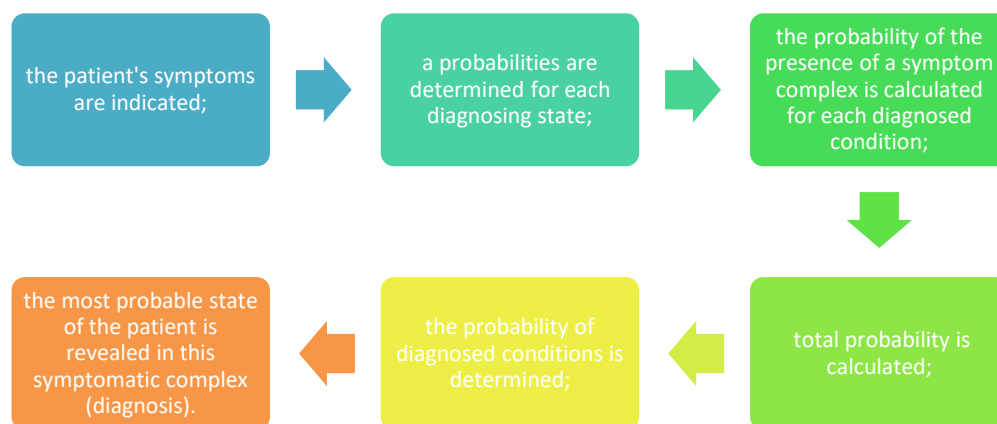


Figure 2: Algorithm for the process

3. Differential diagnosis of benign and malignant gastric ulcer using a mathematical method

The studies carried out have shown that for the differential diagnosis of benign and malignant gastric ulcers, a mathematical model, previously developed, is applicable, based on a decision-making method with qualitative and probabilistic uncertainty [6]. Let's consider the differential diagnosis of benign and malignant gastric ulcers. There is a diagnostic table [6] indicating signs and corresponding qualitative descriptions of utilities (weight) regarding the listed diseases.

Let's consider two cases: Case 1

The patient has constant aching pain, aggravated by eating. The patient turned gray and lost a lot of weight. His anemia progresses, Gregersen's reaction is observed, the acidity of gastric juice is reduced.

Furthermore, apply the developed mathematical model of diagnosis, based on the methods of fuzzy set theory, to diagnose these diseases, which will correspond to the problem of finding the optimal alternative.

Supposably, we have many alternatives (diseases):

$$A = \{A_1, A_2, \dots, A_m\},$$

belonging to the same nosological class. The selection of the optimal alternative (diagnosis) depends on the weight of the symptoms (utility), presented as a matrix for possible conditions and different alternatives (diseases).

Using the diagnostic table [6], we compile a utility matrix for the listed diseases. Utilities are presented qualitatively: often (Ч), rarely (Р), extremely rarely(KP), and therefore it is advisable to apply the mathematical method of decision making with qualitative and probabilistic uncertainty.

$$U = \left\{ \begin{array}{l} X1, X2, X3, X4, X5, X6, X7, X8, X9, X10, X11, X12, X13, X14, \\ A1 KP, B., B, X, .P, X, B, P, P, KP, KP, KP, X., X \\ A2 B, KP, C, P, X, .P., C, Ч., X, ОЧ, ОЧ, X, KP, P \end{array} \right\}$$

Linguistic criteria are represented as a fuzzy set:

$$Ч\{0,5/9;1.0/10\}; P\{0,5/6;1.0/7;0.5/8\}; KP\{0,5/2;1.0/1\};$$

The index, which accounts for the maximum degree of membership, is set by the expert. Matrix is being formed

$$U = \begin{pmatrix} u_{11} & \dots & u_{1n} \\ u_{21} & \dots & u_{2n} \\ \dots & & \dots \\ u_{m1} & \dots & u_{mn} \end{pmatrix}$$

elements are $\tilde{U}_{ij} = \bigcup_k \mu_{u_{ij}}(u_k) / u_k$, where $u_k = \mu \sim (x_k)$, represented as a fuzzy set. Then it is consisting of fuzzy subsets:

$$\mu_{u_i} \sim (u_k) / u_k = [\mu(u_i) / u_i] / [\mu_{u_k}(u_i) / u_i]. \quad (1)$$

Set u_i simplify as follows:

$$\mu_{u_i} \sim (u_k) = \min [\mu_x(x_k), \mu_{u_{ik}}(u_i)] \quad (2)$$

Minimization leads to reduced risk of misdiagnosis.

Set \tilde{U}_{io} , which is found as the intersection of the sets: U_{im} и U_i and $\mu_{z_{io}} \sim (u_k) = \min_{z_{im}} \{ \mu_{z_{im}}(u_k); \mu_{z_i}(u_k) \}$ allows you to subtract the best alternative, which means a probable disease with these symptoms:

$$A^* = \mu_{A_o} \sim (a_o) = \max_{A_o} \mu_{A_o} \sim (a_i) \quad (3)$$

$$\text{where } \mu_{A_o} \sim (a_i) = \max_{u_{io}} \mu_{u_{io}} \sim (u_k)$$

There are two variants:

- Fuzzy features and clear state (diagnosis is based on one known factor);
- Fuzzy features and unclear state (observed symptoms is taken into account).

Then, there is clear state:

$$x_j = \in X$$

Let the state be known: X3 (pain is constant).

Let's diagnosing correctly (choosing the best alternative). Let's find fuzzy utilities for a given state:

$$U_1=[B]=\{0.5/3; 1.0/4; 0.5/5\};$$

$$U_2=[C] =\{0.5/9; 1.0/10\};$$

$$u_{\max} = \sup Y, \text{ where } Y = S(U_1) \cup S(U_2) = \{3, 4, 5, 9, 10\}; \quad u_{\max} = 10;$$

The maximizing set will be respectively:

$$U_{1m} = \{3:10/3; 4:10/4; 5:10/5\} = \{0.3/3; 0.4/4; 0.5/5\};$$

$$U_{2m} = \{0.9/9; 1.0/10\}.$$

And the optimizing set can be found as:

$$U_{1o} = \{\min(0.5, 0.3)/3; \min(1.0, 0.4)/4; \min(0.5, 0.5)/5\} = \{0.3/3; 0.4/4; 0.5/5\};$$

$$U_{2o} = \{0.5/9; 1.0/10\},$$

then the set defining the best alternative:

$$\mu \sim(A1) = \max(0.3, 0.4, 0.5) = 0.5;$$

$$\mu \sim(A2) = \max(0.5, 1.0) = 1.0,$$

$$A(*) = \max(0.5, 1.0) = 1.0(A2).$$

Diagnosis: in this condition, the most likely disease is a malignant stomach ulcer.

Consider the *second* variant, namely:

- the state of the system is given by a *fuzzy* set

$$X = \bigcup_k \mu \sim (Xk) / Xk$$

The state of the system is imprecisely specified and, moreover, the utilities are imprecisely defined. Inaccurate condition means: the severity of diagnostic signs may be different, which is more consistent with reality. So, the patient's condition, listed above, is represented by the following set:

$$\{0.7 / X3; 0.5/X5; 0.7/X7; 0.6/X9; 0.5/X10; 0.7/X11; 0.5/X12\}$$

The severity of symptoms is set and should correspond to the real condition of the patient at the moment. And the fuzzy utilities of the alternatives for a given state are taken from the matrix compiled on the basis of statistical data. Taking into account the utility, we find for various alternatives (diseases):

$$\tilde{U}_{ij} = \bigcup_k \mu_{u_{ij}}(u_k) / u_k, \text{ where } u_k = \mu \sim (x_k)$$

$$\text{and } u_{\max} = \sup Y, \text{ where } Y = S(U_1) \cup S(U_2) = \{3, 4, 5, 9, 10\}; \quad u_{\max} = 10;$$

Let's present the set with fuzzy utilities for the given state:

$$U_1 = \{0.7 / B; 0.5/P; 0.7/B; 0.6/P; 0.5/KP; 0.7/KP; 0.5/K. \} = \{0.9 / B; 0.8/P; 0.85/KK\};$$

$$U_2 = \{0.7 / C; 0.5/X. 0.7/C. 0.6/X. 0.5/O.5 0.7/O.7 0.5/X\} = \{0.9 / C; 0.9/X.9/X;/OO\};$$

then,

$$U_1 = \{0.9/[0.5/3; 1.0/4; 0.5/5]; 0.8/[0.5/1; 1.0/2; 0.5/3]; 0.85/[0.5/2; 1.0/1]\} = \\ \{0.75/3; 0.5/4; 0.5/5; 0.9/2; 0.9/1\};$$

$$U_2 = \{0.9/[0.5/9; 1.0/10]; 0.9/[0.5/8; 1.0/9; 0.5/10]; 0.85/[0.5/6; 1.0/7; 0.5/8]\} = \\ \{0.95/9; 0.95/10; 0.75/8; 0.5/6; 0.85/7\};$$

$$U_{1m} = \{3 : 10/3; 4 : 10/4; 5 : 10/5; 2 : 10/2; 1 : 10/1\};$$

$$U_{2m} = \{0.9/9; 1.0/10; 0.8/8; 0.6/6; 0.7/7\};$$

Finding an optimizing set

$$U_{1o} = \{0.3/3; 0.4/4; 0.5/5; 0.2/2; 0.1/1\};$$

$$U_{2o} = \{0.9/9; 0.95/10; 0.75/8; 0.5/6; 0.7/7\};$$

Finally

$$\mu \sim(A1) = \max (0.3, 0.4, 0.5, 0.2, 0.1) = 0.5;$$

$$\mu \sim(A2) = \max (0.9, 0.95, 0.75, 0.5, 0.7) = 0.95$$

$$A (*) = \max (0.5, 0.95) = 0.95(A2).$$

Diagnosis: in this condition, the most likely disease is a malignant stomach ulcer.

Let's consider second case: Case 2

Anamnesis: the patient is quite old, long (more than 2 years). There is local pain in the epigastria on palpation (Mendel's symptom), appetite is normal, and fluoroscopic studies of the stomach showed that the "beggar" has the correct shape.

Again, there are two variants might be:

- clear state;
- fuzzy features and unclear state.

$$x_j = \in X$$

Let the state be known: X4 (local tenderness in the epigastria during palpation). Using the data of the diagnostic table for diseases of the digestive system, we will make a diagnosis. Let's find fuzzy utilities for a given state:

$$U 1=[X] = \{0.5/8; 1.0/9; 0.5/10\};$$

$$U 2=[P] = \{0.5/1; 1.0/2; 0.5/3\};$$

$$u_{max} = \sup Y, \text{ where } Y = S(U 1) \cup S(U 2); \quad u_{max} = 10;$$

The maximizing set will be respectively:

$$U1m = \{8:10/8; 9:10/9; 10:10/10\} = \{0.8/8; 0.9/9; 1.0/10\};$$

$$U2m = \{0.1/1; 0.2/2; 0.3/3\}.$$

And the optimizing set can be found as:

$$U1o = \{\min (0.5, 0.8)/8; \min (1.0, 0.9)/9; \min (0.5, 1.0)/10\} = \{0.5/8; 0.9/9; 0.5/10\};$$

$$U2o = \{0.1/1; 0.2/2; 0.3/3\},$$

Finally:

$$\mu \sim(A1) = \max (0.5, 0.9, 0.5) = 0.9;$$

$$\mu \sim(A2) = \max (0.1, 0.2, 0.3) = 0.3,$$

$$A (*) = \max (0.9, 0.3) = 0.9(A1).$$

Diagnosis: in this condition, the most likely disease is a benign stomach ulcer, which corresponds to the conclusions of experts.

Now, let's consider second variant of the second case:

Fuzzy features: $X = \bigcup_k \mu \sim (Xk) / Xk$, which corresponds: the state of the system is not precisely specified (the severity of diagnostic features is different for the corresponding patient) and, in addition, the utilities are not precisely defined. So, the patient's condition, listed above, is represented by the following set

$$\{0.5 / X1; 0.7/X2; 0.8/X4; 0.9/X6; 0.3/X7; 0.2/X10; 0.9/X13\}$$

The severity of the symptoms is given and corresponds to the patient's condition, and the fuzzy utility of the alternatives for this condition are taken from the diagnostic table [6].

$$\tilde{U}_{ij} = \bigcup_k \mu_{u_{ij}}(u_k) / u_k, \text{ where } u_k = \mu \sim (x_k)$$

Let's present the set with fuzzy utilities for the given state:

$$U_1 = \{0.8 / X; 0.9/X; 0.3/B; 0.2/KP; 0.9/X; 0.5/KP; 0.7/B\} = \\ \{0.99 / X; 0.75/B; 0.6/KP\}; \\ U_2 = \{0.8 / P; 0.9 / P; 0.3 / X; 0.2 / O\mathcal{C}; 0.9 / KP; 0.5 / B; 0.7 / KP\} = \\ \{0.98 / P; 0.3/X. 0.5/B. 0.2/O.2 0.7/K. \}$$

then,

$$U_1^* = \{0.99/[0.5/8;1.0/9;0.5/10]; 0.75/[0.5/3;1.0/4;0.5/5]; 0.6/[0.5/2;1.0/1]\} = \\ \{0.5/8; 0.99/9; 0.5/10; 0.5/3; 0.75/4; 0.5/5; 0.5/2; 0.6/1\}; \\ U_2^* = \left\{ \begin{array}{l} 0.98/[0.5/1;1.0/2;0.5/3]; 0.3/[0.5/8;1.0/9;0.5/10]; 0.5/[0.5/3;1.0/4;0.5/5]; \\ 0.2/[0.5/6;1.0/7;0.5/8]; 0.7/[0.5/2;1.0/1] \end{array} \right\} = \\ \left\{ \begin{array}{l} 0.5/1; 0.98/2; 0.5/3; 0.3/8; 0.3/9; 0.3/10; 0.5/3; 0.5/4; 0.5/5; \\ 0.2/6; 0.2/7; 0.2/8; 0.5/2; 0.7/1 \end{array} \right\};$$

$$u_{\max} = \sup Y, \text{ where } Y = S(U_1) \cup S(U_2) = \{3,4,5,9,10\}; u_{\max} = 10;$$

$$U_{1m} = \{8 : 10/8; 9 : 10/9; 10 : 10/10; 3 : 10/3; 4 : 10/4; 5 : 10/5; 2 : 10/2\} = \\ \{0.8/8; 0.9/9; 1.0/10; 0.3/3; 0.4/4; 0.5/5; 0.2/2; 0.1/1\}$$

$$U_{2m} = \left\{ \begin{array}{l} 0.1/1; 0.2/2; 0.3/3; 0.8/8; 0.9/9; 0.1/10; 0.3/3; 0.4/4; \\ 0.5/5; 0.6/6; 0.7/7; 0.8/8; 0.2/2; 0.1/1 \end{array} \right\};$$

Finding an optimizing set

$$U_{1o} = \{0.5/8; 0.9/9; 0.5/10; 0.3/3; 0.4/4; 0.5/5; 0.2/2; 0.1/1\}; \\ U_{2o} = \left\{ \begin{array}{l} 0.1/1; 0.2/2; 0.3/3; 0.3/8; 0.3/9; 0.1/10; 0.3/3. 0.4/4; \\ 0/5/5; 0.2/6; 0/2/7; 0/2/8; 0.2/2; 0.1/1 \end{array} \right\};$$

Then,

$$\mu \sim (A1) = \max (0.5, 0.9, 0.5, 0.3, 0.4, 0.5, 0.2, 0.1) = 0.9;$$

$$\mu \sim (A2) = \max (0.5, 0.2, 0.1) = 0.5$$

$$A (*) = \max (0.5, 0.9) = 0.9(A1).$$

Diagnosis: in this condition, the most likely disease is a benign stomach ulcer, which corresponds to the conclusions of experts.

The following Table 1 represent the results of computations.

Table 1
 Result of computations

Cases	Anamnesis	Diagnosis
Case 1 variant 1	The patient has constant aching pain, aggravated by eating. The patient turned gray and lost a lot of weight. His anemia progresses, Gregersen's reaction is observed, the acidity of gastric juice is reduced	a malignant stomach ulcer
Case 1 variant 2	The patient has constant aching pain, aggravated by eating. The patient turned gray and lost a lot of weight. His anemia progresses, Gregersen's reaction is observed, the acidity of gastric juice is reduced	malignant stomach ulcer
Case 2 variant 1	Anamnesis: the patient is quite old, long (more than 2 years). There is local pain in the epigastria on palpation (Mendel's symptom), appetite is normal, and fluoroscopic studies of the stomach showed that the "beggar" has the correct shape	benign stomach ulcer
Case 2 variant 2	Anamnesis: the patient is quite old, long (more than 2 years). There is local pain in the epigastria on palpation (Mendel's symptom), appetite is normal, and fluoroscopic studies of the stomach showed that the "beggar" has the correct shape	benign stomach ulcer

According to the table above, it can be concluded that the main advantage of making a diagnosis using a mathematical model is its objectivity, which can eliminate over diagnosis during the initial patient 'survey [6]. As can be seen from the results obtained, it follows that the severity of symptoms (the state of the system) affects the diagnosis (the most likely disease in a given symptoms). Such combinations of the severity of symptoms are also possible, when the symptoms characteristic of both disease of case 1 and disease of case 2 are pronounced. As a result, we obtain the probabilities of the disease listed above, the same in value.

3.1. Current diseases diagnosing methods

The process of diagnosing a disease is the process of obtaining, processing and analyzing various types of information about a patient. The following steps can be distinguished in the diagnostic process:

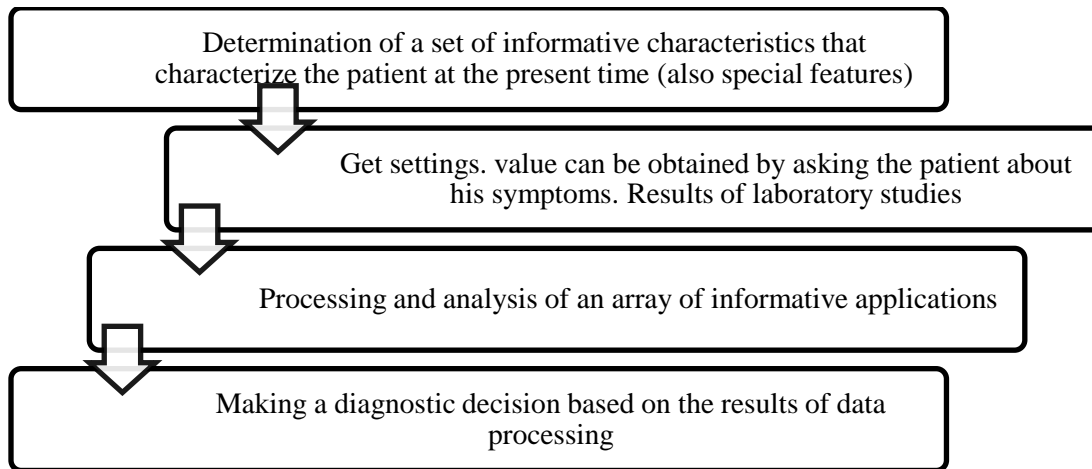


Figure 3: Diagnosing steps

The main problem is the third and fourth stages, illustrated on Figure 3, because:

- Not enough outgoing data to analyze the object;
- Difficulty in processing a large amount of data.

Processing such data can take a long time. And an automated diagnostic system can solve this problem. Specialists need to take into account indications and contraindications, patient characteristics, known cases of diseases. To work effectively, you need to process an avalanche of information. Automation of all part of these tasks can truly save resources and improve the quality of services. Also the development of such a system helps to solve the problem with a shortage of medical workers. A district hospital doctor may not have sufficient expertise or experience to determine at an early stage oncology or ischemic stroke, digital technologies will help him make the correct primary diagnosis and make a decision on the urgent referral of the patient to a specialized medical institution. Tasks that should be solved during project are:

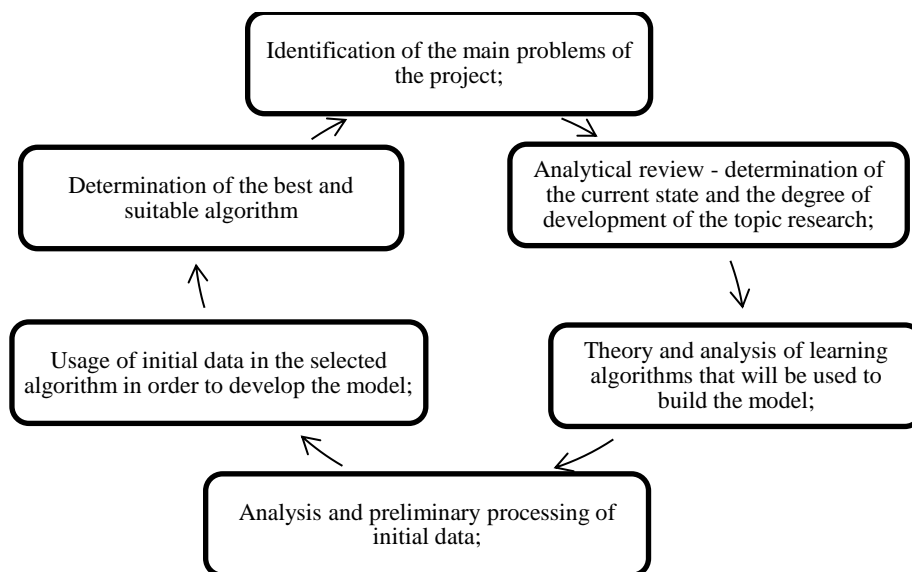


Figure 4: Tasks

Moreover, the Figure 4 illustrates the tasks to analyze and study materials on modern medicine, choose actual field in healthcare sphere. Second task is to make analytical review researches related to automated diagnosing systems, which are in world and in Kazakhstan. Third task is to study the algorithms and methods used for current topic. The fourth task is to create dataset in order to use in developing model. The fifth task is to develop a several models for diagnosing and prediction of disease using mathematical methods. The sixth task is to choose the best and suitable model, then create user interface, which will integrate with created model.

4. Conclusion

Finally, it can be argued that new technologies make it possible to quickly analyze huge amounts of information on a specific task, on the basis of which make predictions and issue recommendations to doctors. AI is especially in demand in the field of diagnostics this kind of innovation frees people from routine processes. A computer assistant, for example, can help a doctor analyze visual information. Differential diagnosis of diseases of the digestive system is based on the available diagnostic tables [6], which contain modern data on the etiology and pathogenesis of diseases of the internal organs. Timely nosological diagnosis is facilitated by the correct choice of approaches leading to the solution of the problem. One of these approaches is the use of mathematical methods of diagnostics, leading to objective decision-making. To analyze the existing symptoms, as well as laboratory and instrumental data, allows modern automated information technology diagnostic systems, based on the developed mathematical models. People should always concern about early diagnosis and prompt treatment as it is fundamental to control and need to be available wherever an epidemic occurs. In this paper, mathematical method proves to be one of the methods that could be used to estimate the relative risk of disease. Nevertheless, further research must be done to improve the current method.

5. References

- [1] Digital Kazakhstan. 2018 URL:<https://digitalkz.kz/o-programme>.
- [2] E.P. Balogh, T.B. Miller, The National Academies of Sciences. Improving Diagnosis in HealthCare. Washington: National Academies Press (2015).
- [3] E.K. Kaidar, A. Kenesova, G. Sabyrov. "Statistical digest Health of the population of the Republic of Kazakhstan", (2009-2017) available: <http://www.rcrz.kz/index.php/ru/statistika-zdravookhraneniya-2> p 43-59.
- [4] A.B. Myrzakerimova, M.O. Nurmaganbetova, K.S. Duisebekova. "Modeling the decision making process for automated system for diagnosing diseases of internal organs." GLOBAL SCIENCE AND INNOVATIONS 2019: CENTRAL ASIA № 2(3).
- [5] Healthcare Development State Program of the Republic of Kazakhstan available: http://www.dsm.gov.kz/en/pages/densaulyk-healthcare-development-state-program-republic-kazakhstan-2016-2019?theme_version=mobile.
- [6] M.O. Nurmaganbetova. Mathematical methods in medicine (2012)- Germany, Lambert Academic-Publishing.
- [7] K. Suzuki, Y. Chen. "Artificial Intelligence in Decision Support Systems for Diagnosis in Medical Imaging." Springer International Publishing (2018).
- [8] A.B. Myrzakerimova, M.O. Nurmaganbetova. "Information Technology in Medical Research." III International conference « Digital technologies in science and industry - 2017», Kazakhstan, Almaty, 19-20 may 2017, p.522-524.
- [9] A.B. Myrzakerimova, M.O. Nurmaganbetova, K.S. Duisebekova, M. Shaizat. "Forecasting risk of diseases in Kazakhstan with using mapping technique based on 9 years statistics." The 11th International Conference on Ambient Systems, Networks and Technologies (ANT) April 6-9, 2020, Warsaw, Poland.

Modelling of a Filter-Compensating Device with a Controlled Reactor Compensator

Oleksandr Zhuk¹, Serhii Trybulkevich¹, Dmytro Zhuk¹, and Volodymyr Ryabenskij¹

¹ National University of Shipbuilding n.a. Admiral Makarov, Mykolaiv, Ukraine

Abstract

Improvement directions of the adjustable power line conditioners (APLC) intended for an autonomous electric power system (EPS) with semiconductor converters (SC), which contains a resonant LC filter (RF) and a reactor compensator (RC) with pulse width regulation (PWR) are considered. The conditions for alignment the frequency characteristics of electric power systems with the spectra of harmonics generated in the power network by both semiconductor converters and reactor compensators are defined. The possibility and expediency of using the proposed improved structure of the controllable filter-compensating device, in which the main reactor filter is also interference-proof in relation to the reactor compensator with pulse-width regulation, have been proven. Theoretical conclusions are confirmed by a model experiment.

Keywords

Controlled filter compensating device, reactor compensator with pulse-width control, non-sinusoidal coefficient, model experiment.

1. Introduction

1.1. The problem of electric power quality in the autonomous electric power systems

The problem of electric power quality assurance and electromagnetic compatibility in autonomous electric power systems (EPS) in modern marine vessels and platforms is very relevant in connection with use of powerful semiconductor converters (SC) on them as part of electric propulsion systems, propulsion devices and various technological electric drives. In such power systems the decrease of electric power quality is due to two reasons: presence of higher harmonics in consumption current and main harmonic of this current phase shift relative to the mains voltage.

The development of effective adjustable power line conditioners (APLC) for autonomous (ship) electric power systems with SC is associated with specific, often contradictory requirements, fulfillment: reactive power compensation accuracy in statics and dynamics, high speed, higher harmonics effective reduction in a wide frequency range to limit non-sinusoidal coefficients of network voltage and consumption current, minimum number of adjustable circuits.

The task is complicated by the fact that modern active or hybrid adjustable power line conditioners themselves are sources of higher harmonics, due to the presence of semiconductor switches in their composition [1,2,3,4,5,6].

Ensuring power quality and conditions of electromagnetic compatibility by improving adjustable power line conditioners structure and control principles, by using a high-speed reactor compensator (RC) and also by matching electric power systems frequency characteristics with harmonics spectra generated by both SC and RC.

1.2. Research tasks and objectives

1. Power unit improved structures construction principles development and high-speed adjustable power line conditioners control methods substantiation.
2. Electric power systems equivalent resistances frequency characteristics analysis and current harmonics, which are generated by SC and RC, reduction coefficient analysis, with adjustable power line conditioners different versions. Harmonics resonant increase exclusion conditions determination.
3. Analysis results and practical recommendations verification by means of a model experiment.

2. The autonomous electric power system structure with SC and APLC

An autonomous electric power system with SC and adjustable power line conditioner generalized scheme is shown in Fig. 1, a. The generator (supply network) is represented by a sinusoidal EMF with an amplitude and short-circuit resistance, a transformer or an input reactor SC – by resistance. The adjustable power line conditioners include a resonant series LC filter (RF) consisting of resistances X_{L0} , X_{C0} and a reactor compensator conditionally indicated by an adjustable equivalent resistance at the fundamental harmonic X_{RCE} .

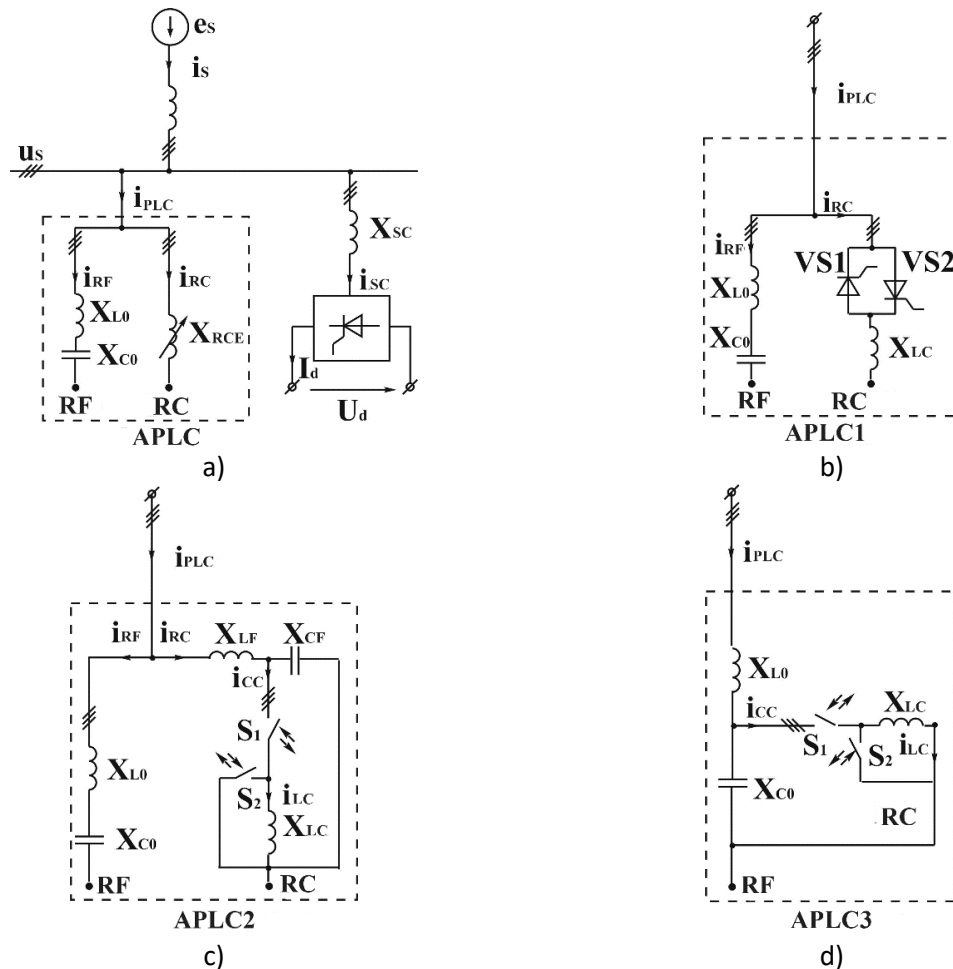


Figure 1: The autonomous electric power system structure with SC and APLC: a) generalized scheme; b) APLC1 – with RC phase control; c) APLC2 – with RC pulse-width regulation and its own anti-interference filter; d) APLC3 – with RC pulse-width regulation and RF use as an anti-interference filter

RF tuning frequency order corresponds to zero of the system frequency characteristics and is selected from the condition $v_{RF0} = \omega_{RF0} / \omega = \sqrt{X_{C0} / X_{L0}} = p - 1$, where ω_{RF0} – the filter resonance frequency, ω – the network frequency, and p – SC pulsation.

Reducing higher harmonics, RF is simultaneously a reactive power generator at fundamental harmonic $Q_{RF} = 3U_{ph}^2 / (X_{C0} - X_{P0})$, where U_{ph} – effective value of the phase voltage of the network ($U_{ph} \approx E_m / \sqrt{2}$).

RC consumes reactive power $Q_{RC} = 3U_{ph}^2 / X_{RCE}$. The RC scheme with phase regulation on the basis of counter-parallel connected single-operation thyristors (APCL in Fig. 1, b) was widely used [4]. The main disadvantages of this scheme are low-frequency harmonics generation in the input network, as well as a significant regulation delay time, which is half of the network period $T/2 = \pi/\omega$.

The listed shortcomings are limited to the high-speed reactor compensator with pulse-width regulation (PWR) at high frequency (Fig. 1, c, d).

The three-phase reactor compensator with a semiconductor pulse-width regulator based on alternating current keys main structures are shown in Fig. 2.a,b. Thanks to connectedness properties of three-phase circuits without a neutral wire, simplification is achieved in these schemes compared to the direct combination of single-phase regulators. For example, four and five keys are used instead of six in the diagrams in Fig. 2a, b, respectively. Semiconductor alternating current switches made on the basis of transistors and diodes are presented in Fig. 2, c, d. Two-operation thyristors can be used instead of transistors. The key version in Fig. 2, c is preferable, as it contains a smaller number of controllable elements.

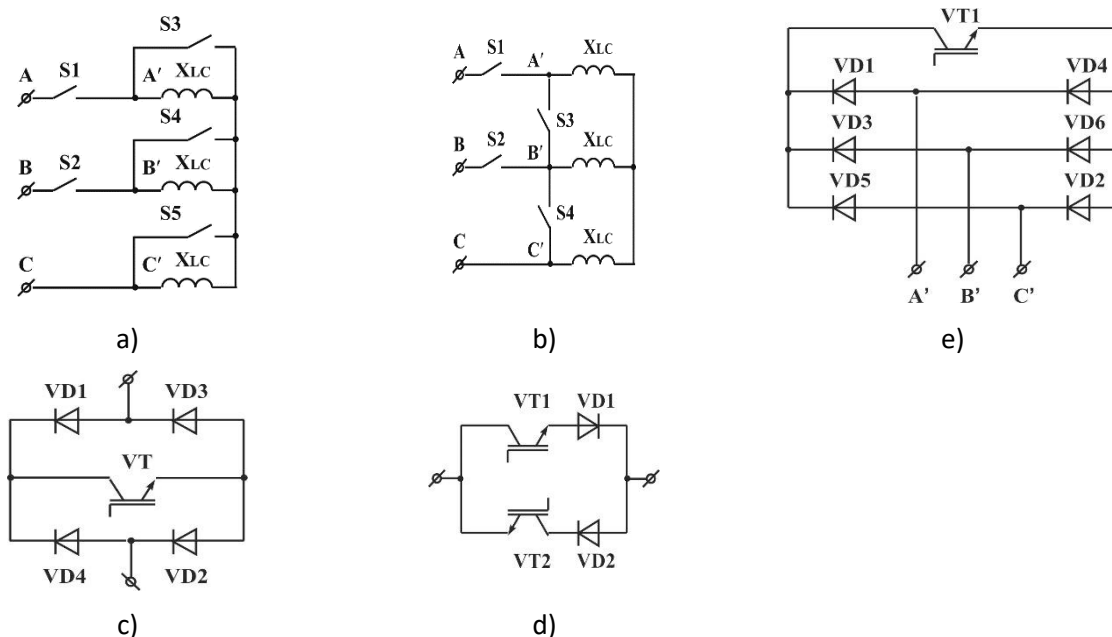


Figure 2: Three-phase RC with a semiconductor PWR: a, b – RC basic structures, c, d – alternating current semiconductor switches, e – short circuit on one direct current semiconductor switch

Switches S1 and S2, periodically switched at the same time, connect the reactor X_{LC} to the three-phase voltage during the time interval t_1 . Switches S3, S4, and S5 are switch on only when S1 and S2 are switch off and serve to short the reactor phases for a time t_2 . Thus, the PWR commutation period $T_C = t_1 + t_2$. RC

inductance control is carried out by changing the conductive state relative time of the keys S1, S2 (duty cycle) $\gamma = (t_1 + t_2)/T_C$. During the pulse-width regulator operation, there is a periodic alternation the reactor connecting modes to three-phase voltage the and the modes of its three-phase short circuit. Variable RC phase equivalent resistance $X_{RCE} = X_{LC} / \gamma^2$.

In contrast to Fig. 2a, in the diagram in Fig. 2b, instead of shorting the reactor phases with three parallel switches, interphase shorting with two switches S3 and S4 is used.

In the diagram in Fig. 2, b, instead of two AC switches S3 and S4, a short-circuit breaker with one DC switch, shown in Fig. 2, d, can be used.

Fig. 3 shows a modified three-phase RC circuit with PWR. Here, the serial switches made on transistors and diodes connected in opposite parallel. The current and voltage forms in phases of the regulators made according to the schemes of Fig. 2, a, b and Fig. 3 are the same and are presented in Fig. 4.

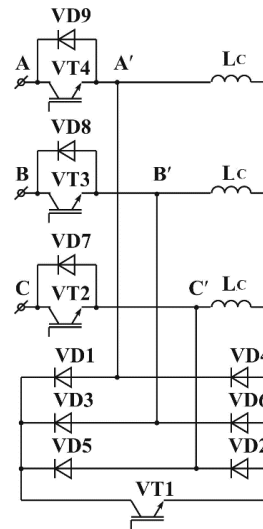


Figure 3: Modified scheme three-phase RC with PWR

So that the phase currents and voltages of system with RC and PWR do not contain constant components, it is necessary to ensure the switching frequency $f_\kappa = 1/T_\kappa = n_\kappa \omega / 2\pi$, where $n_\kappa = 6k$, $k = 1, 2, 3, \dots$. Under these conditions, in steady states, the voltage and current curves will be periodic, and their spectra have a discrete character. For modern power modules based on IGBT keys, the switching frequency can reach 20 kHz.

Each branch of the RC with a serial switch in relation to the external circuit is a source of pulsed quasi-sinusoidal current. These current higher harmonics (interference) have orders of $\nu = kn_\kappa \pm 1$, where $k = 1, 2, 3, \dots$. RMS values of these harmonics.

$$I_{CC(\nu)} = \frac{2\sqrt{2}\gamma U_{ph} \sin \nu\pi\gamma}{X_{LC} \nu\pi} \quad (1)$$

To protect supply network from HF interference created by the PWR, it is possible to include an L-shaped low-frequency anti-interference filter (LFF) formed by elements X_{LF}, X_{CF} (Fig. 1c) at the input of the RC.

It is recommended to choose $X_{LF} \ll X_{LC}$ (for example $X_{LF} = 0,05X_{LC}$). The value X_{CF} is selected from the ensuring the necessary filtration coefficient condition, which shows how many times the final

interference amplitude in the composition of the compensator phase current i_{PC} at the switching frequency is less than the initial one in the current composition i_{CC} .

Filtration coefficient

$$K_F \approx (2\pi f_K)^2 / \omega_{IF0}^2, \quad (2)$$

where $\omega_{IF0} = \sqrt{1/(L_F C_F)}$ – own resonant frequency of anti-interference filter. Therefore,

$$X_{CF} < n_k^2 X_{LF}. \quad (3)$$

It follows from (3) that, for example, when $K_F = 100$, $\omega_{IF0} \approx 0,1\omega_K = 0,1(2\pi f_C)$.

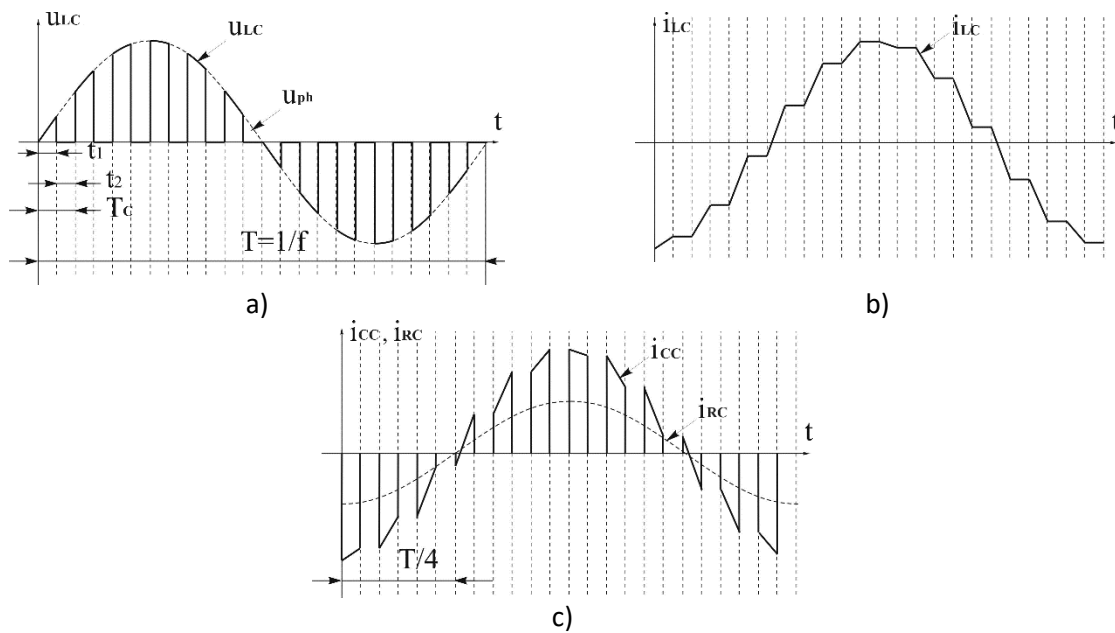


Figure 4: RC with PWR phase voltages and currents time diagrams : a) voltage on the reactor u_{LC} ; b) reactor current i_{LC} ; c) series switch branch current i_{CC} and the input phase current of the RC i_{RC}

When choosing a sufficiently high switching frequency ($f_C \approx 20$ kHz), in contrast to the power resonance filter included in the PKU, the RC anti-interference filter is "light" [7].

Due to the anti-interference filter presence, the RC input current i_{RC} has an almost sinusoidal shape. Its RMS value

$$I_{RC} = I_{CC(1)} = \gamma^2 U_{ph} / X_{LC}. \quad (4)$$

RC reactive power consumption

$$Q_{RC} = 3U_{ph} I_{RC} = 3\gamma^2 U_{\Phi}^2 / X_{LC}. \quad (5)$$

RF parameters are selected based on two conditions: limiting the supply voltage non-sinusoidal nature and SC reactive power compensation. The condition for full reactive power compensation for any SC-APLC system mode is the ratio

$$Q_{RF} - Q_{RC} - Q_{SC} = 0. \quad (6)$$

Here and further, we will assume that a thyristor converter (TC) is considered as a SC. Reactive power consumed by SC

$$Q_{SC} \approx I_d \sqrt{U_{d0}^2 - U_d^2}, \quad (7)$$

where U_{d0} is the maximum rectified voltage corresponding to the control angle $\alpha = 0^\circ$; U_d, I_d – current values of rectified voltage and current.

If the rectified current is equal to the nominal ($I_d = I_{dnom}$) in the entire regulation range of the SC, then Q_{SC} takes the maximum value at the minimum value $U_d = U_{dmin}$ corresponding to the maximum control angle α_{max} :

$$Q_{SCmax} \approx I_{dnom} \sqrt{U_{d0}^2 - U_{dmin}^2}. \quad (8)$$

In this case, the necessary RF and RC reactive powers are determined from the ratio

$$Q_{RFmax} = Q_{RCmax} = Q_{SCmax}. \quad (9)$$

In accordance with [8,9,10], it is necessary to determine the system voltage non-sinusoidal coefficient value K_{US} with the APLC parameters found in (9). It may turn out that condition (9), necessary for reactive power compensation, will be insufficient to limit K_{US} , i.e. to compensate for the distortion power. In this case, at the next stage of the calculation, the initial values will assumed

$$Q'_{RFmax} = Q'_{RCmax} = Q_{SCmax} + \Delta Q, \quad (10)$$

where ΔQ is the step of iteration.

The final RF and RC parameters selected values must ensure the limitation of the non-sinusoidal system voltage coefficient in the most intense mode at the permissible level, i.e. the condition must be met

$$K_{USmax} \leq K_{USlim}. \quad (11)$$

In order to develop recommendations for the APLC schematic solution as part of autonomous electric power systems with SC, it is necessary to consider the system's resistances frequency characteristics [11,12,13,14,15].

Proceeding from the superimposition principle, it is advisable to perform an equivalent circuits analysis of system with APLC2 for higher harmonics brought to the inputs of SC and RC, which are shown as higher harmonics currents sources I_{SCv} and I_{RCv} (Fig. 5, a, c). The corresponding equivalent reactive resistances frequency characteristics are determined from the expressions

$$X_{ESCv} = (((vX_S)^{-1} + (vX_{L0} - vX_{C0}/v)^{-1} + (vX_{LF} + ((vX_{RCE})^{-1} - v/X_{CF})^{-1})^{-1})^{-1}, \quad (12)$$

$$X_{ERCv} = (((vX_S)^{-1} + (vX_{L0} - vX_{C0}/v)^{-1})^{-1} + vX_{LF})^{-1} - v/X_{CF})^{-1}. \quad (13)$$

The frequency characteristics have zeros and poles corresponding to voltage and current resonance modes. It is of interest to determine poles frequencies order at which an undesirable higher harmonic generated by the source's resonance increase is possible.

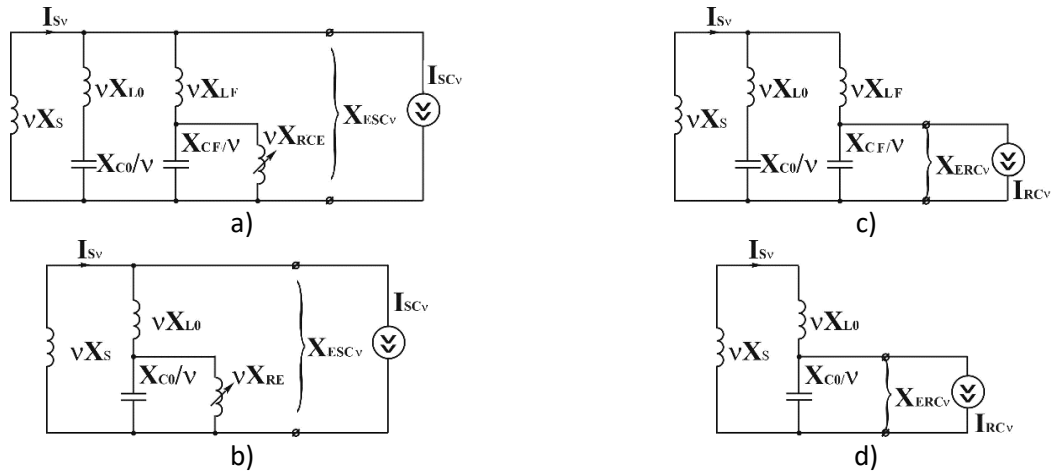


Figure 5: System SG-SC-APLC equivalent replacing schemes, given respectively to the SC and RC inputs: a, c – for the system with ALCC2; b, d – for system with APLC3

The analysis shows that frequencies order of two poles μ_1 and μ_2 , which each of the characteristics has X_{ESCv} and X_{ERCv} , turn out to be the same and weakly depend on the RC equivalent resistance value. When $X_{RCE} = \infty$ they are defined as positive real roots of biquadratic equation

$$Av^4 + Bv^2 + C = 0, \quad (14)$$

Where

$$\begin{aligned} A &= X_{L0}X_{LF} + X_S X_{LF} + X_S X_{L0}, \\ B &= X_{L0}X_{CF} + X_{C0}X_{LF} + X_S X_{CF} + X_S X_{C0}, \\ C &= X_{C0}X_{CF}. \end{aligned}$$

Consequently

$$\mu_1 = ((B - (B^2 - 4AC)^{1/2}) / 2A)^{1/2}, \quad (15)$$

$$\mu_2 = ((B + (B^2 - 4AC)^{1/2}) / 2A)^{1/2}. \quad (16)$$

On the basis of (15) and (16) it is possible to establish that

$$\mu_1 < \nu_{RF0}; \nu_{RF0} < \mu_2 < \nu_{RF0}, \quad (17)$$

where $\nu_{IF0} = \omega_{IF0} / \omega$.

The smallest higher harmonics generated by SC and RC orders are respectively equal

$$\nu_{SCmin} = p - 1 \text{ и } \nu_{RCmin} = n_\kappa - 1. \quad (18)$$

In order to exclude the resonant harmonics, increase in the system the following matching the frequency characteristics of the equivalent resistors with the spectra of SC and RC harmonic condition must be fulfilled.

$$(\mu_1 \& \mu_2) < (\nu_{I\min} \& \nu_{K\min}). \quad (19)$$

It is not difficult to make sure that for the system with APLC2 (Fig. 1, c), this condition is almost always not observed in relation to SC harmonics. For example, at $p=6$ and $n_k = 396$ ($f_k = 19800$ Hz) in accordance with (20) $\nu_{SC\min} = 5$ and $\nu_{RC\min} = 395$. The orders of RF and IF tuning frequencies are made $\nu_{RF0} = 5$ and $\nu_{IF0} \leq 0, \nu_{k\min} = 39$ in accordance with the above.

At the same time, according to (19), $\mu_1 < 5$ and $5 < \mu_2 < 39$. Thus, the separate "light" anti-interference filter for RC use creates an additional system frequency characteristic pole, the order of which is $\mu_2 > \nu_{SC\min}$. Therefore, in the APLC2 scheme, presented in Fig. 1, c and providing effective reduction of high-frequency harmonics generated by RC, conditions arise for resonant increase of relatively low-frequency harmonics generated by SC. The specified shortcoming can be eliminated using an improved the APLC3 scheme (Fig. 1, d), in which the RC is connected directly to the RF at the connection point X_{L0} and X_{C0} . With such a schematic solution, the RF with the tuning frequency order $\nu_{RF0} = \nu_{SC\min}$ the simultaneously performs two functions: a power resonant system filter in relation to the SC and an L-shaped low-pass filter in relation to the RF.

Thus, the additional second pole of system resistance frequency characteristics and the resonant harmonics increase are excluded, as well as the simplification of the APLC is achieved. The frequency characteristics of the system equivalent reactive resistances with the improved APLC3 relative to the SC and RC are determined in accordance with the substitution schemes (Fig. 5, b, d) from the expressions

$$X_{ESC} = ((\nu X_S)^{-1} + (\nu X_{L0} - ((\nu X_{RFE})^{-1} - \nu / X_{C0})^{-1})^{-1})^{-1}, \quad (20)$$

$$X_{ERFV} = ((\nu(X_S + X_{L0}))^{-1} - \nu / X_{C0})^{-1}. \quad (21)$$

Additional analysis shows that when switching from APLC2 to APLC3 and unchanged RF parameters, based on the full reactive power compensation condition, the value X_{LC} should be reduced by $\nu_{RF0}^2 / (\nu_{RF0}^2 - 1)$ times (by 4%). At the same time, the order of the zero frequency of the system resistance characteristic increases compared to ν_{RF0} by $\sqrt{1 + 1/\nu_{RF0}^2}$ times (by 2%), which practically does not affect the higher harmonics reduction efficiency. Therefore, the APLC2 main parameters determining method described above is also applicable for APLC3.

Using the obtained frequency characteristics expressions X_{ESCv} , X_{ERCv} – (12), (13) and (20), (21), it is possible to determine the SC and RC currents harmonic reduction coefficients frequency dependences of the systems with the investigated APLC:

$$K_{ISCv} = I_{SCv} / I_{Sv} = |\nu X_S / X_{ESCv}|, \quad (22)$$

$$K_{IRCv} = I_{RFv} / I_{Sv} = |\nu X_S / X_{ERFv}|. \quad (23)$$

3. The results of calculation and modeling of the autonomous electric power system (taking into account APLC)

Autonomous electric power system with SC harmonic distorted voltages and currents frequency characteristics comparative analysis was performed based on the corresponding analytical calculations and modeling for various variants of the APLC results. The following circuit and mode parameters $U_{ph} = 220$

V , $X_S = 0,02 \text{ Ohm}$, $X_{SC} = 0,01 \text{ Ohm}$, $p = 6$, $\alpha_1 = 30^\circ$, $\alpha_2 = 60^\circ$, $I_{dnom} = 1400 \text{ A} = \text{const}$ with $\alpha = 0.90^\circ$ are accepted as initial parameters.

The APLC with the PWR calculated parameters are determined in accordance with the above methodology. $X_{C0} = 0,227 \text{ Ohm}$, $X_{P0} = 9,07 \cdot 10^{-3} \text{ Ohm}$, $X_{LC} = 0,218 \text{ Ohm}$, $f_K = 19800 \text{ Hz}$, $X_{CF} = 15,7 \text{ Ohm}$, $X_{LF} = 0,011 \text{ Ohm}$.

Calculated equivalent reactive resistances frequency characteristics for systems with APLC2 and APLC3 are presented in Fig. 6, a, b and Fig. 6, c, d, respectively. SC currents harmonics reduction coefficients frequency dependences graphs are shown in Fig. 7. The characteristics (curves 1, 2) limiting positions of the corresponding to the values $X_{RCE1} = X_{LC}$ and $X_{RCE2} = \infty$ are shown.

For the system with APLC2, the characteristic has 2 poles: $\mu_1 = 2,8$ and $30,65 \leq \mu_2 \leq 31,75$, and the harmonics reduction coefficient in the range $27,9 < v < 33,3$. Consequently, when using APLC2, a the 29th and 31st harmonics orders resonant increase generated by SC is possible. In the system with APLC3, the only characteristic pole X_{ESCv} $\mu_1 \approx 2,8$ is on the left $v_{SCmin} = 5$. Therefore, for this variant, the resonant harmonics increase is impossible.

Follows from Fig. 7b that at $v = 5$ $K_{ISCv} \rightarrow \infty$, and in the range $5 < v < \infty$ $K_{ISCv} \geq 3,33$, i.e. APLC3, completely eliminating the 5th harmonic, provides effective reduction of all other higher harmonics generated by SC. The calculation K_{IRCv} according to (23) shows that APLC3 also provides a RC generated high-frequency harmonics reduction by more than 20,000 times. To compare the APLC efficiency, the summary MATLAB package (Simulink) modeling results of the specified options and modes are presented by the generator (network) voltage and current non-sinusoidal coefficients values in the table. 1, as well as the corresponding time graphs and spectra in Fig. 8. The model experiment corresponds to the theoretical analysis results.

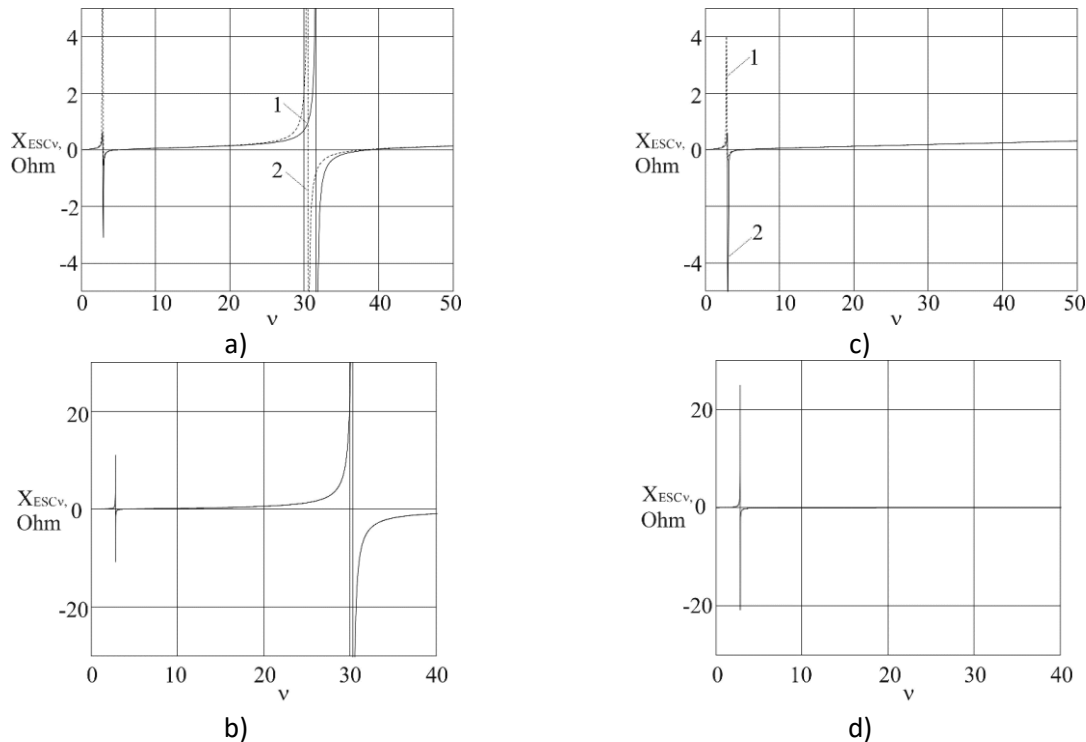


Figure 6: System equivalent reactive resistances frequency characteristics X_{ESCv} and X_{ERKv} : a, b – for the system with APLC2; c, d – for the system with APLC3

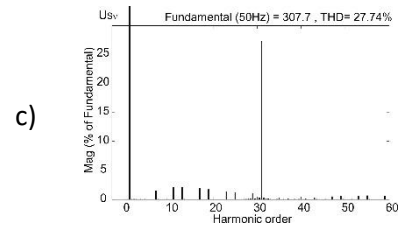
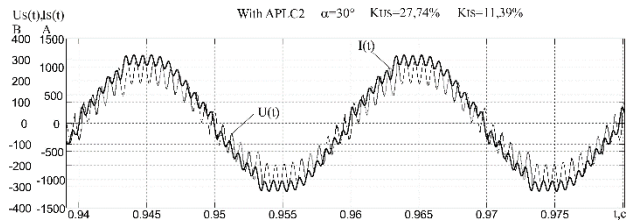
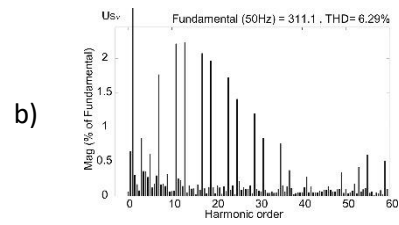
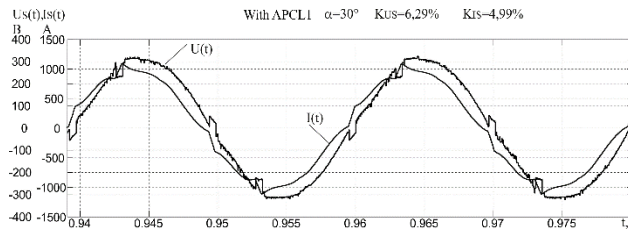
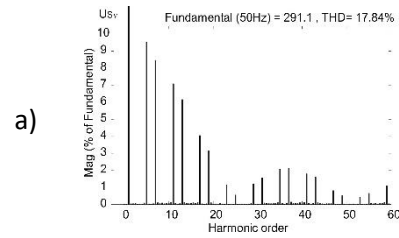
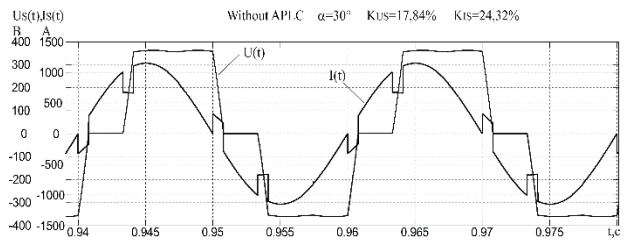


Figure 7: Current harmonics reduction coefficients frequency characteristics K_{IIIv} : a) for APLC2; b) for APLC3

Table 2

Voltage and current non-sinusoidal coefficients in an autonomous electric power system with SC

Thyristor control angle	Without APLC		APLC1		APLC2		APLC3	
	$K_{US}, \%$	$K_{IS}, \%$	$K_{US}, \%$	$K_{IS}, \%$	$K_{US}, \%$	$K_{IS}, \%$	$K_{US}, \%$	$K_{IS}, \%$
$\alpha_1 = 30^\circ$	17,84	24,32	6,29	4,99	27,74	11,39	5,97	4,79
$\alpha_2 = 60^\circ$	23,47	26,55	8,96	9,95	34,28	24,06	8,61	9,54



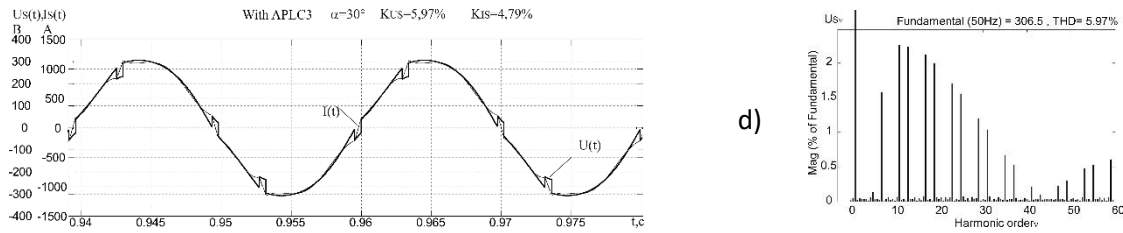


Figure8: Electric power system with SC modeling results: a) without APLC; b) APLC1 (RC phase regulation); c) APLC2 (PWR with a separate low-pass filter for RC); d) APLC3 (PWR using RF as low-pass filter for RC)

4. Conclusions

1. The use of all considered variants of APLC provides almost complete reactive power compensation, that is, the mains voltage and current consumption main harmonics phase shift elimination ($\cos\varphi_{(1)} = 1$).

2. The APLC1 and APLC3 use provides a significant generator (mains) voltage non-sinusoidal coefficients reduction in the compared to the option without compensation (by 2.84 and 2.98 times, respectively). However, APLC3 has an undoubted advantage – a 200-fold reduction in the regulation delay time.

3. The RC with the PWR and a separate anti-interference filter use in the composition of the APLC2 leads to a significant increase in the non-sinusoidal voltage coefficients (by 1.55 times) compared to the case without compensation due to the resonant increase of the 31st order harmonic. This phenomenon is explained by the fact that a separate low-frequency interference filter, effectively reducing the generated by the PWR RC harmonics, simultaneously causes the system resistance frequency characteristic pole occur at the frequency of the 31st order, that is, the resonance mode of corresponding current harmonics generated by the SC. Thus, the use of the APLC2 schematic version is inappropriate.

4. The modeling results confirm the correctness of the obtained conditions for matching the SC and RC system frequency characteristics harmonic spectra, according to which the most effective version of the improved APLC3, in which the RC with PWR is connected to the reactor and RF capacitor connection point, is the most effective. In this case, there is no need to use a separate anti-interference filter, since the branch with resistance X_{L0} and X_{C0} simultaneously performs the functions of both a resonant filter for harmonics generated by SC and an L-shaped low-pass filter for harmonics generated by RC with PWR.

5. This scheme, being approximately the same in configuration complexity as APLC1 (with RC phase regulation), is 4% superior to the latter in terms of the reducing non-sinusoidal voltage and current of SG (distortion power compensation) efficiency.

5. References

- [1] E.I. Sokol, G.G. Zhemerov, D.V. Tugay, Power electronics and energy development concept «Smart Grid», Special issue: Energy saving. Power Engineering. Energy Audit 8 (114) volume 1 (2013) 7-16. URL: <http://repository.kpi.kharkov.ua/handle/KhPI-Press/8418>.
- [2] A.F. Zharkin, D.O. Novskiy, D.O. Malakhatka, Hybrid filter-compensating converters for the three-phase systems with nonlinear and variable loads, Technical electrodynamics 4 (2015) 48-52.
- [3] V.M. Mikhal'skiy, V.M. Sobolev, V.V. Chopyk, I.A. Shapoval, The minimization strategy of undesirable instantaneous power components with different topologies of shunt active filter, Technical electrodynamics 1 (2014) 41-50.

- [4] Dayi Li, Tingkang Wang, Wenhao Pan, Xinzhi Ding, Jie Gong, A comprehensive review of improving power quality using active power filters, *Electric Power Systems Research* 199 (2021). doi: 10.1016/j.epsr.2021.107389.
- [5] Yifei Wang†, Youxin Yuan, Jing Chen, Study of Harmonic Suppression of Ship Electric Propulsion Systems, *Journal of Power Electronics* 5 volume 19 (2019) 1303-1314. doi: 10.6113/JPE.2019.19.5.1303.
- [6] Yifei Wang, Kaiyang Yin, Huikang Liu, Youxin Yuan, A Method for Designing and Optimizing the Electrical Parameters of Dynamic Tuning Passive Filter, *Symmetry* 13 (2021) volume 7 1115. doi: [10.3390/sym13071115](https://doi.org/10.3390/sym13071115).
- [7] J. Dixon, L. Moran, J. Rodriguez, R. Domke, Reactive power compensation technologies: State-of-the-Art review, *Proceedings of the IEEE* 12 (2005) volume 93 2144-2164. doi: 10.1109/JPROC.2005.859937.
- [8] A.K. Zhuk, Investigation of network filters influence on total harmonic distortion in autonomous electric power systems with thyristor converters, *Special issue: Power electronics and power efficiency Part. 2* (2004) 93-98.
- [9] O. Zhuk, D. Zhuk, D. Kryvoruchko, Voltage Harmonic Distortion in Autonomous Electric Power System with an Adjustable Power Line Conditioner, *Proceedings of the 3rd International Conference on Intelligent Energy and Power System, IEPS '2018, IEEE, Kharkiv, Ukraine, 2018*, pp. 33-39. doi: 10.1109/IEPS.2018.8559532.
- [10] O. Zhuk, D. Zhuk, D. Kryvoruchko, Non-sinusoidal voltage in an autonomous electric power system with a controlled filter compensating device, *Technical electrodynamic* 5 (2018) 26-30.
- [11] Harmonic filters and EMI, 2018. URL: <https://www.metartec.com/DataEditorUploads/R7 - Harmonic Filters and EMI.pdf>.
- [12] R. Klempka, Z. Hanzelka, and Y. Varetsky, Bank Harmonic Filters Operation in Power Supply System – Cases Studies, *Power Quality Issues* (2013) 201–230. doi: 10.5772/53425.
- [13] Y. Varetsky, Switching on power harmonic filters, *Energy Engineering and Control Systems* 2 volume 4 (2018) 51 – 58. doi: 10.23939/jeeecs2018.02.051.
- [14] J.P. Torreglosa, E. González-Rivera, P. García-Triviño, D. Vera, Performance Analysis of a Hybrid Electric Ship by Real-Time Verification, *Energies* 15 (2022). doi: 10.3390/en15062116.
- [15] ABB, Power Quality Filter, 2003. URL: <https://library.e.abb.com/public/0f61159109c44f58c1256f2e00445c57/2GCS401012A0070.pdf>.

Features of computer simulation of flight vehicles in teaching technical specialties in the field of the aviation industry in the Republic of Kazakhstan

Khuralay Moldamurat¹, Galia Mukhamedrakhimova¹, Samal Kalieva¹, Niyaz Belgibekov¹,
Asel Zhumabayeva¹, and Makhabbat Bakyt¹

¹ *L.N. Gumilyov Eurasian National University, Astana, Kazakhstan*

Abstract

The article discusses the features of computer simulation of flight vehicles in teaching technical specialties in the field of the aviation industry in the Republic of Kazakhstan. With the help of a computer program, a student learns to find and explore new products by designing an unmanned aerial vehicle (UAV), as well as modeling. Digital education emphasizes the importance and usefulness of a computer program. The combat UAV "Berkut" used in the military sphere was designed as an object of study. A 2D UAV model and an effective UAV model are obtained. The use of a computer software environment will allow the student to become a strong engineer, designer, programmer. When designing the UAV "Berkut" in the environment of the SolidWorks computer program, the student must learn mathematical, physical, UAV ballistics, and ergonomic assembly of the UAV. The most effective aspects of the use of computer technologies are outlined in the education system.

Keywords

Digital educational system, training, development, virtual laboratory, research facility, SolidWorks program, design of Berkut combat unmanned aerial vehicle (UAV), computer software environment, computer research, modeling, aerodynamics, static, ergonomic assembly, 2D and 3D model, student, teacher

1. Introduction

Eurasian National University named after L.N. Gumilyov in the Republic of Kazakhstan has a special specialty - space technology and technology, which trains specialists in the field of the aviation industry. It considers the place and features of computer simulation of flight vehicles in teaching a profession. The significance features and effectiveness of teaching students of technical specialties in the environment of a computer program are given. Students study a combat UAV and are offered a task to design a 3D model [1]. The UAV design process was very helpful for the students, they learn a lot. On the basis of effective UAV samples available in the research method, the fighter designed the unmanned aerial vehicle "Berkut" (UAV). Effective aspects of determining the goals and use of the UAV are given. An effective model of aerodynamics, static and ergonomic assembly of the UAV in flight has been developed in the SolidWorks computer program. In addition, it is very useful in the field of education to use a large number of computer programs. Computer research is of great importance in special disciplines studied in technical and engineering specialties. In the educational process, the technical base, research sites, engineering design laboratories and outer space, nuclear research are very expensive - nanotechnology centers, remote reconnaissance, military ranges, the study of aircraft ballistics. Even inaccessible becomes impossible in the learning process. Therefore, to solve these problems, special software environment. The article teaches students to find new products when designing UAVs using a computer program, get 3D models and conduct ballistic studies and explore complex objects.

When designing air transport, students studying in the specialty of space engineering and technology provide for the design of a special fighter unmanned aerial vehicle (UAV) "Berkut". Students learn the importance of creating new products and qualified service in their field as a future specialist. Also, the student must understand what the UAV must learn. What you need to know in the specialty. Constant UAV

readiness for global competition in war conditions. When using a UAV, it is important to know the most effective points and features. A fighter, designed together with students, must have a remote automatic control of the UAV "Berkut" [2]. In addition, it must perform the task in real time and quickly. In any case, a Berkut UAV fighter must conduct reconnaissance of an object marked from above and independently make a decision during the flight. A method of hardware input of numbers in a random situation of the drone was obtained [3, 21]. Terms of reference for the fighter UAV "Berkut" are prepared in the environment of a computer program. Ballistics is studied taking into account the effective net mass of the UAV and the load weight of the weapon used. The fighter simulated the aerodynamics and static in flight of the Berkut UAV, as well as the ergonomic assembly of the Berkut UAV fighter in a computer program. The student must complete tasks in the process of work and fully design the Berkut UAV. To complete the tasks, the student must master the SolidWorks computer software environment. Technical and engineering disciplines are also important - physics, mathematics, computer science, mechanics, aircraft ballistics, aircraft design, design in the environment of computer programs, knowledge of microprocessor systems and digital devices.

2. Theoretical part

With the help of a computer program, the student conducts a review and research of information about the UAVs of the whole world when designing the Berkut UAV. Based on the achievements of the world UAVs, it is necessary to choose an effective UAV architecture. We get the result that the UAV has been repeatedly used in practice and fully fulfilled its target tasks [3]. Based on the result obtained, the student should be able to design the Berkut UAV.

We consider the UAV device existing in the world - "Baykar Makina UAV. It was designed and engineered in the Turkish state. The Baykar Makina UAV has an internal combustion engine and a pusher-type propeller. "The strike speed of the Baykar Makina UAV is a tactical average altitude of 4 km, s guided weapons. Bayraktar TB2 operates in the air from 12 to 24 hours. The maximum control range is up to 150 km. This allows you to conduct constant duty in the air and fully fulfill your goals. At the same time, the Turkish industry was not able to fully equip the UAV, so it purchased foreign components, mostly Canadian-made. The main ones are the 100 horsepower Rotax 912 piston engine and the company's L3HARRIS WESCAM stabilized infrared device. "The inter-archive parametric parameters of the Baykar Makina UAV and the 3D model [4].



Figure 1: In-flight vision of UAV "Baykar Makina"

The Office of Naval Research (ONR) of the US Department of Defense has announced a major project to use UAV groups for military purposes. The project was named Low Cost UAV Swarm Technology - LOCUST ("grasshopper"). According to the developers of the project, the autonomous Roy of the UAV allows the control system to receive significant tactical advantages on the battlefield [5]. In the case of flying a swarm control system, UAVs interact with each other based on a decentralized architecture. In this case, the launch of drones can be carried out from a variety of platforms installed on various vehicles, ships and aircraft. The flight of the UAV is controlled by the operator, monitoring the implementation of the mission and making the necessary adjustments in the course of its implementation [6].



Figure 2: After the flight of the UAV, the tail and wings open

One of the latest solutions with UAV control system around the world. One of the tasks solved with the help of group control is automatic refueling in the air. A complex scientific and technical problem has been solved. UAV flights in formations are studied by many scientific centers of the world [7, 8]. As one example, a research team from the University of Sydney (Australia) has done a lot of work on the creation and management of UAVs, which in their project has developed not only autonomous refueling between two U&A, but also a navigationsystem based on computer vision, intelligent control for these goals (Fig. 2). In the article, the system of capturing intelligent tasks and methods of solution development were obtained [7,20].

3. Practical part

The student must learn and be convinced of the efficiency and features when designing in the environment of the SolidWorks computer program, attaching importance to the structural characteristics of the Berkut UAV.

A fighter with a shock operational-tactical, turbofan engine is provided for by the Berkut UAV.

The frame of the projected UAV "Berkut" consists of a composition of bluish color, combined with the blue color of the sky, built to visually deceive the enemy from the opposite direction. The connecting armature of the UAV is made of aerospace aluminum alloy composite material, it is light in flight and has high strength. The total mass and length are developed in the environment of the SolidWorks computer program for an effective model of the Berkut UAV for use with obtaining special aerodynamic complex mathematical calculations. Figure 3 Below is a 3d view of the Berkut unmanned aerial vehicle (UAV) [9].

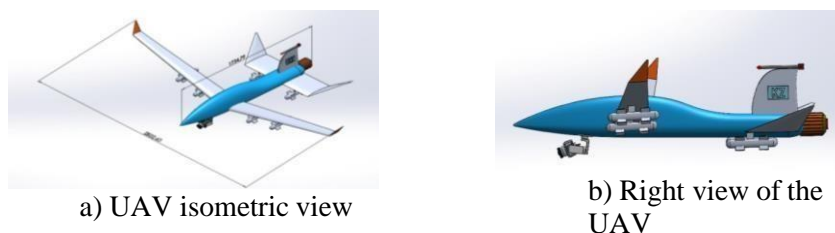


Figure 3: Fighter isometric view of UAV "Berkut", overall size and weight, right view

The description of the combat UAV "Berkut" is given below:

- Weight: 142 kg UAV net weight;
- Wingspan: 2.83;
- Total length of the lake: 1.74 meters;
- Maximum flight altitude: 4.1 km;
- Travel speed: 200 km;
- Control ranges from ground station -123 km;
- Operational-tactical with shock engine, turbofan engine -1;

- Fuel-aviation kerosene;
- A microprocessor system is applied to the on-board control system;
- Material used - aviation aluminum alloy 7075-T6.

The student is equipped with 6 missiles as weapons for the UAV "Berkut" when designing in a computer program. We place the missiles equally, observing the laws of stabilization. The center of gravity of the combat UAV "Berkut" plays an important role in the alignment of direct flight and maneuvering in the air. Since the center of gravity cannot find the most suitable place, we must eliminate the risk of increased morbidity and increased energy consumption and loss of control [10]. (Made from an explosive fragment or armor-piercing warhead) - 2.5 kg In Fig. 2 below, the total size of the Berkut combat unmanned aerial vehicle (UAV) and the total weapon weight of 157 kg were obtained.

The fighter is represented by an unmanned aerial vehicle (UAV) "Berkut" with a total size and a total weight of 157 kg in service.

The Berkut UAV fighter must have a high sense of proportion and speed [11]. The winglet is simple, one-color, the internal structure of the wing consists of many cells, thanks to which the entire design is optimized. On a small light aircraft, a turbofan engine regulates thrust with a proportional coefficient of lift and flight This is good for maneuvers such as increasing lift and braking but adds weight to controls and is often not suitable for operator control.

4. Input data

Global Mesh Options Automatic starting grid: enabled Problem solution level: 3

Narrow Channel Resolution Enhancement: Disabled Geometry Resolution

Determination of the minimum cleaning: automatic mode Minimum wall thickness determination: automatic mode

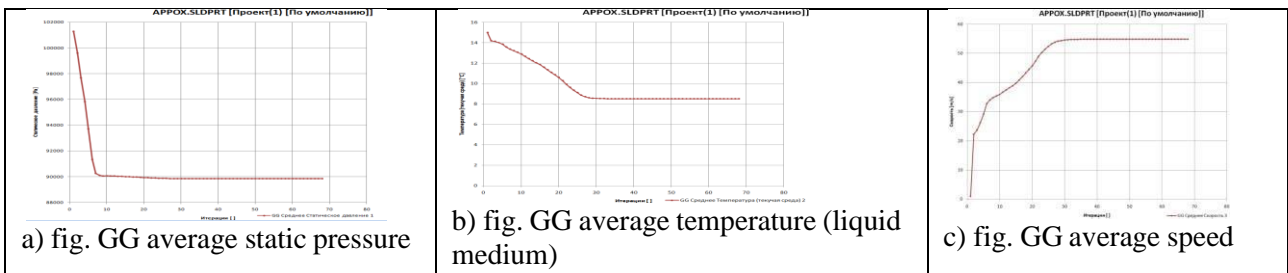


Figure 4: The fighter will learn how to build parametric graphs of the impact on the launch of the Berkut UAV and explore the graphs

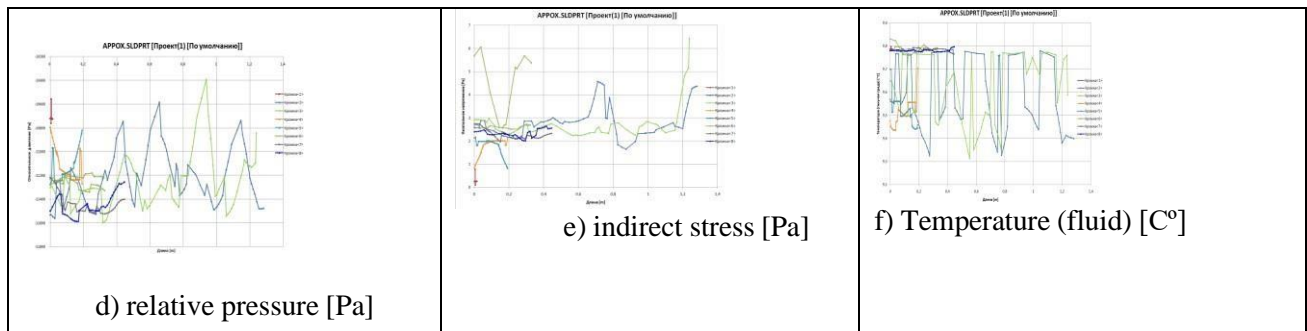


Figure 5: Graph of ribs attached to the wings and stabilizers of ROV "Berkut"

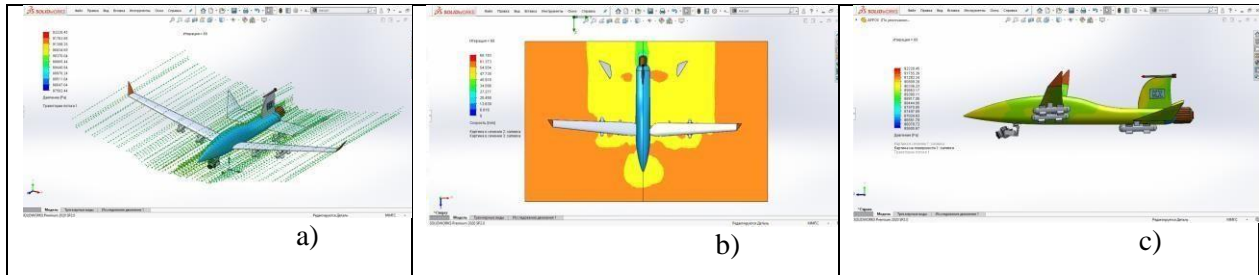


Figure 6: Aerodynamic flow and fluidity of the aircraft in flight combat ROV "Berkut" learn how to design in the CAE environment

All of the above UAV design processes should be fully mastered by the student. The angle of the hull in the direction of flight affects its stability, but if the projection area of the hull and the angle of its direction are not large, then the balance bar has a lesser effect [12, 13]. The stabilizer is stable when the light aircraft is moving at low speed. Tip - light aircraft rise from the ground and gain altitude is not difficult, and when the regulator is reduced, the nose of the aircraft stabilizes. In addition, high speed is not required for a safe landing. A special program in the middle of the computer. In addition, the quality and durability of the aircraft is very important. Using the program, we can observe the area where the air flow strongly affects the aircraft. In the future, we will take into account the strength of that area when creating a 3D image. In this program, we will create a 3D design of the aircraft and make a model. As you can see in the 4 pictures above.

Table 1

Min / Max indicators of studies according to the SolidWorks program in flight of the UAV "Berkut"

Name	Minimum	Maximum
Pressure [Pa]	87582.44	92228.45
Density (liquid medium) [kg / m ³]	1.08	1.14
Speed [m/s]	0	68.193
Speed (X) [m/s]	-14.321	12.168
Speed (Y) [m/s]	-28.819	31.922
Speed (Z) [m/s]	-67.731	3.331
Temperature [°C]	7.52	11.65
Temperature (liquid medium) [°C]	7.52	11.65
Torsion [1/s]	8.09e-03	779.96
Speed in rotating coordinate system [m/s]	0	68.193
Speed in rotating coordinate system (X) [m/s]	-14.321	12.168
Speed in rotating coordinate system (Y) [m/s]	-28.819	31.922
Speed in rotating coordinate system (Z) [m/s]	-67.731	3.331
Mach number []	0	0.20
Shear stress [Pa]	0	12.37
Relative pressure [Pa]	-13730.55	-9084.54
Non-collinear heat flow indicator []	2.2683383e-06	1.0000000
Thermal resistance indicator []	1.4559651e-07	1.0000000
Heat transfer coefficient [W / M ² / K]	0	0
Surface heat flux density [W / M ²]	0	0
Surface heat flux density (convection) [W / M ²]	0	0
Acoustic power [W / M ³]	0	1.833e-06
Acoustic power level [dB]	0	62.63

At normal speed of sound, at a distance of $\frac{1}{4}$ from the leading edge of the wing, there is a point of aerodynamic force, and when the angle of attack changes, the aerodynamic moment does not change. The student was convinced experimentally and theoretically in the process of designing the UAV "Berkut". This position is called the aerodynamic center of the wing. At a high speed of sound, the wing span occurs at the aerodynamic center point. For wings other than rectangular (triangular, trapezoidal, etc.), Mean The Aerodynamic Center (MAC) is the middle center of the wing [14, 15]. Taking into account all the above tasks, the "Berkut" ROV received a complete set in the SolidWorks program, with the help of a manual and an instructive manual for special education teachers.

5. Discussion

In the article, the student will learn to find and explore, as well as to model new products, designing UAVs using a computer program. For students of technical and engineering direction, computer modeling and design is important. The formation of a specialist provides great opportunities. A computer program develops the thinking of students. In addition, new technologies allow to invent modern products. The computer program will fully teach you how to do scientific research, investigate complex objects, and perform engineering design. So, in the SolidWorks program, you can design products and get 2D and 3D models of products and determine the strength and quality of products. Thus, it is possible to improve digital educational competencies with the help of computer programs, increasing technological, engineering, and information literacy [16, 17]. Allows you to compare, evaluate the concepts and results of work performed in a computer environment, as well as analyze the differences in the results. Educational scenarios in the technical and engineering areas should be well planned by the teachers-student. In the processes of development and advanced training of future young professionals, as well as the formation of new technologies. In computer modeling, research, the teacher must increase the interest and qualifications of the student through the correct task. It is important to educate learners by offering a wide range of digital learning methods. The development of engineering and technology is growing rapidly in the 21st century. To do this, the teacher must constantly seek and improve himself in education. Digital educational innovations: the evaluative perspective of digital learning and computer technology training increase the interest of students [18, 19]. The effective use of a computer program provides great opportunities for studying the topics of scientific research undergraduates and PhD students. The conditions for the formation of the physical worldview were considered in the solution of aerodynamic calculation methods [22] Can complete scientific research topics with results. Differentiators in the development of science and education are computer research and the development of digital competencies. Computer modeling and research can use virtual structures and devices with different sizes. In conclusion, a series of reflections is formed on the importance of the development of computer design and modeling, research. Also important is the constant provision of institutional guidelines and transversal training and updating of educational programs (bachelor's, master's and PhD) in higher education institutions.

6. Final part

Together with students and teachers, the Berkut combat UAV was developed in the environment of the SolidWorks computer program. In the process of application, research methods were studied. As a result of the calculation, an optimized 3D model of the product was obtained.



Figure 7: Photo of the teacher and students who took part in the design of the Berkut UAV

In the process of training, he learned how to work in the SolidWorks complex of complex objects in the environment of a virtual computer program. He also mastered the design, calculations, research and invention of a new product.

In SolidWorks in a CAE application, calculate aircraft pressure force, fluid density, aerodynamic force, aircraft speed change rate, and aircraft fluidity, as well as aircraft center of gravity, average speed, and force.

In addition, the quality and durability of the aircraft were studied in SolidWorks in a CAE application. It is very important to increase the strength of areas that are heavily affected by air flow. Therefore, in the future, it is better to make a mixture of high-quality materials when making a full-fledged model of an aircraft.

The system of topological optimization of the relative parameters and stress-strain states of the combat UAV "Berkut" has been improved in the SolidWorks complex. The fighter was awarded the technical units of measurement of the UAV "Berkut" and a 3d architectural sample was prepared. The fighter considered specific patterns based on the additional weapon load during assembly and launch UAV Berkut.

In conclusion, students of the specialty "space engineering and technology" received the technical parameters of the combat UAV "Burkit" in the environment of a computer program and were examined in a vertical simulation.

The SolidWorks computer-aided design program has learned the basics of using mathematical and other models, computer-aided design procedures and computer technology. Distinguish features and effectiveness of computer-aided design of technical objects and their components. The use in the process of practice in the education system of a large number of types of computer programs related to the profession develops the quality of education. In addition, students develop interest in the profession and professional knowledge.

7. References

[1] DARPA collects drones in a swarm [Electronic resource]. – Resource access mode: <http://military.rf/2017/%D0%91%D0%BF%D0%BB%D0%B010/>.

[2] Samigullina G. A., Masimkanova Zh. A., modified algorithm based on the multifunctional multi-agent Smart system of swarm intelligence, Bulletin of the Kazakh-British Technical University, no2 (49), 2019 pp. 158-163.

[3] Samigulina, G.A., Samigulina, Z.I., Development of a Unified Artificial Immune System for Intelligent Technology of Complex Industrial Automation Objects Control in the Oil and Gas Industry, Smart Innovation, Systems and Technologies, 2021/

[4] Is Kazakhstan ready for a technological race? [Electronic resource]. Resource access mode: https://forbes.kz//process/intellektualnaya_zadacha_1588745463/

- [5] Yemelyev, A.K., Moldamurat, K., Seksenbaeva, R.B. Development and Implementation of Automated UAV Flight Algorithms for Inertial Navigation Systems, SIST 2021 - 2021 IEEE International Conference on Smart Information Systems and Technologies, 2021, 9465965.
- [6] Kyzyrkanov, A.E., Atanov, S.K., Aljawarneh, S.A.R. Formation control and coordination of swarm robotic systems, ACM International Conference Proceeding Series, 2021, 3492704.
- [7] Moldamurat Kh. «Mobile fire robot» invention patent – No.2020/0819.1 dated November 26, 2020.
- [8] Baimukhamedov M.F., Moldamurat K., Akgul M.K. Optimal control model of the automobile transport, Transport Means - Proceedings of the International Conference, 2019, 2019-October, pp. 1312–1316.
- [9] Adilzhan K.K., Sabyrzhan A.K., Timur T.Z. The Usage of Extended Kalman Filter to Increase Navigation Accuracy of Mobile Units in Closed Spaces, SIST 2021 - 2021 IEEE International Conference on Smart Information Systems and Technologies, 2021, 9465903.
- [10] Atanov, S.K., Bigaliyeva, A.Z., Apachidy, N.K., Rusak, A.V. Process control issues of fine grinding in a planetary mill. Vestnik Sankt- Peterburgskogo Universiteta, Prikladnaya Matematika, Informatika, Protsessy Upravleniya, 2020, 16(3), pp. 277–292.
- [11] Erol, B. A., Majumdar, A., Benavidez, P., Rad, P., Choo, K. - R., & Jamshidi, M. (2020). Toward artificial emotional intelligence for cooperative social human-machine interaction. IEEE Transactions on Computational Social Systems, 7(1), 234-246. doi:10.1109/TCSS.2019.2922593. Retrieved from: <https://www.scopus.com/record/display.uri?eid=2-s2.0-85068161401&origin=resultslist&sort=plf-f>.
- [12] Craig John, Introduction to Robotics. Mechanics and control: a monograph / - Moscow: Institute for Computational Research. 2013, 564.
- [13] Nikhil Sethi, Saurav Ahlawat, Raghava Nallanthighal. Low Fidelity VTOL UAV Design Optimization using an Open Source Framework – South Asian University, Delhi, India bDelhi Technological University, Delhi-110042, India.
- [14] Emilio Botero and Juan J. Alonso. Conceptual Design and Optimization of Small Transitioning UAVs using SUAVE, AIAA (5-9 June 2017).
- [15] Ashraf M. Kamal, Alex Ramirez-Serrano. Design Methodology for hybrid (VTOL+ Fixed wing) Unmanned Aerial Vehicles // Aeronautics and Aerospace Open Access Journal, 2018.
- [16] Rishabh Dagur, Vikrant Singh, Shabir Grover, Nikhil Sethi, B.B. Arora. Design of Flying Wing UAV and Effect of Winglets on its Performance // IJETAE, March 2018.
- [17] Matthew Clarke, Jordan Smart, Emilio Botero, Walter Maier and Juan J. Alonso. Strategies for Posing a Well-Defined Problem for Urban Air Mobility Vehicles // AIAA SciTech (7-11 January 2019).
- [18] Viktorovna, U. N., Kulmukhambetovna, I. G., Serikovna, B. K., Pavlovna, R. L., & Kydyrbaevna, K. A. (2017). Formation of communicative competence as a condition of development of social orientation of the future teacher. Man in India, 97(16), 407 -414. ISSN 00251569. Retrieved from: <https://www.scopus.com/record/display.uri?eid=2-s2.0-85074669298&origin=resultslist>.
- [19] Moldamurat K., Akhmedjanov S., Kariyeva K., Omarov Zh., Kalibekov D., Sayassat N. Design and optimization of parameters of a hybrid unmanned aerial vehicle in the SolidWorks complex. 2022 IEEE Smart Information Systems and Technologies (SIST) 28 -30 April, 2022, Nur-Sultan, Kazakhstan.
- [20] Atanov, S.K., Seitbattalov, Z.Y., Moldabayeva, Z.S. Development an Intelligent Task Offloading System for Edge-Cloud Computing Paradigm // Proceedings - 2021 16th International Conference on Electronics Computer and Computation, ICECCO 2021, 2021
- [21] Maidanov, A., Atanov, S., Tailak, B. Hardware Implementation of Pseudo-Random Numbers on CPLD // Proceedings - 2021 16th International Conference on Electronics Computer and Computation, ICECCO 2021, 2021.
- [22] Mukhamedrakhimova, G., Kenzhaliyev, D., Kenzhebekov, B., Mukhamedrakhimov, K. Conditions of formation of a general physical world view in students for the improvement of their future profession // Espacios, 2017, 38(48), 26.